The Effects of Daily Exercise Duration on Cardiac Responses and Atrial Fibrillation

Renée Ann Gorman

A Thesis submitted to the Faculty of Graduate Studies in Partial Fulfillment of the Requirements for the Degree of Master of Science

Department of Biology
York University
Toronto, Ontario

August 2023

The Effects of Daily Exercise Duration on Cardiac Responses and Atrial Fibrillation

Renée Ann Gorman

Department of Biology, York University

August 2023

Abstract

Atrial fibrillation (AF) is a supraventricular tachyarrhythmia strongly associated with cardiovascular disease (CVD) and sedentary lifestyles. Despite the abundant benefits of regular exercise, AF incidence for professional endurance athletes is proportionate to CVD patients. To assess exercise dose and AF, we compared the effects of strenuous endurance training on mice by varying daily swim durations (120, 180 and 240 minutes). After receiving the same cumulative work while swimming (estimated from O_2 consumption), all exercised groups showed similar elevations (P<0.04) in skeletal muscle mitochondria content and ventricular hypertrophy (P<0.02). By contrast, inducible AF increased (P<0.04) progressively with daily swim dose without markedly affecting atrial refractoriness (P>0.05). Associated with a dose dependency is pronounced (P<0.0001) bradycardia, (P<0.003) hypertrophy, (P<0.0007) fibrosis and (P<0.0001) macrophage accumulation in the atria, that is not observed in the ventricles. Our results demonstrate that prolonging daily swim exercise promotes progressively adverse atrial-specific remodelling leading to increased AF susceptibility.

Keywords: atrial fibrillation; daily exercise duration; endurance training; cardiovascular; arrhythmias

Acknowledgements

First and foremost, I would like to thank my supervisor, Dr. Peter Backx, for his invaluable guidance throughout my Masters degree. I am incredibly fortunate to learn from one of the foremost authorities in cardiology and electrophysiology. I am grateful for his willingness to teach me the fundamentals of becoming a successful researcher and honoured for the opportunity to train under such a distinguished academic.

I would also like to thank Dr. David Hood for joining my Master's committee, who has been a wonderful addition and considerably helpful regarding his exercise expertise.

I am also inclined to thank Naz Polidovitch for his patience and willingness to teach me many of the employed experimental techniques and his intellectual contribution, especially during the early stages. His efforts were instrumental to the success of the project. Additionally, I would like to thank Dr. Robert Lakin for his continual support and for teaching surgical endpoint measurements.

I would also like to thank the present and past members of Dr. Backx's laboratory for their assistance and support. In particular, I would like to thank Ryan Debi for his knowledge of invasive hemodynamics. Moreover, thank you to my volunteers - Jhonny Mendoza, Elana Dhaigham and Jarrett Chow - for their help with the swims.

Lastly, I extend my utmost gratitude to my family and close friends for their unconditional support and encouragement.

Copyright Acknowledgements

Table of Contents

Abstract ii

Acknowledgements iii

Copyright Acknowledgements iv

Abbreviations List vii

Figures and Tables List viii

Chapter 1: Introduction 1

1.1 Characterizing Atrial Fibrillation 1
1.2 Cardiac Electrophysiology and Function 1
1.3 Cardiac Arrhythmogenesis 4
1.3.1 Triggered Automaticity 4
1.3.2 Re-entry and Conduction Block 5
1.3.3 Autonomic Modulation 7
1.4 Atrial Fibrillation Epidemiology 7
1.4.1 Nonmodifiable Risk Factors: Age, Sex and Race/Ethnicity 8
1.4.2 Modifiable AF Risk Factors 8
1.4.3 AF Comorbidities and Prognosis Impact 9
1.5 Atrial Fibrillation Pathogenesis 10
1.5.1 Electrical Remodelling 10
1.5.2 Structural Remodelling 11
1.5.2.1 Atrial Hypertrophy 11
1.5.2.2 Atrial Fibrosis 11
1.5.2.3 Atrial Inflammation 14
1.6 The Relationship Between Physical Activity, Excessive Endurance Training and AF 14
1.7 Potential AF Pathophysiology in Endurance Athletes 16
1.7.1 The Athlete's Heart Phenotype 16
1.7.1.1 Cardiac Chamber Morphology and Function 17
1.7.1.2 Sinus Bradycardia 18
1.7.2 Skeletal Muscle Mitochondrial Adaptations 19
1.7.3 Atrial Fibrosis and Inflammation 19
1.8 Synopsis and Hypothesis 20

Technical Contributions Acknowledgement 22

Chapter 2: Materials and Methods 23

2.1 Experimental animals 23
2.2 Swim Training Protocol 23
2.3 O_2 Measurements 25
2.4 Echocardiography 25
2.5 Surface Electrocardiography with Pharmacological Blockade 25
2.6 Invasive Hemodynamics 26
2.7 In vivo Electrophysiology: Effective Refractory Period and AF Inducibility 26
2.8 Tissue Morphometry of Hearts 30
2.9 Histology and Immunohistological Staining 31
2.10 Cytochrome c oxidase activity 33

2.11 Statistical Analysis 34
Chapter 3: Manuscript for Journal Submission 35
3.1 Abstract 36
3.2 Introduction 37
3.3. Methods 37
3.4 Results 38
3.4.1 Exercise Quantification 38
3.4.2. Cardiac Adaptations in Swim-Trained Mice 42
3.4.3. Dose-Dependent Arrhythmia Inducibility in Swim-Trained Mice 49
3.4.4. Atrial Macrophage Infiltration in Swim-Trained Mice 58
3.5 Discussion 61
3.5.1 Limitations 63
3.5.2. Conclusion 63
3.5.3. Future Directions 64
Chapter 4: Extended Discussion 65
4.2 Possible Pathways Between AF Remodelling with Exercise versus CVD 65
4.3 Scaling of Exercise Dose and Response from Mouse Models to Humans 66
4.4 Dose-Response Relationship and Heterogeneous Cardiac Remodelling in Athletes 67
4.4 Future Directions 68
Chapter 5: References 70
Appendix 86
A.1 Swim O_2 Calculation Corrections 86
A.1.1 Calibration 86
A.1.2 Pressure Compensation 86
A.1.3 Baselining 86
A.1.4 Conversion to Molarity and Volume 87
A.1.5 Humidity Compensation 87
A.2 Oxygen Consumption and Total Exercise Dose Calculations 88

Abbreviations List

ACh	Acetylcholine
AF	Atrial fibrillation
AP	Action potential
APD	Action potential duration
AR	Aortic regurgitation
AT1-R	Type 1 angiotensin receptor
AV	Atrioventricular
CO	Cardiac Output
CRP	C-reactive protein
cTnI and cTnT	Cardiac troponin I and T
Cx	Connexin
DAD	Delayed afterdepolarization
DM	Diabetes mellitus
EAD	Early afterdepolarization
ECC	Excitation-contraction coupling
ECM	Extracellular matrix
EF	Ejection Fraction
ERP	Effective refractory period
FHS	Framingham heart study
HF	Heart failure
HR	Heart rate
IC	Interstitial fibrosis
ICANS	Intrinsic intracardiac autonomic nervous system
IL	Interleukin
LA	Left atria
LV	Left ventricle
LVEDP	LV End-Diastolic Pressure
LVSP	LV Systolic Pressure
MI	Myocardial infarction
MΦ	Macrophage
M2	Muscarinic receptor 2
NCX	Na^{2+}/Ca^{2+} exchanger
PA	Physical activity
PC	Pericapsular fibrosis
RA	Right atria
RAAS	Renin-angiotensin-aldosterone system
RMP	Resting membrane potential
RV	Right ventricular
SAC	Stretch-activated ion channel
SR	Sarcoplasmic reticulum
SERCA2a	Sacro/endoplasmic reticulum Calcium ATPases 2a
SV	Stroke volume
TGF-β	Transforming growth factor β
TNF	Tumour necrosis factor
VNS	Vagal nerve stimulation
VO_2	Oxygen consumption
VO_{2max}	Maximal oxygen consumption

Figures and Tables List

Figure 1.1. Representative cardiac action potential (AP) waveforms. 3
Figure 1.2. A Model of Re-entry. 6
Figure 1.3. Cardiac Fibrosis Types and the Effects on Anisotropic Conduction 13
Figure 1.4. J-shaped Dose-Response Curve Between Atrial Fibrillation Risk and Physical Activity. 16
Figure 2.1. Mouse Swimming Apparatus 24
Table 2.1. Acclimation Period for the Swim Duration Protocols. 24
Figure 2.3. Intracardiac 2F Electrophysiology Catheter Placement. 28
Figure 2.4. Atrial Effective Refractory Period (AERP) Measurements. 29
Figure 2.5. Atrial Arrythmias Detection Using an Intracardiac 2F EP Catheter. 30
Figure 2.6. The Threshold Method for Collagen Content Quantification. 33
Figure 3.1. Self Regulation Behaviour During Swimming. 39
Figure 3.2. Exercise Characterization using a Mouse Swim Model. 40
Figure 3.4. Skeletal Muscle Mitochondrial Adaptation. 42
Table 3.1. Extended Surface Electrocardiogram Heart Rate Data. 43
Figure 3.5. Effect of Swim Training on Heart Rates (HRs) and Autonomic Regulation. 44
Table 3.2. Physical Ventricular Parameters of Mice Swim-Trained for Variable Daily Durations. 46
Figure 3.6. Expanded Ventricular Morphometric Data. 47
Figure 3.7. Linear Regression of Echocardiographic Measurements. 48
Table 3.3. Functional Ventricular Parameters of Swim-Trained Mice. 49
Figure 3.8. Variable Training Duration Increases Atrial Fibrillation Inducibility, Without Refractory or Action Potential Shortening. 50
Figure 3.10. Atropine Effects on Atrial Refractoriness and AF Susceptibility in Swim-Trained Mice 52
Figure 3.11. Swim Training at Variable Daily Durations Induces Atrial Fibrosis. 54
Figure 3.12. Discrimination Between Swim Training Induced 55
Figure 3.13. Swim Training Induced Minimal Ventricular Fibrosis. 56
Table 3.4. Physical Atrial Parameters of Mice Swim-Trained for Variable Daily Durations 57
Figure 3.14. Linear Regression of Atrial Hypertrophy Measurements. 57
Figure 3.15. Swim Training at Variable Daily Durations Induces Atrial Inflammation. 59
Figure 3.16. Swim Training at Variable Durations Does Not Cause Ventricular Inflammation. 60
Appendix Figure A.1. Dose-Dependent AF Susceptibility in Swim-Trained Mice (Extended). 89
Appendix Figure A.2. Effect of Swim Training on Heart Rates (HRs) and Autonomic Regulation (Extended). 90
Appendix Figure A.3. Refractory Periods With and Without Parasympathetic Blockade (Extended). 91
Appendix Figure A.4. Swim Training Induced Atrial Collagen Deposition (Extended). 92

Chapter 1: Introduction

1.1 Characterizing Atrial Fibrillation

Atrial fibrillation (AF) is the most commonly diagnosed cardiac arrhythmia worldwide, and involves rapid, irregular atrial activity, causing cardiac desynchrony and exacerbating thrombosis formation, stroke tendency and overall mortality risk [1]. AF can be paroxysmal (episodes that terminate spontaneously), persistent (continue for more than seven days and are not self-terminating) or permanent. Furthermore, symptoms vary from asymptomatic to palpitations, chest pain, shortness of breath, nausea, dizziness, diaphoresis and generalized fatigue [1]. Various treatments and risk modifiers exist, including anticoagulation, rate- or rhythm-control medication, cardioversion and ablation yet AF management has numerous inadequacies, reflecting the complex multifactorial pathophysiology [2]. Notably, AF patients display a multitude of atrial electrical and structural changes, termed remodelling. Electrical remodelling includes reduced atrial refractoriness and increased cellular heterogeneity that can initiate AF. Structural remodelling, such as atrial hypertrophy and fibrosis, can also predispose conduction propagation barriers and alter conductivity. Together, these changes promote electrical re-entrant stability, underlying AF, and are discussed in detail below.

1.2 Cardiac Electrophysiology and Function

To understand AF pathogenesis, normal cardiac physiology must first be addressed. The heart functions as a mechanical pump, supplying blood to the body. Each contraction initiates from a bioelectrical signal, the action potential (AP), due to excitation-contraction coupling (ECC) [3]. An AP originates in the sinus nodal cells and propagates through the heart via impulse conduction, measured by the intra- and extracellular voltage differences. Impulse conduction extends through the atria causing contraction, then passes through the atrioventricular (AV) node, His bundle along the septal wall and into the subendocardial Purkinje fibres, stimulating synchronized ventricular contraction.

The AP consists of five phases, determined by the opening and closing of various transmembrane proteins, consisting of ion channels and transporters [4,5]. The resting membrane potential (RMP) in working myocardial cells, or the maximal diastolic potential in spontaneously beating cells, ranges from -95 to -40 mV and represents the lengthiest period in a cardiac cycle (phase 4) [6]. The RMP is primarily attributable to the conductance of inwardly rectifying K^+ currents and the electrogenic ATP-dependent Na^+-K^+ pump that exports 3 Na^+ ions and imports 2 K^+ ions per ATP [7].

Subsequently, phase 0 represents the fast depolarization period caused by an abrupt increase in Na^+ influx and characterized by the upstroke velocity typically peaking at 130 to 140 mV from the RMP [8]. Membrane repolarization (i.e., the return to negative potentials) follows the upstroke period and includes

phases 1, 2 and 3. A relatively fast transient characterizes phase 1 caused by a decrease in Na^+ influx and an increase in K^+ efflux. Phase 2 consists of the plateau period (still at a depolarized voltage) via a small net current carried by simultaneous Ca^{2+} influx and counteracting K^+ efflux. Lastly, phase 3 represents the large repolarization toward the RMP due to increased K^+ efflux and decreased Ca^{2+} and Na^+ influx. **Figure 1.1** describes the specific channels contributing to AP ionic currents.

Cardiomyocytes do not beat spontaneously, resulting in a stable voltage at the RMP. In contrast, nodal cells exhibit automaticity and undergo gradual membrane potential changes toward positive values, termed spontaneous diastolic depolarization. Upon reaching the threshold potential, a new AP initiates. In healthy conditions, AP duration (APD) determines the effective refractory period (ERP)- the shortest interval required before a new stimulus can elicit a subsequent AP. However, AP shape is not uniform and differs in various cardiac regions. Moreover, there are interspecies differences [9], even when recording from similar locations.

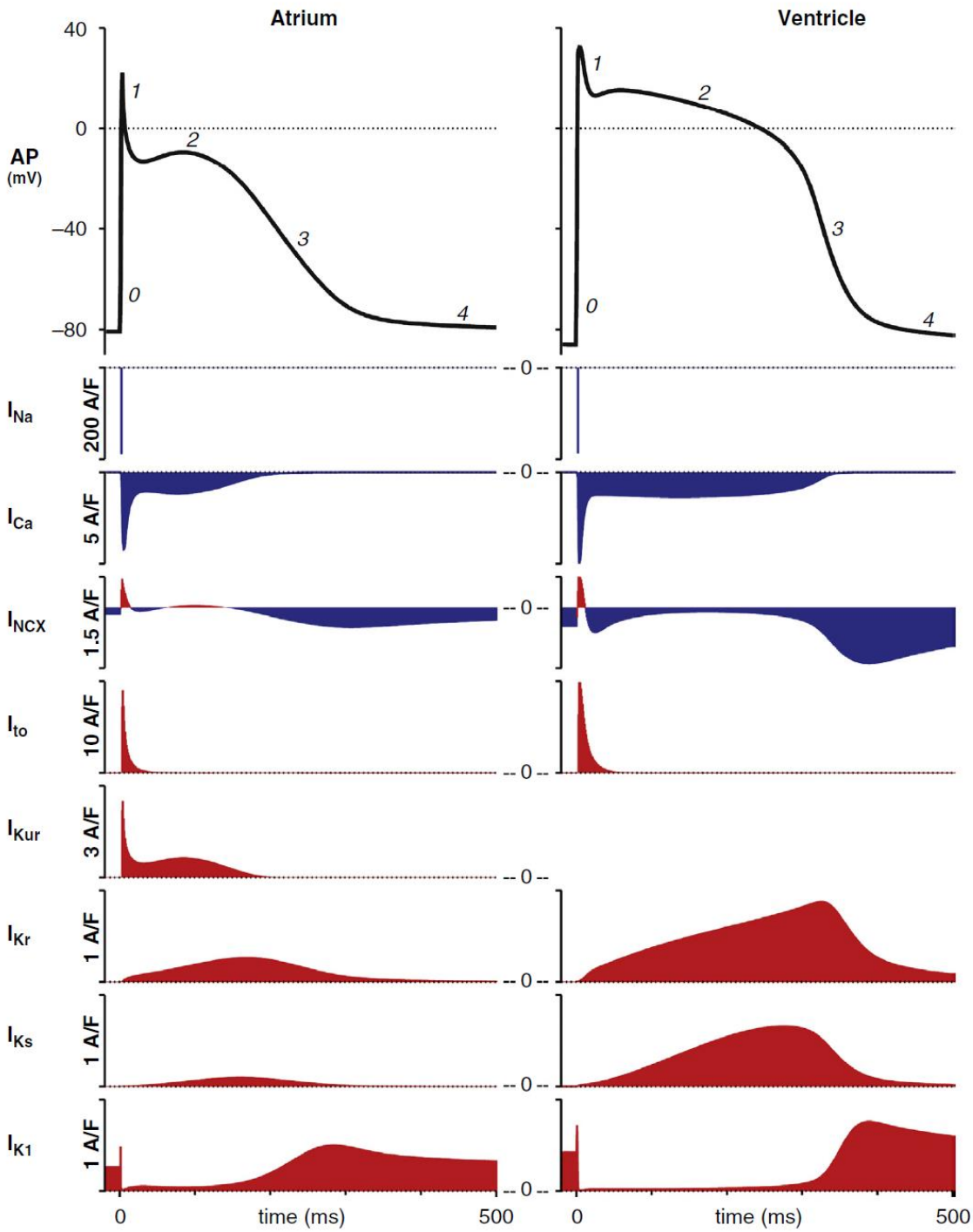

Figure 1.1. Representative cardiac action potential (AP) waveforms. The *top panel* are tracings from atrial (*left*) and ventricular (*right*) human myocytes. The five phases of the AP are labelled above. AP rate of change is directly proportional to the sum of the underlying transmembrane ion currents (*lower panels*). Inward currents (blue) depolarize the membrane, while outward currents (red) repolarize. Compared to an atrial AP, the ventricular AP typically has a higher plateau potential (phase 2), longer duration and a more negative resting membrane potential (phase 4). Copyright©2017, Elsevier Health Sciences [10].

1.3 Cardiac Arrhythmogenesis

As mentioned above, spontaneous diastolic depolarization in sinoatrial nodal cells can provoke a new AP following a preceding AP. Furthermore, ectopic foci, referring to triggered automaticity outside of the sinoatrial node, can yield wavefront-wavetail interactions and *re-enter* previously depolarized tissue when appropriately timed (i.e., kindling). If triggered automaticity and wavefront re-entry occur, this can yield irregular heart rhythms termed arrhythmias [11]. Cardiac arrhythmias demonstrate considerable variability in appearance, type, location (supraventricular or ventricular) and underlying disease, with numerous proposed mechanisms. Arrhythmias can also become exacerbated by pathological conditions, including AF, myocardial infarction (MI), heart failure (HF), genetic diseases or adverse drug reactions [12]. Nonetheless, most result from *triggers* and *modulators* combined with an enhanced pro-arrhythmic *substrate* [11].

1.3.1 Triggered Automaticity

Abnormal myocardial pacing is an established source for arrhythmia initiation [13]. One example is triggered automaticity, which requires a preceding AP for subsequent spontaneous (yet irregular) firing [14]. The temporal relationship between the preceding AP and succeeding depolarization determines whether triggered automaticity is termed early or delayed afterdepolarization. Early afterdepolarization (EAD) occurs prior to termination of the preceding AP during phase 2 or 3 and can arise from APD prolongation. Mechanistically, this results in a period where L-type Ca^{2+} channels have recovered from inactivation and can reopen [15], causing positive voltage oscillations during the plateau (phase 2 EAD) or terminal repolarization (phase 3 EAD). The Luo-Rudy studies [15] also proposed another phase 3 EAD type, resulting from spontaneous Ca^{2+} release during repolarization, which then translates into Na^{+}/Ca^{2+} exchanger (NCX) depolarization [16]. This type of EAD mechanistically resembles delayed afterdepolarizations but differs in timing (i.e., during the AP rather than after). EADs are also rate dependent, with the reactivation-driven EADs occurring predominantly with slow pacing, whereas the release-driven EADs occur with fast pacing [13]. Contrastingly, delayed afterdepolarizations (DADs) involve a depolarizing potential that occurs during diastole after the preceding AP terminates. DADs generally result via Ca^{2+}-sensitive depolarizing currents following overloaded sarcoplasmic reticulum (SR) spontaneous Ca^{2+} release [17]. In particular, when the Ca^{2+}-sensitive conductance from the forward-mode I_{NCX} overcomes the opposing I_{K1} (which attempts to maintain RMP) it activates I_{Na}, triggering depolarization [18]. Together, afterdepolarizations contribute to the formation of ectopic foci and AF initiation.

1.3.2 Re-entry and Conduction Block

Re-entry then occurs when a propagating impulse fails to terminate following initiation and persists due to continuous circuit activity that can re-excite the heart post-refractory period (**Figure 1.2**); it is the electrophysiological mechanism responsible for the majority of clinical arrhythmias. There are three criteria for a re-entrant event: unidirectional conduction block, return to the origin and interruption possibility [8]. In an idealized setting, the re-entry circuit wavelength is a useful concept whereby a wavelength equals the impulse conduction velocity times the refractory period (~APD) and represents the best predictor of arrhythmia inducibility [19,20]. As such, a decreased wavelength (via slowed conduction velocities and refractory periods) promotes re-entry conditions. Moreover, any event which leads to AP heterogeneity in conduction [21] or repolarization [22] predisposes re-entry via unidirectional block [23]. Re-entry and conduction block are also intimately linked as pathological impulse propagation occurs alongside structural abnormalities [24].

Re-entry classification can further divide into anatomical and functional. The former refers to a central block that remains fixed regarding location and circuit speed, and is caused by distinct anatomical structures (i.e., necrotic myocardium, scar tissue or fibrous valve rings). In contrast, functional re-entry is highly complex as central blocking and circuit formation arise from electrophysiological heterogeneity in cell conductivity, refractoriness and excitability. Thus, a wavefront propagating in regions with considerable cell variability can encounter a functional block, rather than anatomical, and form a re-entrant circuit [12]. There are also many concepts of functional re-entries, such as leading circle, spiral rotor wave and multiple wavelet theory. Notably, the multiple wavelet theory was first proposed as the basis of AF, stating that wavefronts do not spontaneously abolish but four to six simultaneous re-entrant wavelets maintain the arrhythmia [25].

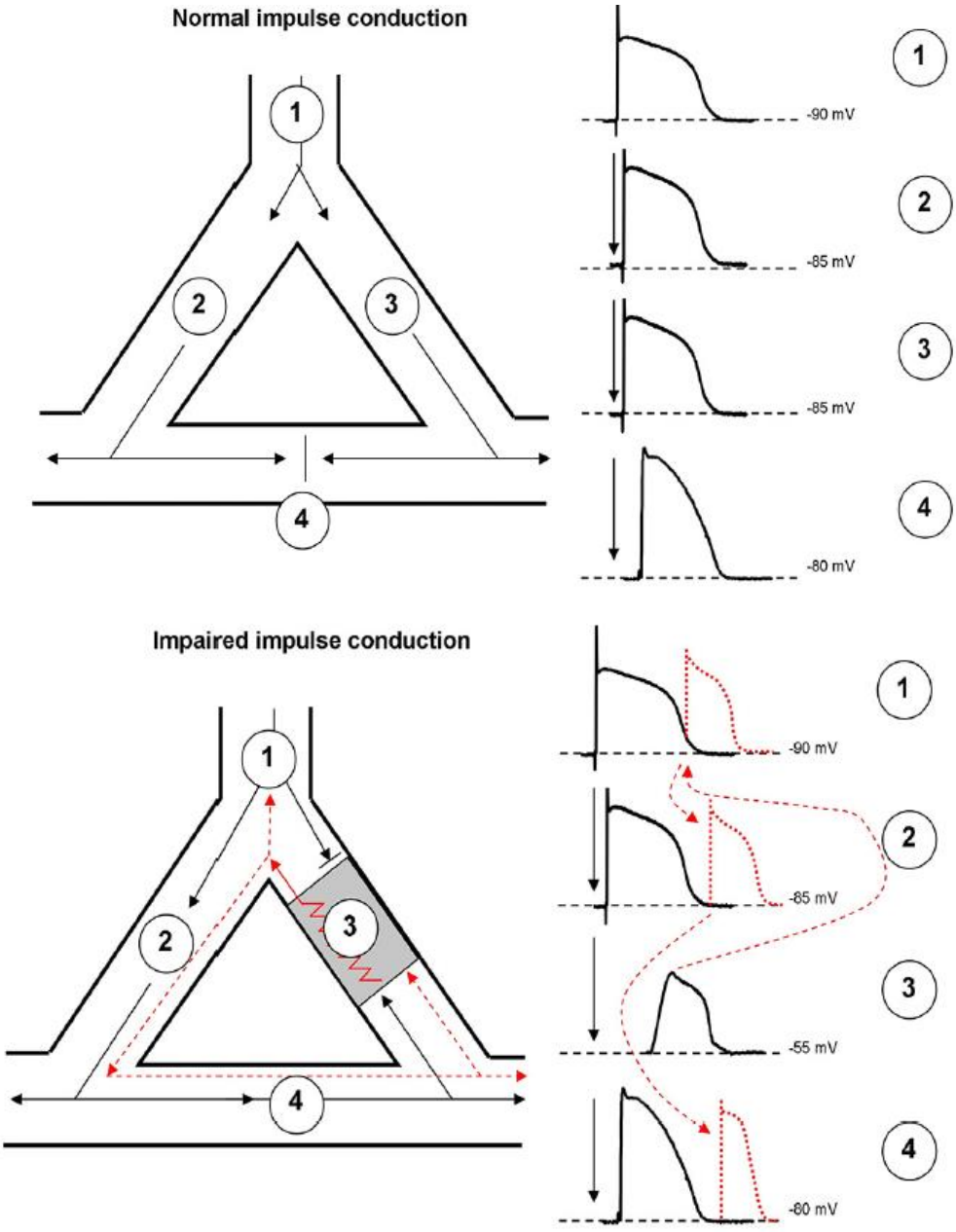

Figure 1.2. A Model of Re-entry. An area of branching cardiac tissue provides separate paths (2 and 3) for impulse propagation. An electrode positioned at each site (1-4) records a single action potential as it travels in the proximal to distal direction. In healthy tissue, impulse conduction is fast, and the effective refractory period (ERP) is relatively long, causing wavefronts to collide at site 4 and propagate distally (*top panel*). However, re-entry can occur with unidirectional block causing retrograde impulses rather than anterograde (*bottom panel*). Unidirectional block can result from non-conducting fibrotic tissue or cellular heterogeneity, whereby the depolarized myocardium at site 3 blocks anterograde conduction, yet the site 4 impulse can slowly propagate retrogradely into the affected region. If propagation from site 4 is slow enough to outlast the previous ERP, the impulse can re-excite the proximal tissue and travel toward both sites 1 and 2 (i.e., *re-enter*), establishing a circus movement. Thus, impulse timing (related to conduction velocity), refractory state (related to ERP), and tissue substrate (condition and length) are critical for re-entry precipitation. Copyright©2021, American Physiological Society [8].

1.3.3 Autonomic Modulation

The final component of arrhythmogenesis involves cardiac autonomic input which can modulate development. The intrinsic system consists of parasympathetic and sympathetic afferent and efferent neuronal circuits, with overlapping influence on cardiac functional regulation [26]. Parasympathetic cardiac innervation is mediated primarily by the vagus nerve which contains 80% afferent fibers and emerges from four nuclei in the medulla oblongata [27]. Preganglionic parasympathetic fibers synapse at the surface or inside the myocardium whereas preganglionic sympathetic fibers course through the spinal intermediolateral column and synapse at para-vertebral extra-cardiac ganglia [27]. Postganglionic fibers then directly innervate the atrial and ventricular myocardium to varying degrees. Moreover, there is an intrinsic intracardiac autonomic nervous system (ICANS). The ICANS can interact with the efferent nerve supply and express multiple neurotransmitters, particularly of parasympathetic cholinergic input to the myocardium [28]. These ICANS neurons are primarily located in 5 groups of atrial ganglionated plexi and may represent local spatial control of cardiac muscle.

Together, the neuro-cardiac feedback system is essential for cardiac parasympathetic and sympathetic tone and ensures well-balanced autonomic input [29]. However, acute hemodynamic stress and chronic CVD promote imbalances that enhance arrhythmia vulnerability. For example, vagal nerve stimulation (VNS) has been associated with arrhythmia onset in experimental [30] and clinical studies [31]. VNS increases arrhythmia risk through acetylcholine (ACh), wherein ACh binds to muscarinic receptors (primarily M2) that inhibit the G protein α-subunit causing decreased sympathetic activation [32]. In addition, ACh shortens repolarization by activating $I_{K,ACh}$ which can also prevent AP firing by inducing hyperpolarization of the cardiac RMP. Interestingly, the pore-forming Kir3.x α-subunits of $I_{K,ACh}$ display atria-specific expression, restricting its effects to the atrial myocardium [33]. APD shortening can then promote arrhythmias by reducing the wavelength, and thus facilitating re-entry [34]. Furthermore, the regional heterogeneity of autonomic activity, rather than elevated VNS alone, can drive arrythmia susceptibility [35].

1.4 Atrial Fibrillation Epidemiology

Having established the fundamentals to arrhythmogenesis, we can now focus on AF and its research significance. In particular, AF incidence continues to rise globally, whereby the Framingham Heart Study (FHS) revealed a 3-fold increase over the last 50 years [36], and the Global Burden of Disease project estimated 46.3 million individuals were living with AF in 2016 [37]. In 2018, lifetime risk then rose to 1 in 3 for white populations over 40 and 1 in 5 for blacks [38]. AF incidence also effects nearly 1 million Canadians [39], 14 million Europeans by 2060 [40] and approximately 72 million Asians by 2050 [41]. However, despite advancements in AF awareness and detection, the global burden remains underestimated

due to asymptomatic cases. Thus, understanding the fundamental causes of AF is critical for future prevention and treatment.

1.4.1 Nonmodifiable Risk Factors: Age, Sex and Race/Ethnicity

Age is the most predictive AF risk factor, with incidence rising sharply after 65 [36]. The population of individuals >65 will also double from 12% in 2010 to 22% by 2040 [42]. As such, chronic subclinical inflammation is a hallmark of biological aging associated with elevated reactive oxygen species, endothelial dysfunction, increased collagen deposition and extracellular matrix changes [42]. Age-dependent left atria (LA) dilation and senile amyloidosis can also alter the myocardial tissue structure [43], and spontaneous Ca^{2+} releases from the SR that is associated with aging can trigger AF [44].

Another common risk factor is sex [45,46]. Despite age-related prevalence being 1.5x greater in men [36], women typically experience worsened symptoms related to a reduced quality of life and adverse outcomes such as strokes [47]. Potential sex-based differences include ion current expressions [48], hormone influence [49] and anatomical variations [50]. Women with AF also demonstrate elevated fibrotic remodelling and inflammation compared to men [42].

Concomitantly, AF prevalence is highest for individuals with European ancestry despite an increased comorbidity burden in black populations. For example, the Multi-Ethnic Study of Atherosclerosis showed that AF incidence was 46-65% lower in Hispanics, Asians and blacks over 65 than non-Hispanic whites [51]. Possible explanations include genetic, socioeconomic and environmental health determinants, including smaller average LA in black populations [52], unfavourable single-nucleotide polymorphisms associated with European ancestry [53] and (or) under detection with worsened healthcare access in predominantly non-white communities. The same paradox exists with ethnic groups originating from India, Pakistan, Nepal, Sri Lanka and Bangladesh, where reduced AF incidence could relate to smaller LA size [54] and ethnic variations in cardiac ion channels [55].

1.4.2 Modifiable AF Risk Factors

Aside from nonmodifiable factors, well-established AF predictors also include hypertension, diabetes mellitus (DM), obstructive sleep apnea, MI, HF, poor lifestyle choices and valve-related disorders. For example, the FHS determined hypertension portended AF risk by 50% in men and 40% in women, ranking fourth after aging, valvular heart disease and HF [56]. However, due to its higher prevalence in the population, affecting 80% of individuals >65 and 26% of adults <45, hypertension accounts for more cases of AF than any other modifiable risk factor [57]. Mechanistically, chronic blood pressure elevations promote structural remodelling in the left cardiac chambers, including profibrotic changes that promote AF development [58]. Moreover, DM is associated with a 1.6-fold increased AF risk

[36] linked to elevated oxidative stress, inflammation and mitochondrial dysfunction, consequently promoting AF in metabolically stressed hearts [59].

Additionally, lifestyle choices play an important role. Multiple studies report a dose-dependent association between smoking and increased AF risk, whereby nicotine can activate profibrotic responses and block K^+ channels contributing to the electroanatomic pathophysiology [60,61]. Long-term excessive alcohol consumption also has direct toxic, inflammatory and oxidative effects on the LA myocardium, causing enlargement and AF substrate formation [36]. Lastly, obesity prevalence continuously increases worldwide and is associated with hypertension, metabolic syndrome, DM, coronary heart disease and obstructive sleep apnea, providing the substrate for AF initiation and perpetuation [62].

However, patients with the most aggressive AF onset are those with volume overload from valve-related disorders, such as aortic regurgitation (AR) [63]. AF is observed in up to 19% of patients with severe AR [64] and AR prevalence in AF patients has almost doubled between 1998 and 2010 [65]. Moreover, in the FHS, valvular heart disease was a significantly more potent AF risk factor in females than males (18% vs. 5%) [66]. As AF and AR are associated with elevated atrial pressures and stretch, the resultant effect is atrial hypertrophy, fibrosis and inflammation that contributes to the arrhythmogenic substrate [63,67]. Our laboratory has also previously established that adverse atrial remodelling and AF vulnerability with AR requires tumour necrosis factor (TNF), a profibrotic and proinflammatory cytokine, providing a mechanistic link between elevated atrial stretch, adverse remodelling and AF susceptibility associated with CVD [68].

1.4.3 AF Comorbidities and Prognosis Impact

Although AF patients generally survive the arrhythmia, the accompanying comorbidities and complications, including HF, MI, stroke, dementia and possibly cancer, considerably increase mortality risk. HF and AF appear to have a bidirectional relationship, whereby 37% of the FHS participants with new AF onset had previously been diagnosed with HF [36]. Vice versa, 57% of participants with HF had pre-existing AF. The most common pathological feature for both surrounds LA vulnerability; AF episodes involve an irregular heart rate (HR), shortened diastole and unsynchronized atrial contractions, causing reduced cardiac output and contributing to HF development [42]. Long-term, both can result in cardiomyopathy that promotes LV dysfunction and can increase the presence of diffuse fibrosis and cardiomyocyte apoptosis [69]. MI and AF are also closely associated, whereby fibrillatory episodes may directly cause type 2 MI through insufficient coronary perfusion [70]. Most notably, AF is associated with a 4 to 5-fold increased stroke risk, such that thrombus formation and stroke result from AF-mediated atrial fibrosis [71], enlargement [72] and alterations in blood flow [67].

1.5 Atrial Fibrillation Pathogenesis

Accepting the multiple wavelet theory, ectopic foci from the pulmonary veins and coronary sinus myocardium are widely recognized as the site for AF initiation by interrupting sinus rhythm and promoting re-entrant events when kindled [8]. As a result, cardiac excitability will vary from cell-to-cell during fibrillation: some fibres are refractory, others almost fully recovered and few conduct impulses at slow velocities. Consequently, APs propagate in multiple wavelengths, re-enter excitable tissue and become self-sustaining. Studies regarding chronic AF patients and animal models also show significantly shorter and more triangular-shaped atrial APs than those in sinus rhythm [11,73]. Furthermore, atrial extrasystoles or electrical stimulation can induce AF in remodelled atria, with prolonged and frequent episodes causing more pronounced remodelling and increased AF vulnerability such that *AF begets AF* [74].

1.5.1 Electrical Remodelling

AF-related electrical remodelling is highly complex, yet the most well-established phenomenon involves the downregulation of L-type Ca^{2+} channels along with its corresponding mRNA and proteins. I_{Ca} reductions are understood to occur irrespective of the underlying AF cause [11] and act as the primary mechanism for APD shortening in chronic AF. Other studies have also observed Kir2.1 upregulation, the main channel protein of I_{K1} [75], along with constitutively active components of the $I_{K,ACh}$ channel (Kir3.1/3.4) that typically has weak currents in sinus rhythm [76]. Moreover, a recent study indicated that cholinergic M1 receptors are simultaneously upregulated, further activating $I_{K,Ach}$ and thereby shortening atrial repolarization [77]. I_{to} downregulation has also been reported in chronic AF [11], as reflected in the widening of early atrial repolarization. Lastly, abnormal intracellular Ca^{2+} handling seen in severe AF patients can increase the open probability of the SR ryanodine receptors, resulting in more frequent Ca^{2+} release from the intracellular store [78]. Increased cytosolic Ca^{2+} can then enhance the frequency of spontaneous depolarization via I_{NCX}, contributing to triggered activity in AF [79].

Connexins (Cx)- proteins that form hemichannels and ensure functional syncytium at intercalated disks- can also become dysfunctional with AF, including abnormalities in expression, function and localization [80]. For example, Cx43 and Cx40 are either ubiquitously expressed in cardiac tissue or primarily found in the atria, respectively. Atrial tissues of paroxysmal AF patients show reduced Cx40 distribution, while persistent AF patients demonstrate severe reductions in Cx40 immunostaining [81]. Goats with AF-induced atrial remodelling also demonstrate considerable increases in Cx40 distribution heterogeneity and relocalization to the lateral margins [82]. Together, these alternations can impair electrical propagation and promote re-entry circuits.

1.5.2 Structural Remodelling

Although AF is fundamentally an electrical phenomenon, the atria of patients also demonstrate profound changes in tissue structure, characterized primarily by hypertrophy [83], fibrosis [84] and inflammation [85], collectively promoting AF.

1.5.2.1 Atrial Hypertrophy

Atrial hypertrophy is often considered a precursor to AF onset and develops in response to pressure and volume overload from physiological stimuli, such as exercise and pregnancy, or pathological stimuli, including left ventricular dysfunction, systemic hypertension and valvular disease [67]. While acute atrial overload can cause transient electrophysiological changes, chronic exposure leads to sustained atrial stretch [86] that can exacerbate AF risk [87]. For instance, Fraser and Turner [88] reported the degree of atrial dilation correlated with AF incidence, and Henry *et al*. [89] showed that AF was rare (3%) when the left atrial diameter was less than 40 mm, but common (54%) when exceeding 40 mm in patients with valvular disease. The FHS also revealed every 5 mm elevation in LA diameter increased AF risk by 39% [56] and LA size is reported to predict AF, even following age, sex and CVD adjustment [90].

The effect of acute and chronic overload on AF vulnerability has also been studied in several animal models. In Langendorff-perfused rabbit hearts, acute increases in atrial pressure caused ERP and APD shortening leading to increased AF inducibility that dissipated within 3 minutes following pressure release [91]. Cellularly, stretch-activated ion channels (SACs) have been implicated in the cardiomyocyte mechanoelectrical response to overload and is linked to conduction slowing [92], heterogeneity [93] and increased pulmonary vein activation rates [94], providing the optimal substrate for re-entrant events. Moreover, animal models have demonstrated that chronic atrial overload increases AF stability through increased conduction heterogeneity, rather than AERP shortening [95], linked to fibrosis [96] and possibly immune remodelling [97]. Moreover, due to high atrial compliance [98], the response to chronic overload is thought to disproportionately effect the atria compared to the ventricles.

1.5.2.2 Atrial Fibrosis

In this regard, cardiac fibrosis results from an accumulation of the extracellular matrix (ECM)- the three-dimensional elastic network of collagen fibers and non-structural proteins that embed cardiomyocytes, fibroblasts, immune cells and vessels- i.e., the scaffold of the healthy heart. Atrial fibrosis is observed in biopsies from AF patients [99] and classified as a primary determinant in AF development and reoccurrence [84]. Notably, atrial fibrosis is reported to have limited reversibility [100], making preventative strategies crucial.

In the normal myocardium, perimysial fibrous tissue separates myocyte bundles, while endomysial fibrous tissue surrounds individual myocytes. These structures are composed of type I and type III collagen, serving primarily to reinforce myocardial stiffness [101] and coordinate contraction [102]. In contrast, excessive fibrotic remodelling is characterized by an increase in fiber separation via elevated deposition of type I collagen bundles [103]. Historically, there are two forms of cardiac fibrosis: reparative, also called replacement fibrosis, and reactive, also called diffuse myocardial fibrosis (**Figure 1.3 top panel**). Reparative fibrosis occurs following tissue damage and cardiomyocyte death as evidenced through profound collagen deposition *replacing* the myocardium [104]. During the acute injury phase, inhibition of the reparative fibrotic pathway leads to local rupture and increased mortality [105]. In contrast, reactive fibrosis describes diffuse collagen deposition and cross-linking in pericapsular and interstitial areas that occur in chronic cardiac conditions [106].

To understand fibrosis-related AF pathology, anisotropic myocardial conduction must first be defined. Wavefront propagation requires a cell supplying adequate current to depolarize itself and charge the neighbouring tissue capacitance. Normal atrial conduction exhibits uniform anisotropy, wherein propagation occurs rapidly in one direction (longitudinal) and slower in another (transverse). Discontinuities in the cellular interconnections increase unidirectional conduction slowing caused by increased membrane resistance between cells [107] (**Figure 1.3 bottom panel**). For example, interstitial fibrosis predominantly separates longitudinal cellular bundles, resulting in decreased transverse conduction [108]. The loss of side-to-side fiber connection then causes microstructural disturbances that result in dissociated, non-uniform conduction with longer propagation periods and complex "zig-zag" patterns due to the alternative route the waves must travel [109]. Together, these changes can lead to unidirectional conduction block, creating the excitable gap required for a re-entrant circuit [7].

Cellularly, cardiac fibrosis can involve the activation of numerous signalling pathways, including the renin-angiotensin-aldosterone system (RAAS) and tumour transforming growth factor β (TGF- β) [110]. In brief, RAAS primarily controls haemodynamic stability through regulation of fluid volume, salt balance and blood pressure. Angiotensin II (Ang II), a component of RAAS, interacts with the type 1 angiotensin receptor (AT1-R) and stimulates mitogen-activated protein kinase, regulating gene transcription of factors involved in elevated ECM protein production [111]. Additionally, TGF-β is one of the strongest stimulators of collagen synthesis by cardiac fibroblasts and exerts its effect through binding to specific receptors expressed on all cell types, causing a phosphorylation cascade in which the inactive Smad 2 and 3 proteins form a Smad complex [112]. Smad complexes then translocate to the cell nucleus and induces fibrosis-related gene expression. Notably, murine models have demonstrated that increased and prolonged TGF-β expression leads to atrial-specific elevated fibrosis content that does not extend to the ventricles [113].

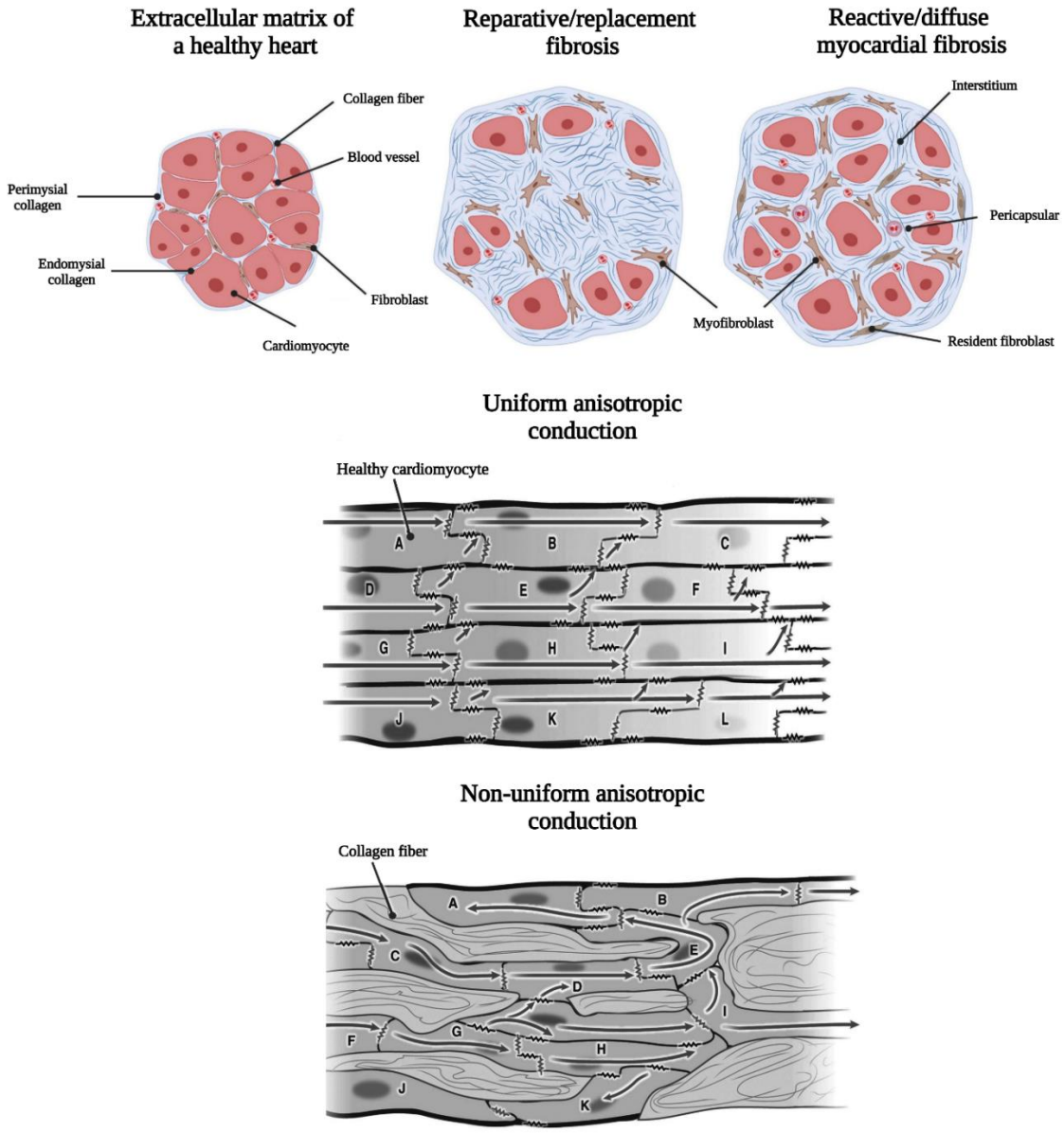

Figure 1.3. Cardiac Fibrosis Types and the Effects on Anisotropic Conduction. There are two fibrotic tissue types in comparison to the extracellular matrix in a healthy heart (*top left*). Replacement/reparative fibrosis is classified as collagen-based scarring that *replaces* dying cardiomyocytes (*top middle*). In contrast, reactive/diffuse myocardial fibrosis manifests as cross-linked collagen deposition in pericapsular and interstitial areas (*top right*). Both types alter cardiac anisotropic conduction, but to varying degrees. As such, uniform anisotropic conduction in a healthy muscle bundle demonstrates longitudinal and transverse conduction between cells, as indicated by the arrows, and is facilitated by gap junctions (*middle panel*). Due to the naturally elongated shape of cardiomyocytes, an impulse propagating in the transverse direction will encounter more gap junctions (i.e., resistors) compared to an equivalent distance in the longitudinal direction, slowing conduction. Conversely, non-uniform anisotropic conduction occurs when there is increased connective tissue that disrupts connections such that propagation occurs only where myocardial regions can penetrate the large amount of collagen (*bottom panel*). In the above example, transverse conduction is considerably impacted. Each cardiomyocyte bundle in the bottom panels contains 12 cells labelled A to L for reference. Figure based on Schimmel *et al*. [106] and Anter [114] and assembled using BioRender.

1.5.2.3 Atrial Inflammation

AF precipitation and progression also involves considerable immune remodelling regarding cell recruitment and activation [115], yet the precise mechanisms remain speculative. Some studies suggest that inflammation-related conditions, including hypertension, obesity and obstructive sleep apnea, can increase the release of pathogen-associated molecular patterns and (or) damage-associated molecular patterns, invoking an immune response [116]. For instance, studies have reported markedly increased CD45+ infiltration, a common marker of all inflammatory cells, in the atria of AF patients compared to those with sinus rhythm [117]. Additionally, atrial rapid and irregular electrical activity is reported to cause intracellular Ca^{2+} overload and oxidative stress, promoting resident immune cell activation and cytokine release [118]. For example, inflammatory cytokine factors, including C-reactive protein (CRP), TNF, interleukin (IL) IL-1β, IL-6 and soluble TNF receptors are commonly released during AF [119]. Moreover, these cytokines can promote changes in numerous cardiac cell types, playing an important role in the overall biochemical and structural changes observed with AF [120]. In particular, animal studies have demonstrated changed proportions of cardiac immune cells, primarily with increased macrophages, during AF onset and maintenance [121]. Moreover, CRP received attention as an inflammatory marker and several studies have shown a positive correlation between CRP and AF, arrhythmia duration and LA dimensions [121,122]. Additionally, TNF can disrupt the intracellular Ca^{2+} homeostasis in atrial myocytes by repressing SR Ca-ATPases (SERCA2a) expression [124] and promoting atrial fibrosis through TGF-β signalling activation (Liew *et al*., 2013). TNF also promotes contractile dysfunction, fibroblast activity and cardiomyocyte hypertrophy [7,124] wherein TNF LA levels directly correlated with LA size in AF patients [126]. Macrophages are also major sources of TGF-β1 during the fibrotic process and can induce fibroblast transdifferentiation to myofibroblasts [127]. Thus, there seems to be a positive feedback loop between immune and electrophysiological remodelling, which is pivotal in AF substrate development and maintenance.

1.6 The Relationship Between Physical Activity, Excessive Endurance Training and AF

Regular physical activity (PA) is essential to a healthy lifestyle and provides numerous benefits, including improved energy economy, mental health and overall quality of life [128]. As such, most international guidelines recommend 150 minutes of moderate exercise or 75 minutes of vigorous PA per week [129]. These guidelines not only lower the risk for metabolic disorders [130], selected cancers [131] and CVD [132], but also independently reduce AF burden with a 45% lower all-cause mortality risk compared to inactive patients [133]. Nevertheless, recent studies have reported a dichotomous effect of exercise with the age-dependent incidence of AF, wherein risk is greater for individuals partaking in

excessive and strenuous exercise, particularly with endurance sports such as swimming, cycling, running and cross-country skiing [134]. Moreover, numerous studies suggest that the relationship between endurance exercise and AF risk is not linear, but rather J-shaped [135] (**Figure 1.4**).

Coelho and colleagues [136] were the first to document the association between endurance training and AF, whereby 26% of athletes presented with paroxysmal AF and had reproducible arrhythmia inducibility with programmed stimulation and exercise. Mont *et al*. [137] then conducted a retrospective analysis by reviewing lone AF patient records- a subclassification previously used to describe AF without pre-existing comorbidities- and observed 63% (44/70) engaged in long-term sports practice compared to the general population. In agreement, Myrstad *et al*. [138] found that older Norwegian men with a history of endurance sport practice had elevated AF incidence to a degree comparable with cardiovascular-diseased patients. Critically, as more and more professional athletes engage in extreme endurance training for up to 4-6 hours each day, 6 days per week, for several months without sufficient (if any) scheduled days of appropriate recovery [139], understanding the role of exercise dose in cardiac responses and AF susceptibility is crucial.

Notably, the relationship between excessive endurance training and AF appears to depend on exercise parameters, including intensity, duration, frequency and cumulative dose. For example, Gerche and Schmied [140] concluded that low-intensity exercise reduced AF risk, whereas moderate and high-intensity gradually increased AF prevalence. Andersen *et al*. [141] then assessed arrhythmia prevalence in cross-country skiers (n>52,000), revealing a positive association between AF and the number of completed races (i.e., total cumulative dose), increasing with prolonged race durations. Another study also found that >1500 total hours of aerobic-dominated exercise caused increased AF risk [142] and Aizer *et al*. [143] identified that AF incidence correlated with the frequency of jogging bouts per week. Lastly, Jin *et al*. [144] found that >17 MET hours per week demonstrated increased AF prevalence. Together, available data thus suggests that the type (endurance), intensity, duration, frequency and total dose of PA may play a crucial role in AF precipitation and maintenance.

Also important to note is that although there is some controversy surrounding the relationship between professional endurance athletes and increased AF risk, with studies reporting conflicting results [144,145], these differences primarily arise from research design [147]: most are case-controlled, possess poor methodological quality (not prospective and randomized) and characterized by considerable heterogeneity in PA reporting, involving mainly questionnaires. Thus, in this present study, a swimming mouse model will be used whereby workload is internally quantified through oxygen consumption (VO_2), with the primary aim to observe whether endurance training predisposes AF while determining its dependability on varying exercise dose.

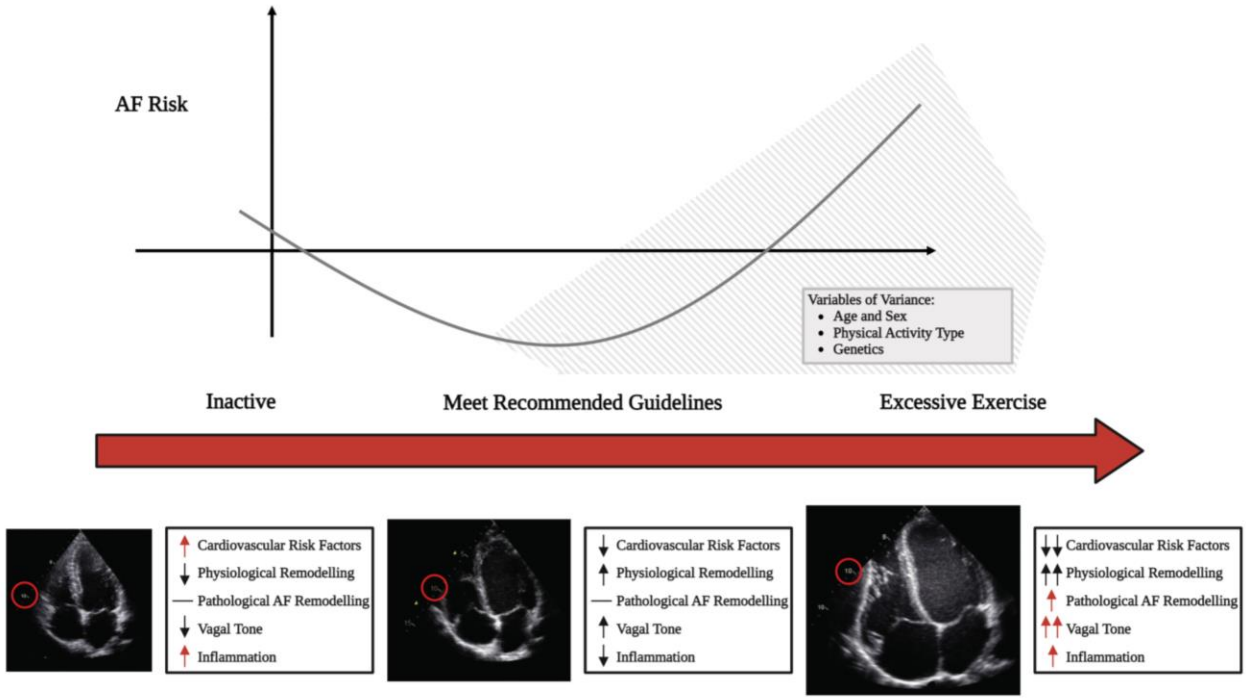

Figure 1.4. J-shaped Dose-Response Curve Between Atrial Fibrillation Risk and Physical Activity. Beyond guideline amounts (150 minutes of moderate-intensity or 75 minutes of vigorous-intensity per week), excessive exercise levels (e.g., vigorous endurance training) can result in an increased atrial fibrillation (AF) risk. The echocardiogram examples demonstrate the progressive cardiac remodelling from a typical sedentary subject (*left*), leisure-time athlete (*middle*) and professional cyclist (*right*). The physiological benefits of regular, moderate exercise (*middle*) and the proposed pathological mechanisms of inactivity (*left*) and excessive exercise (*right*) are also presented. The shaded area denotes the variance in AF risk caused by individual differences in age, sex, type of physical activity and genetic predisposition. Note, there are also research caveats relating to sample size, a variety of trial designs and small participant numbers at the highest of activity levels (*far right*). Figure based on Buckley *et al*. [135] and created using BioRender. Copyright©2013, Oxford University Press regarding the echocardiogram images [140].

1.7 Potential AF Pathophysiology in Endurance Athletes

Characteristics of AF in athletes often include patients <60 that excessively engaged in endurance sports and do not exhibit the common modifiable risk factors [148]. However, the underlying pathological mechanisms of AF in trained athletes remain unclear. Regular exercise promotes structural, functional and electrical remodelling, often termed the *athlete's heart* [149], and the phenotypic changes, and possible maladaptive alterations proposed in the literature, will now be discussed.

1.7.1 The Athlete's Heart Phenotype

Cardiac exercise adaptations have been systematically defined and are conditioning-type dependent: endurance training (sometimes described as isotonic, dynamic or aerobic) includes activities such as marathon running and swimming, while strength training (also referred to as isometric, static or anaerobic) includes weightlifting and wrestling [150]. Furthermore, there are combined endurance and

strength-related activities, including cycling and rowing, with most athletic disciplines possessing some overlap in conditioning modes [151]. Nonetheless, endurance training is associated with sustained elevations in cardiac output (CO) and VO_2, independent of increased peripheral vascular resistance [152]. Moreover, VO_2 is intrinsically dependent on CO: the product of stroke volume (SV) and HR. With each exercise bout, volume overload imposes substantial physiological and metabolic demand on the heart, causing transient modulation of CO [153] while chronically prompting complex dose-dependent adaptations of the cardiovascular system [153,154].

1.7.1.1 Cardiac Chamber Morphology and Function

Cardiac dimensional alterations associated with athletic endurance training are well documented using echocardiographic and magnetic resonance imaging [156]. The first study investigating the athlete heart was by Morganroth *et al*. [157], who described endurance athletes possessing eccentric LV hypertrophy, characterized by an increased LV internal dimension and mass, with minor changes in wall thickness. Similarly, right ventricular (RV) remodelling is documented in endurance athletes [158] and demonstrates an increased RV:LV ratio [159], supporting the concept that the right chambers are more sensitive to volume overload due to lower resting pressures and thinner walls [160]. Concomitantly, functional changes also occur, characterized by reductions in LV ejection fraction (EF) [161] and fractional shortening (FS) [161,162] at rest. The observation of depressed LV function in these athletes is a geometric consequence of ventricular dilation with concomitant eccentric hypertrophy [163]. As such, reduced preload states (such as rest) will demonstrate misleading impaired function as the LV is adapted to high CO with chronic aerobic exercise. Thus, although ventricular function may appear depressed *at rest*, LV dynamics are instead markedly improved in trained athletes, made evident *during* exercise bouts. Work by Fagard *et al*. [152] supports this interpretation as they studied marathon runners completing cycling ergometry and demonstrated elevated FS during cycling with faster ventricular relaxation than non-athletes. These observations also contribute to the higher SV and contractile reserves commonly seen in trained athletes during exercise [152]. To determine whether similar ventricular adaptations occur in swim-trained mice, this study will utilize echocardiography, ventricular weights normalized to body weight and tibia length as well as non-invasive hemodynamics with dobutamine to assess ventricular morphology and function.

Strikingly, chamber enlargement with endurance training is not ventricle-specific but extends to the atria. In fact, LA enlargement is the echocardiographic parameter most associated with AF risk in athletes [164] and is supported by similar findings in hypertensive, obese and HF patients [165]. In this regard, Hauser *et al*. [166] first described atrial enlargement in a small group of marathon runners, with similar increases subsequently observed in veteran athletes [167]. Pelliccia *et al*. [168] then demonstrated LA enlargement in a sizeable athlete population (n=1777), and Oxborough *et al*. [159] identified a large,

indexed LA volume in 90 of the 102 endurance-trained participants, with values well above the American Society of Echocardiography's normal range [169].

Mechanistically, there are considerable atrial volume challenges during strenuous endurance exercise (i.e., in response to hemodynamic and metabolic demand) that can activate the aforementioned remodelling pathways related to atrial stretch and hypertrophy [170]. Interestingly, ventricular dimensions in veteran athletes return to typical age-associated ranges years after training cessation, yet LA hypertrophy appears to persist [167] and contribute to AF precipitation by providing an extended path length that promotes re-entry. Thus, atrial stretch to volume overload may provide another mechanism for increased AF vulnerability in endurance athletes. Due to the exceedingly difficult task of atrial echocardiographic imaging in mice, this study will use atrial weight relative to body weight and tibia length as an index of hypertrophy to assess its role in training-induced AF risk.

1.7.1.2 Sinus Bradycardia

Similar to cardiac morphology and function, common ECG patterns are observed with endurance training, including sinus bradycardia and conduction delays [171]. Specifically, sinus bradycardia, or reduced resting HR <60 bpm, occurs in up to 90% of elite endurance athletes [172], and is suggested to involve increased parasympathetic and possibly decreased sympathetic tone [147]. Moreover, these reductions are thought to persist for up to 10 years following athletic training termination [173].

Enhanced vagal tone can modulate AF risk based on findings that sleeping and eating represent the most common periods for arrhythmia events in athletes (i.e., when the parasympathetic system is highly active) [173,174]. Mechanistically, increased vagal activity can shorten the atrial refractory period and enhance spatially heterogeneous APDs through activation of $I_{K,Ach}$ channels, thereby reducing the excitation wavelength and facilitating re-entry [7]. Furthermore, there is an atrial gradient of $I_{K,ACh}$ current that, when combined with the heterogeneous distribution of parasympathetic ganglia, may augment the dispersion of atrial refractoriness [176]. In addition to increased vagal tone, some pharmacological studies also suggest an intrinsic slowing of the SAN firing rate in athletes [177]. However, as previously mentioned, $I_{K,ACh}$ can hyperpolarize the SAN, which decreases the pacemaker pre-potential slope and may explain those findings [176]. Thus, our present study will assess autonomic tone and HR slowing using atropine and propranolol administration to pharmacologically block cardiac autonomic modulation, with HRs derived from surface electrocardiography. If autonomics mediate bradycardia, the pharmacological blockade will alleviate HR slowing. AF inducibility will also be assessed in the presence and absence of parasympathetic inhibition using atropine to determine the role of vagal tone.

1.7.2 Skeletal Muscle Mitochondrial Adaptations

Coinciding with cardiac remodelling observed following endurance training, skeletal muscle adaptations also occur, and these muscles together account for 85-95% of the CO distribution and oxygen delivery during maximal exercise effort [178]. In this regard, skeletal muscle mitochondria are responsible for oxidizing nutrient substrates and generating ATP in working muscle to meet the energetic demands of exercise. The efficiency of skeletal muscle function and overall physical performance is thus determined by mitochondrial function (i.e., the culmination of content, structure and respiration) [179]. In the 1960s, John Holloszy pioneered the concept of exercise-induced mitochondrial biogenesis [180], whereby training adaptations can elicit steady-state improvements in protein abundance [181], mitochondrial content [182] and functional adjustments such as enhanced mitochondrial respiratory [183]. Moreover, training promotes several highly coordinated adaptive processes, including mitochondrial fission and fusion [184], involving the degradation of damaged and dysfunctional mitochondria (i.e., mitophagy) for improved overall quality [185]. In this regard, there is some evidence to suggest that excessive exercise training in humans causes mitochondrial impairment effecting metabolic activity [186]. Thus, determining the relationship between exercise dose and skeletal muscle mitochondrial remodelling, would provide important insights into changes that occur outside of cardiac tissue in response to prolonged strenuous exercise, and will be assessed by measuring cytochrome c oxidase (COX) activity in the tibialis anterior and gastrocnemius muscle.

1.7.3 Atrial Fibrosis and Inflammation

In contrast to the predominantly beneficial adaptations of endurance sports mentioned above, strenuous exercise has also been linked to reductions in cardiac function and the release of biomarkers associated with cardiomyocyte stress with exhaustive bouts. For example, during extreme endurance exercise (such as participating in ultramarathons), considerable cardiac work is performed to cope with the increasing demands for oxygen and nutrients, along with elevations in core body temperature, altered pH, increased catecholamines, mechanical work and elevated reactive oxygen species. As such, human studies [187] and meta-analyses [188] have found elevated cardiac troponin I and T (cTnI and cTnT) levels following prolonged exercise, which represent markers of cellular damage [188]. Although cTn kinetics post-exercise remain considerably smaller than those seen following myocardial infarction [187], these changes could suggest that unlike the adaptive responses of the athlete's heart phenotype (ventricular dilation, hypertrophy and bradycardia), there may also be adverse responses with chronic strenuous exercise.

Over the last decade, fibrosis and inflammation were speculated to contribute to AF in athletes, as shown in both rodent models and humans [85]. For example, our laboratory previously observed increased

atrial collagen deposition in 6 week swim-trained mice that behaved as AF substrate [189]. Benito *et al*. [190] similarly found evidence of myocardial fibrosis in rodents undergoing high volumes of endurance training, and human studies, although limited, have detected increased atrial fibrosis in elite athletes by late gadolinium-enhancement magnetic resonance imaging [191]. In this study, both atrial and ventricular collagen deposition will be quantified using a histological approach of staining cardiac sections with picrosirius red to assess the role of fibrosis in athletes developing AF.

Furthermore, given the close relationship between atrial fibrosis and inflammation, the immune response to chronic strenuous exercise may also contribute to AF precipitation in endurance athletes. Each exercise bout leads to a robust inflammatory response characterized by leukocyte mobilization and increased circulating inflammatory mediators produced by immune cells or active muscle tissue directly [192]. Depending on the type, duration and familiarity of the exercise [192,193], the release of proinflammatory cytokines (TNF, IL-1β and IL-6) and subsequent anti-inflammatory or regulatory cytokines (IL-4, IL-10 and IL-13) will vary. In this regard, regular PA is regarded as a long-term anti-inflammatory therapy, after the acute increases in proinflammatory cytokines are resolved [195], and may be vital following exercise as apart of the reparative and adaptative response [196]. However, high-intensity and prolonged exercise bouts appear to exacerbate this response, somewhat resembling a pathological state (or a more extreme manifestation of a physiological response). For example, white blood cells are reported to increase immediately after intensive exercise (>75% VO_{2max}), without alteration following moderate exercise [197]. Interestingly, our laboratory previously found no change in mast cells or neutrophils acutely (2 days) or after 6 weeks of swim training mice, whereas Mac-3-positive macrophage/monocyte numbers were significantly increased after 6 weeks [189]. In particular, macrophages are known to play a critical role in tissue repair by releasing proinflammatory cytokines and growth factors, such as TNF, fibroblast growth factor (FGF) and TGFβ1 [198], with mechanical stretch reported to cause atrial macrophage infiltration in rodent models [199]. Importantly, Ulven *et al*. [200] found that pro-inflammatory TNF was only stimulated by intense endurance exercise lasting more than 1 hour, and Moldoveanu *et al*. [194] reported increased TNF after three 2-3 hour moderate bouts of cycling, yet no change was found after a single 45 min moderate bout or one 5 min intense bout. These findings suggest duration plays an important role in regulating the immune response TNF release. Here, inflammation will be assessed using an immunohistochemical approach by staining cardiac sections with F4-80, a known marker for macrophages.

1.8 Synopsis and Hypothesis

Endurance exercise imposes volume overload on cardiac chambers, while longstanding training prompts complex adaptations, including physiological ventricular hypertrophy, sinus bradycardia and enhanced performance [201]. However, it remains disputable whether excessive exercise results in adverse remodelling that increase AF risk [136,152]. Regardless of its cause, atrial changes associated with AF

appear to include enlargement, electrophysiological dysregulation, inflammation and fibrosis [7], collectively termed remodelling. Nonetheless, many knowledge gaps remain concerning the specific pathophysiology for AF in endurance athletes and whether different training parameters variably influence vulnerability. Several studies have assessed AF dependence on training intensity [140], frequency [143], duration [202], cumulative lifetime dose [141] and (or) cardiorespiratory fitness [203]. However, a critical limitation involves the reliance on subjective self-reporting, making the conclusions controversial [147]. Accordingly, this study sought to directly investigate training-induced cardiac responses and AF risk using a mouse swim model, particularly regarding the effects of varying daily exercise dose.

I hypothesize that endurance training and AF vulnerability demonstrate a dose-dependent relationship, and the adverse remodelling underlying AF in swim-trained mice will depend on daily exercise dose.

Based on this hypothesis, the objectives of this study were:

1) Develop a means for exercise quantification in swim mice.
2) Characterize the dose-dependent relationship between daily training and AF.
3) Investigate the pathophysiological mechanisms underlying AF in swim-trained mice who exercised at variable daily doses.

Technical Contributions Acknowledgement

I acknowledge the following individuals for contributing to my M.Sc. project:

1. **Nazar Polidovitch**

Apart from creating the swim apparatuses together, Nazar performed echocardiogram measurements and invasive hemodynamics. He also conducted some morphological and surface electrocardiogram assessments. Moreover, Nazar trained me on most techniques employed, provided technical consultation and assisted with some invigilating swims.

2. **Dr. Robert Lakin**

Dr. Lakin performed the *in vivo* electrophysiological studies, including the refractory period measurements and AF inducibility data. He also generated some of the echocardiograms and provided technical consultation.

3. **Ryan Debi**

Ryan performed some of the invasive hemodynamics assessments and occasionally assisted with invigilating swims.

4. **Victoria C. Sanfrancesco**

Victoria performed the mitochondrial content assessments on the gastrocnemius and tibialis anterior muscles, investigating COX enzyme activity.

5. **Jhonny Mendoza, Elana Dhaigham and Jarrett Chow**

Jhonny, Elana and Jarrett assisted with swimming the mice.

I was responsible for developing the exercise apparatuses, organizing endpoint measurements and predominantly swam the mice. I collected VO_2 measurements during swims (for exercise quantification) and performed histological/immunohistochemical assessments. I also generated most morphometrical and surface electrocardiogram data. Lastly, I was responsible for data analysis and generated all figures and tables.

Chapter 2: Materials and Methods

2.1 Experimental animals

CD1 male mice at six weeks of age (Charles River) were randomly assigned into four groups (sedentary controls or one of three swim groups). All mice were housed in identical environments and consumed the same *ad-lib* diets. All experimental procedures conformed to the Canadian Council on Animal Care standards.

2.2 Swim Training Protocol

Swim training took place in tanks (3.1 gallons, 30 cm diameter and 16.5 cm water depth) filled with thermoneutral water (30-32°C) [204] and equipped with submersible pumps that generate circular currents (**Figure 2.1**). To quantify work and effort associated with daily exercise, we measured O_2 consumption rates (i.e., VO_2) during swimming. Since CD1 mice intrinsically swim against water currents, we initially attempted to vary exercise dose by systematically altering flow rates from 10-20 L/min in the swim tanks. Unfortunately, our VO_2 measurements revealed that after mice swim for greater than ~15 minutes, they self-regulate their swimming effort by intermittently floating or moving toward the centre of the tank where the current is weaker (**Figure 3.1**). **Figure 3.2** demonstrates features of this self-regulation behaviour during a typical swim recording from the first and last week of training. After placement in the water, the VO_2 magnitudes rise quickly and typically peak around 9,500 L of O_2/kg/hr, followed by a decline to a steady state level of 8,600 L of O_2/kg/hr for the remaining duration of the swim during week 1. Interestingly, even with self-regulation, there appears to be some evidence of fatigue based on additional drops in VO_2 beyond 90 minutes which predominately resolves by the final week of training. Also note the rise in achievable VO_2 values for each group by the last week of swim training, possibly suggestive of exercise adaptation and observationally coinciding with improved engagement with the current throughout the swim.

Nonetheless, due to the difficulty in varying exercise intensity, we elected to study the effects of exercise dose on cardiac responses by altering the daily durations of the swims. Since we had previously shown that swimming mice for 90 minutes twice daily resulted in atrial-specific changes [189], we swam mice for either 120, 180 or 240 minutes per day (divided into two daily swims). The two daily swims were separated by a 4-hour rest period. Before exercise mice begin training, each group was acclimatized to the apparatus by completing an initial 30 minute swim session that increased by 10 minutes each day and progressed variably until reaching the target duration (**Table 2.1**). After acclimatization, mice swam twice daily for varying weeks so that each mouse achieved the same cumulative dose of exercise, as determined by the total O_2 consumed (i.e., ~695 L of O_2/kg) during swimming. As a result, mice exercising for 120 minutes each day swam for nine weeks (i.e., ~90 swims) on average, while the 180 minute mice swam for

six weeks (~60 swims), and 240 minute mice swam for four and a half weeks (~45 swims). Sedentary control mice were also placed in water containers without current for 10 minutes twice daily for six weeks.

Figure 2.1. Mouse Swimming Apparatus. CD1 mice swam against a 15 L/min current generated by a submersible pump. The water current prevented floating behaviors and mice swam in pairs to minimize dunking that occurs when three or more exercise together. Pairs either swam in a closed apparatus connected to the calorimetry system (Oxymax, Columbus Instruments, Columbus, OH, U.S.A) (*left image*) or in the 'open air' containers (*right image*). Upon session completion, mice dried under a heating lamp.

Table 2.1. Acclimation Period for the Swim Duration Protocols. The training regimens are outlined in increasing order. For the 240 minute group, two acclimation swims were completed per day in week 2, with a four-hour rest period in between. Training protocols were initiated the following day and carried out to the required termination point, depending on the exercise regimen. All duration groups swam in a water current of 15 L/min.

Final: 120 minutes/day	Monday	Tuesday	Wednesday	Thursday	Friday	Saturday (rest)	Sunday (rest)
Week 1	30 min	40 min	50 min	60 min			

Final: 180 minutes/day	Monday	Tuesday	Wednesday	Thursday	Friday	Saturday (rest)	Sunday (rest)
Week 1	30 min	40 min	50 min	60 min	70 min		
Week 2	80 min	90 min					

Final: 240 minutes/day	Monday	Tuesday	Wednesday	Thursday	Friday	Saturday (rest)	Sunday (rest)
Week 1	30 min	40 min	50 min	60 min	70 min		
Week 2	80 min 90 min	100 min 110 min	120 min				

2.3 O_2 Measurements

Concerning respirometry, a modified Oxymax system (Oxymax, Columbus Instruments, Columbus, OH, USA) measured $\%O_2$ in a closed swim container at a sampling rate of 0.2 Hz (5 seconds). The inflow rate of room air was 4 L/min to assure $\%O_2$ remained within the range of the Oxymax sensors (19.3% to 21.5% O_2) throughout the swim period. To calculate VO_2, we assumed changes in oxygen content were attributed exclusively to mice consumption while swimming. Therefore, VO_2 equalled the atmospheric $\%O_2$ entering the swimming apparatus (inflow) minus the $\%O_2$ leaving (outflow), as outlined in the **Appendix**. Atmospheric $\%O_2$ was set at 20.95% during the initial calibration process, as the manual instructs. Lastly, to determine the volume of O_2 consumed for estimating energy expenditure (ml of O_2/kg/hr), the fractions were multiplied by the inflow and outflow rates (L/min) and divided by the animal's mass. Critical environmental conditions were also monitored and accounted for, including atmospheric pressure, humidity and temperature [204]. VO_2 from each data point was corrected using $\%O_2$ calibration, pressure and humidity compensations and $\%O_2$ drift baselining. Please see the **Appendix** for a detailed breakdown.

2.4 Echocardiography

A 1.5% isoflurane/oxygen mixture anesthetized the mice (with 3% induction) in the supine position. Core temperature was monitored using a rectal probe (THM 150, Indus Instruments, Webster, TX USA) and maintained between 36.9 and 37.3°C on a heating pad. We also regulated the respiratory rate between 90 and 120 per min, and the heating pad contained built-in leads for ECG (lead II) gated acquisition. A depilatory cream removed the chest hair (Nair, Church and Dwight, Princeton, NJ, USA), and an acoustic coupling gel was applied (Aquasonic 100, Parker Laboratories Inc., Fairfield, NJ, USA). The Vevo 2100 system (VisualSonics Inc., Toronto, On, Canada) produced the Transthoracic B-Mode and M-mode echocardiograph measurements and came equipped with ultrasonic linear transducer scanning heads, operating at 30 MHz. Indices were then assessed in the left ventricular (LV) long-axis view using M-mode. These measurements involved using the EKG function whereby cardiac cycle capture simultaneously occurred in the long-axis and was analyzed using the VisualSonics data analysis suite.

2.5 Surface Electrocardiography with Pharmacological Blockade

Animals were maintained under minimal anesthesia in the supine position using a 1.5% isoflurane/oxygen mixture. Core temperature was monitored using a rectal probe and regulated between 36.9 and 37.3°C. Surface electrocardiograms required sub-dermal platinum electrodes (F-E7, Grass Technologies, West Warwick, RI, USA) attached in a lead II arrangement and connected to a Gould ACQ-7700 amplifier with the Ponemah Physiology Platform (P3) acquisition software (Data Sciences

International, New Brighton, MN, USA). Intraperitoneal administration of atropine sulphate (2 mg/kg BW) and propranolol hydrochloride (10 mg/kg BW) caused parasympathetic and sympathetic blockade, respectively. Drug preparation consisted of dissolving 0.0175 g of atropine sulphate (Sigma-Aldrich, Oakville, ON, Canada) and 0.0375 g of propranolol hydrochloride (Sigma-Aldrich, Oakville, ON, Canada) in 10 mL sterile 0.9% sodium chloride saline each. 5-minute stable recordings were made at the end of a 20-minute stabilizing window (following injection) to determine the baseline, +atropine and +atropine and propranolol data. Heart rates were derived from the R-R interval and analyzed using the P3 software.

2.6 Invasive Hemodynamics

After being anesthetized with isoflurane (3% induction and 1.5% maintenance), mice were supine positioned. A rectal probe also monitored core temperature for regulation between 36.9-37.3°C. Insertion of a 1F pressure-transducing catheter (Scisense, London, ON, Canada) into the right common carotid artery allowed guidance through the aorta into the left chambers for subsequent measurements. Data were acquired at 5000 Hz using the Scisense ADV500 control unit (Scisense, London, ON, Canada) with the Acqknowledge acquisition software (Biopic, Goleta, CA, USA). Additionally, a minimum equilibration period of 15 minutes preceded 5 minutes of baseline data acquisition. Inotropic reserve assessment involved intraperitoneal injection of dobutamine (100 µL, 1.5 mg/kg). Given the dobutamine half-life (2 minutes), there were 20 minutes between the administration and subsequent steady-state measurements for drug wash-out.

2.7 In vivo Electrophysiology: Effective Refractory Period and AF Inducibility

A 1.5% isoflurane/oxygen mixture anesthetized the mice for intracardiac measurements. Core temperature was regulated using a rectal probe and maintained between 36.9 and 37.3°C. A small incision exposed the right jugular vein, and a 2F octopolar recording/stimulating catheter (CI'BER Mouse, Numed, Hopkinton, NY, USA) entered the right atrium and ventricle via the superior vena cava. Bipolar electrograms were acquired using a Gould ACQ-7700 amplifier with the P3 acquisition software (Data Sciences International, New Brighton, MN, USA). Each electrode ring is 0.5 mm in length and separated by 0.5 mm. His bundle depolarization represents an isoelectric potential between a P-wave and QRS complex. Catheter positioning required the largest bundle amplitude to appear on lead 34 for consistent placement between animals (**Figure 2.3**). A 15-minute stabilization period then preceded electrophysiological assessments. Stimulations started at a cycle length of 20 ms below the R-R interval and progressively increased to determine the voltage capture threshold. All subsequent measurements used a voltage magnitude of 1.5 times the capture threshold, with a 1 ms pulse duration. Short pulse durations

allow for precise point stimulations, as the size of the atria is small relative to the 0.5 mm platinum stimulation/recording rings.

The atrial effective refractory period (AERP) measurements involved a driving train (S1) of 7 pulses delivered using leads 78 and 56 at 20 ms below the R-R interval, followed by an S2 coupling interval initially below capture (~15 ms) and increased by 5 ms increments until atrial capture with 1-2 ms reductions until loss of capture (**Figure 2.4**).

The AF inducibility protocols came from published work using burst pacing with intervals less than the effective atrial refractory in both trained and sedentary mice [189]. For arrhythmia induction, 27 pulses (of 1 ms duration) at 40 ms intervals were delivered to the right atrium or ventricle and reduced to 20 ms intervals by 2 ms decrements, repeated three times. If there were no arrhythmia events, 20 trains were applied every 1.5 s for 20 pulses (of 1 ms duration) with an interpulse interval of 20 ms. VF inducibility followed an identical protocol. Sustained arrhythmias meant reproducible episodes of rapid, chaotic and continuous atrial or ventricular activity lasting longer than 10 s (**Figure 2.5**).

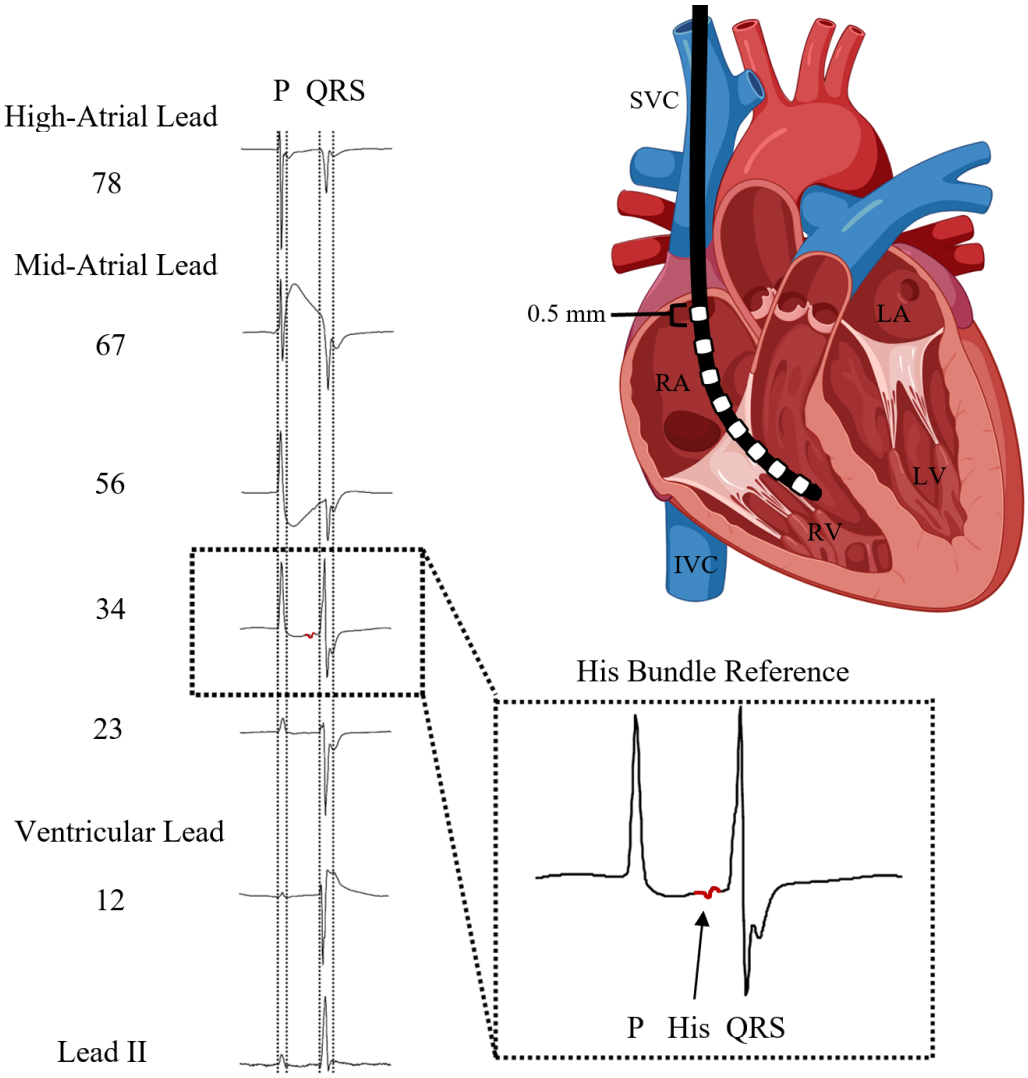

Figure 2.3. Intracardiac 2F Electrophysiology Catheter Placement. The 2F EP Catheter (CI'BER Mouse, Numbed, Hopkinton, NY, U.S.A) was introduced through the right jugular vein, directed through the right atrium and positioned within the ventricle. The ventricular signal (QRS complex) progressively decreases from the distal (12) to proximal (78) leads, whereas the atrial signal (P wave) progressively increases. Leads 78 and 56 were used to stimulate the high and mid right atrium whereas Lead 12 was used to stimulate the right ventricle. Correct positioning was confirmed through observation of the His bundle in Lead 34 as shown on the right. Lead II represents a simultaneous surface ECG recording. The 8 catheter leads are 0.5 mm in length and separated by 0.5 mm between each platinum ring. LA, left atrium; RA, right atrium; LV, left ventricle; RV, right ventricle; SVC, superior vena cava; IVC, inferior vena cava. Based on Aschar-Sobbi *et al*. [189] and created using BioRender.

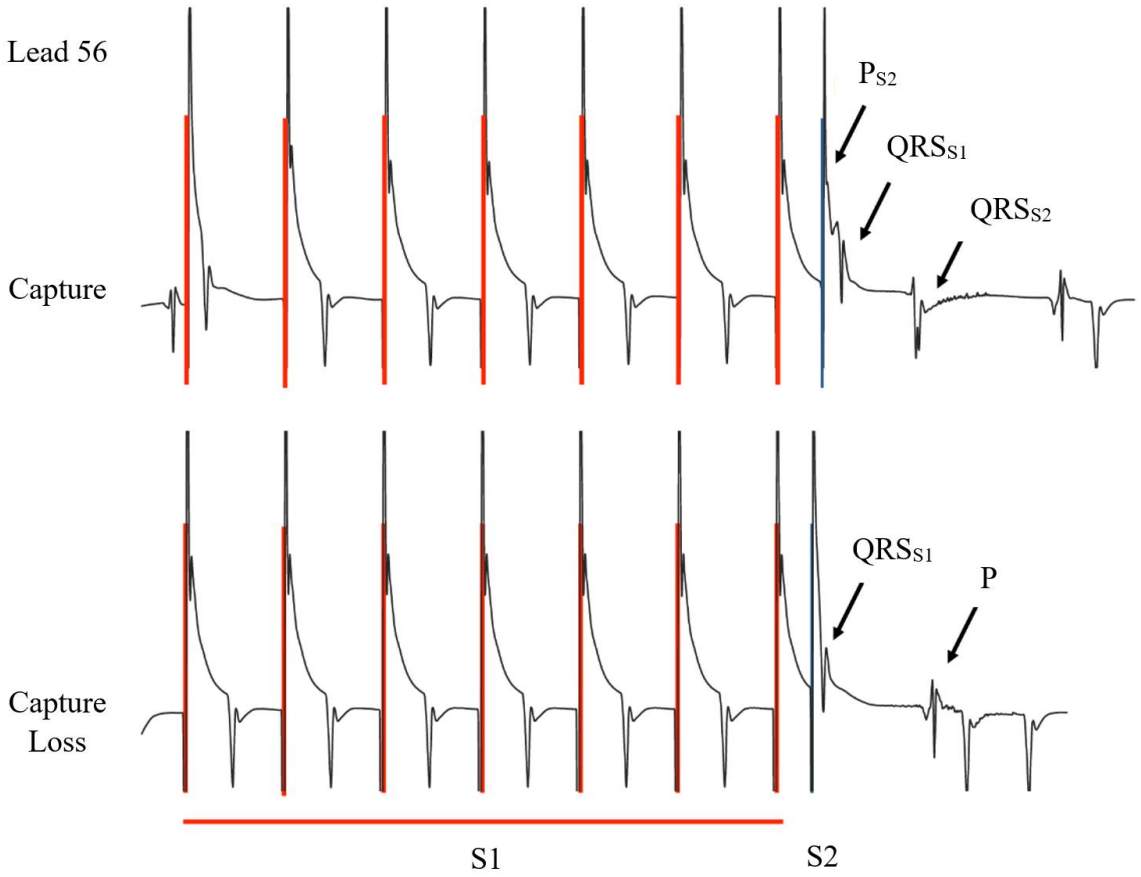

Figure 2.4. Atrial Effective Refractory Period (AERP) Measurements. Seven pulses were delivered at 1.5x voltage capture threshold to the high- and mid-atria via leads 78 and 56, respectively. Pulses were delivered at 20 ms below the R-R interval to control for heart rate (S1; red), followed by a premature stimulation (S2; blue) below atrial capture (15 ms). The S2 interval was then progressively increased by 5 ms until capture and decreased by 1-2 ms until reestablishment of capture loss. Capture results in a P-wave (P_{S2}) prior to the S1-stimulated QRS (QRS_{S1}) and indicates that the atria were not in refractory for S2 (top). Also note the successful propagation of the S2-stimulated P-wave (P_{S2}) to the ventricles (QRS_{S2}). In contrast, S2 coupling intervals, before full atrial recovery, fail to induce atrial activation and results in an S1-stimulated QRS complex (QRS_{S1}) followed by a sinus P-wave.

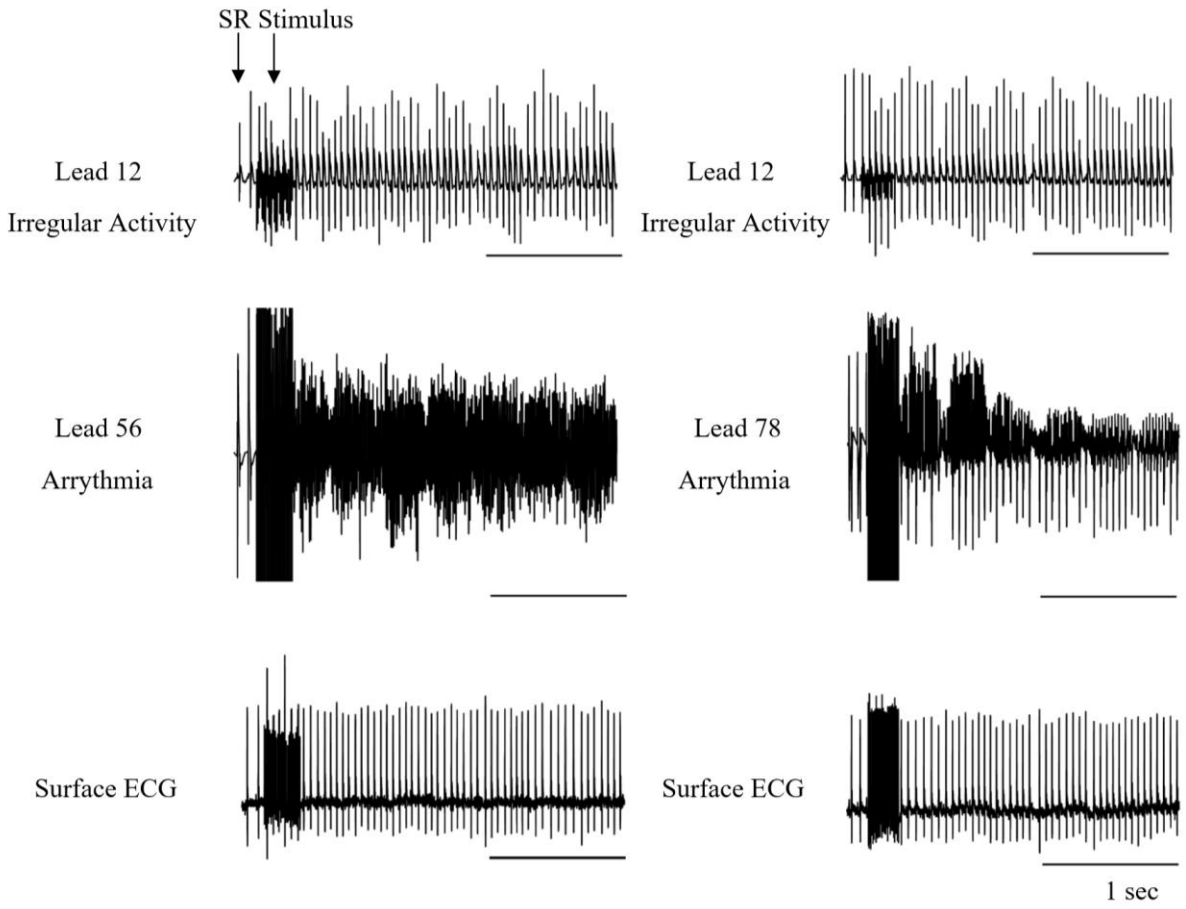

Figure 2.5. Atrial Arrythmias Detection Using an Intracardiac 2F EP Catheter. Atrial arrythmia inducibility was assessed in the mid (Lead 56) and high right atria (Lead 78). Atrial fibrillation was confirmed by the absence of regular P-waves in atrial tracings, chaotic atrial activity and irregularly regular ventricular activation lasting at least 10 seconds. SR, sinus rhythm.

2.8 Tissue Morphometry of Hearts

Intraperitoneal injection with 0.2-0.25 ml heparin (1000IU/ml, Leo Pharma, Thornhill, ON, Canada) preceded isolations to prevent blood clots. A 1.5% isoflurane/oxygen mixture anesthetized the mice, and the toe-pinch method ensured non-responsiveness. A midsternal incision from the abdomen to the chest opened the thorax for heart extraction. Removal of the pericardium and any other residual lung and connective tissue followed. Then, a small lining of adipose tissue guided incisions along the atrioventricular connective tissue until atria and ventricular separation. Tissues were blotted dry and subsequently weighed. The right hindlimb was also excised and stored in bleach to expose the tibia bone. Tibia lengths were determined using a calliper.

2.9 Histology and Immunohistological Staining

Hearts were isolated as described above, yet instead of immediate extraction, the inferior vena cava was severed and followed by heart perfusion through the apex using a 30G needle with 5 mL of 1% KCl in 0.01 M PBS (arresting the heart in diastole) and 15 mL of 4% paraformaldehyde (PFA) in 0.01 M PBS (fixing the tissue). Once excised, the tissues were incubated in 35 mL of 4% PFA overnight. Three 1-hour PBS washes followed, and we subsequently cleaned and sliced the hearts to reveal the 4-chamber view. Individual samples were then placed in tissue processing cassettes and underwent sequential washes with increasing concentrations of ethanol (70%, 80%, 95%, 100% x2), xylene (xylene-ethanol, xylene x2) and paraffin at 60-70°C for embedding. Tissues were then sliced into 5 µm thin sections by the Toronto Centre of Phenogenomics (TCP), including at three levels, 100 µm apart. Lastly, deparaffinization involved a series of 5-minute xylene washes (xylene x2, xylene-ethanol), 5-minute ethanol washes (100% x2, 95%, 70% and 50%) and 10 minutes of tap water. Then, histological staining for one hour using picrosirius red (PSR) occurred to quantify cardiac collagen deposition. Slides were washed in 0.5% acetic acid solution twice, dehydrated using a series of ethanol washes (95% x2 and 100% x2), underwent xylene washes (x3) and mounted with coverslips using Toluene (Fisher Scientific, Waltham, MA, USA). Brightfield laser scanning microscopy imaged the picrosirius red-stained tissue at the Advanced Optical Microscopy Facility (AOMF) in Toronto, Canada. PSR fluorescence properties includes absorption and emission at 550 nm and 635 nm, respectively. Data were then analyzed using ImageJ software with the threshold method, which exploits the brightness of collagen-stained tissue relative to background tissue, expressed as percentages relative to total tissue pixel counts (**Figure 2.6**). The analysis included the left atrial appendage, with interstitial and pericapsular collagen examined separately, and similar-sized sections of the left ventricular free wall for total collagen content.

We conducted immunohistochemical staining of macrophages using a rat anti-mouse primary F4-80 antibody (BIO-RAD, Mississauga, ON, Canada) with secondary goat anti-rat 647 antibodies (Invitrogen, Burlington, ON, Canada). Resembling the PSR protocol, prepared slides were deparaffinized using three xylenes washes for 5 minutes each and rehydrated using a series of increasing alcohol concentrations (100% for 10 minutes 2x, then 95%, 70% and 50% for 5 minutes each). After rinsing with tap water for 10 minutes, heat-mediated antigen retrieval involved slides submerged in 10mM Na-citrate buffer with 0.05% Tween 20 at pH 6.0 in a boiling pressure cooker. After pot pressurization, we counted 3 minutes and then indirectly washed the slides with tap water for 10 minutes. Three washes were then completed for 5 minutes each, using a wash buffer of 1000ml TBS (2.42g Tris base, 8g NaCl, 70 ml ddH2O) with 250 µl of Triton X-100 at pH 7.6. Subsequently, we used a hydrophobic barrier pen to circle the three tissue slices per slide and incubated for 1.5 hours with blocking buffer (1% BSA with 0.3M glycine in TBS) to prevent non-specific binding. Three rinses using washing buffer at 5 minutes each followed, and sections were incubated in a

primary antibody cocktail consisting of 1:100 primary antibodies in TBS with 1% BSA and 0.025% Triton X-100 overnight at 4°C. With the three tissue slices, two were incubated with primary antibody and the other with blocking buffer to act as the negative control. Twelve hours later, slides were rinsed 3x for 5 minutes with wash buffer and incubated with a 1:100 secondary antibody dilution containing WGA (staining the membrane) for 1 hour at room temperature. After three additional washes for 5 minutes each with wash buffer, slides were mounted with anti-fade DAPI-containing medium (Invitrogen, Burlington, ON, Canada) to stain cell nuclei. Confocal laser scanning microscopy imaged the F4-80, WGA and DAPI stained tissue at AMOF in Toronto, Canada. We counted total stained cells in the left atrial appendage, whereby only cells co-staining for DAPI and F4-80 were considered true macrophages. Moreover, we normalized macrophage counts to the total DAPI cell count.

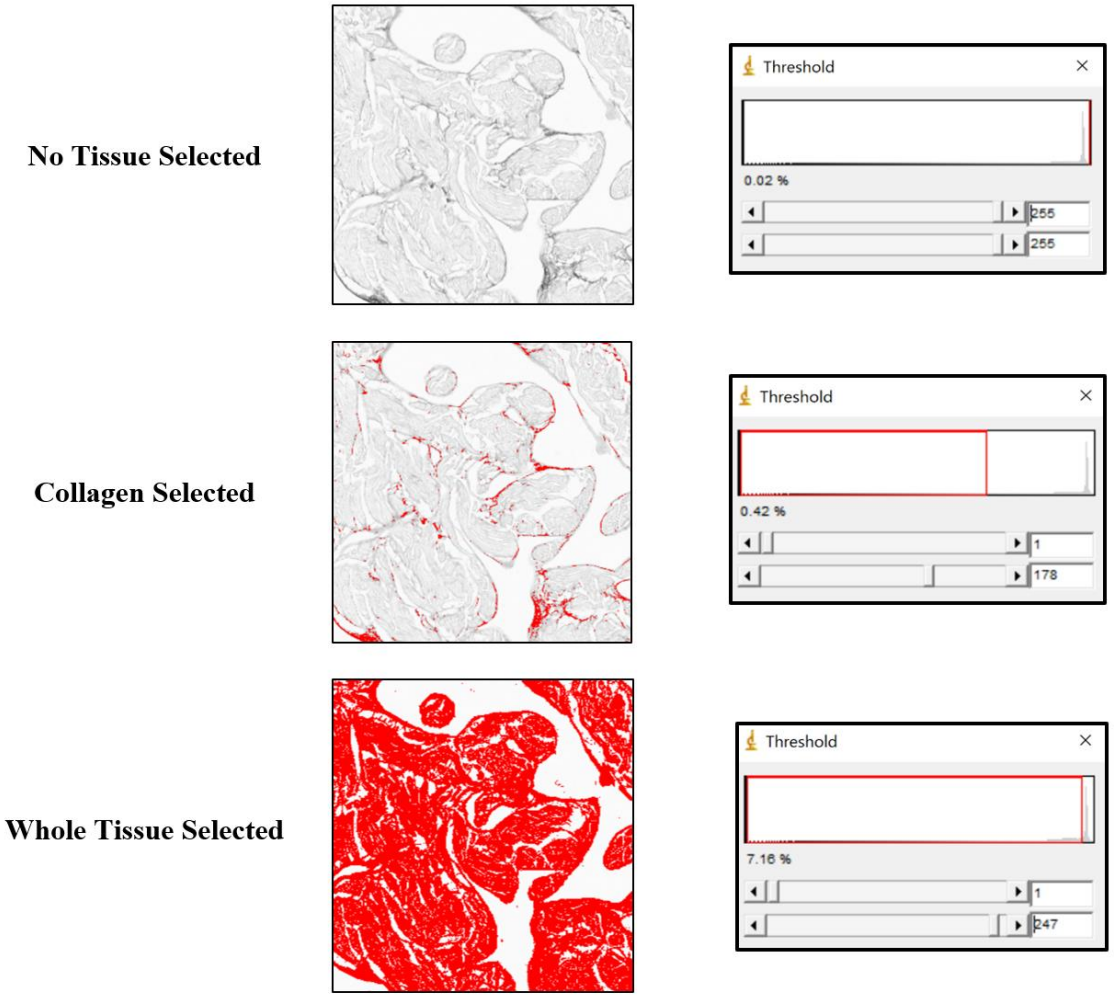

Figure 2.6. The Threshold Method for Collagen Content Quantification. The fluorescent properties of picrosirius red (PSR) were exploited using confocal laser scanning microscopy at 20x objective. Using ImageJ software, collagen quantification involved selecting pixels of varying intensity using manual threshold adjustments for collagen specifically and whole tissue, as shown on the right. Calculation of fibrosis content required measuring pixel counts from collagen-stained regions, expressed as a percentage of total tissue apparent in the field of view. A minimum of five measurements were made for each tissue and averaged. The representative tissue shown is from the left atrial appendage of a 240 minute mouse.

2.10 Cytochrome c oxidase activity

Cytochrome c oxidase (COX) activity acts as a mitochondrial content marker in muscle. As such, a portion (15-30 mg) of the tibialis anterior and gastrocnemius muscle were placed in COX enzyme extraction buffer (100 mM Na–K-Phosphate, 2 mM EDTA, at pH 7.2) on ice and diluted 40-fold separately. Tissues were then homogenized with stainless steel beads at 30 Hz using a TissueLyser II (Qiagen),

repeatedly lysed four times for 1 minute and sonicated three times for 3 seconds. A test solution containing 20 mg of horse heart cytochrome c (C2506, MiliporeSigma) was subsequently prepared and incubated at 30°C for 15 min. In a 96-well plate, we added 50 µl of whole muscle homogenates accordingly and dispensed 240 µl of the test solution into each well in the Citation 5 Bio-Tek Instrument plate reader. The maximal oxidation rate of cytochrome c was then spectrophotometrically assessed by examining 550 nm absorbance change at 30°C. The COX activity measurement for each is an average of eight trials.

2.11 Statistical Analysis

Summary data are presented as Mean±SEM unless otherwise stated. Statistical assessments primarily included the unpaired student's t-test, one-way ANOVA with Tukey's multiple comparison test and linear regression analysis. Exceptions include a Fisher's exact test for atrial arrhythmia data and a paired students t-test for pre- and post-atropine treatment. *$P \leq 0.05$ for significance with analyses performed using Prism or Microsoft Excel.

Chapter 3: Manuscript for Journal Submission

The manuscript below has been slightly modified to conform with the standard thesis guidelines yet contains all the required sections for subsequent submission to a scientific journal.

The Effects of Exercise Dose on Cardiac Responses and Atrial Fibrillation

Renée A. Gorman[1,3], Nazari Polidovitch[1], Ryan Debi[1], Victoria C. Sanfrancesco[2,3], David A. Hood[2,3], Robert Lakin[1,3] and Peter H. Backx[1,3]

[1]Department of Biology, York University, 4700 Keele St, Toronto, ON M3J 1P3,

[2]Department of Kinesiology and Health Science, York University, 4700 Keele St, Toronto, ON M3J 1P3,

[3]Muscle Health Research Centre, York University, 4700 Keele St, Toronto, ON M3J 1P3, Canada

Short Title: Exercise Dose Dependent Atrial Fibrillation

Keywords: exercise dose, atrial fibrillation, daily exercise duration, cardiovascular, atrial remodelling

Address Correspondence to:

Dr. Peter H. Backx, York University, Department of Biology, 354 Farquharson Building, 4700 Keele St., Toronto, Ontario, Canada M3J 1P3. Email: pbackx@yorku.ca, Tel: 647-244-4528

or

Dr. Robert Lakin, York University, Department of Biology, 357 Farquharson Building, 4700 Keele St., Toronto, Ontario, Canada M3J 1P3. Email: lakinrob@yorku.ca

3.1 Abstract

Atrial fibrillation (AF) is a supraventricular tachyarrhythmia strongly associated with cardiovascular disease (CVD) and sedentary lifestyles. Despite the abundant benefits of regular exercise, AF incidence for professional endurance athletes is proportionate to patients with CVD. To assess the relationship between exercise dose and AF, we compared the effects of strenuous endurance training on mice by varying daily swim durations (120, 180 or 240 minutes). After receiving the same cumulative work associated with swimming (estimated from O_2 consumption measurements), all swim-trained groups showed similar elevations ($P<0.04$) in skeletal muscle mitochondria content and ventricular hypertrophy ($P<0.02$). By contrast, inducible AF increased ($P<0.04$) progressively with daily exercise dose without markedly affecting atrial refractoriness ($P>0.05$). Also associated with an exercise dose dependency was bradycardia ($P<0.0001$) as well as atrial hypertrophy ($P<0.003$), fibrosis ($P<0.0007$) and macrophage accumulation ($P<0.0001$), that was not correspondingly observed in the ventricles. Our results demonstrate that prolonging daily swim exercise promotes progressively atrial-specific adverse remodelling, leading to increased AF susceptibility.

3.2 Introduction

International guidelines recommend 150 minutes of moderate physical activity (PA) or 75 minutes of vigorous exercise per week for optimal health outcomes [129]. The benefits of regular exercise are broad, ranging from reduced metabolic disorders [130], lower incidence of selected cancers [131] and improved cardiovascular health, even in patients with heart disease and cardiovascular-related conditions [132]. Nevertheless, some studies have reported that excessive exercise is associated with increased all-cause mortality risk, particularly in vulnerable populations [205], although these conclusions are disputed [206]. The dichotomous effects of exercise are also observed with the age-dependent incidence of atrial fibrillation (AF), wherein these arrhythmias are higher in elite endurance athletes [137] than with sedentary lifestyles [206,207]. Although the relationship between exercise and AF risk is complex [135], self-reporting has suggested that intensity [140], duration [202], frequency [143] and total dose [142] influence AF incidence. A definitive study in competitive cross-country skiers also found that AF tracked with performance and competition numbers (i.e., *cumulative work*) [141].

The underlying electrophysiological basis for AF with high exercise levels remains unclear. However, atrial hypertrophy, reduced atrial refractoriness and enhanced vagal tone are hallmark features reported in endurance athletes [209] that are all linked to AF [210]. Another common feature of AF remodelling seen in patients suffering from cardiovascular disease (CVD) and poor cardiovascular health [211] is atrial fibrosis which has also been reported in veteran marathon runners [191] and rodent exercise models [188,189].

To better understand the complicated dependence of AF on exercise, we compared the cardiac responses of mice undergoing swimming for 120, 180 or 240 minutes per day, split into two sessions. We performed comparisons after all the mice achieved the same total work during exercise as quantified by integrating the total O_2 consumed during swimming. Our results establish that atrial arrhythmia inducibility increases progressively with daily swim dose, corresponding with elevations in vagal tone, hypertrophy, fibrosis and increased immune cell infiltration in the atria. By contrast, the ventricles underwent similar degrees of physiological remodelling without showing increased arrhythmia vulnerability.

3.3. Methods

Please find detailed methodologies described in **Chapter 2**.

3.4 Results

3.4.1 Exercise Quantification

As CD1 mice intrinsically swim against water currents, we initially attempted to vary exercise intensity by altering the flow rates of the submerged water pumps (10-20 L/min). Unfortunately, VO_2 differed negligibly when water flow rates were varied (**Figure 3.1**), because mice self-regulate their effort after swimming for about 15 minutes (see Methods for additional details). Thus, to assess the cardiac responses to exercise dose, we elected to vary daily swim duration (i.e., 120, 180 or 240 minutes per day, divided into two sessions) against a fixed current (15 L/min). We also adjusted the number of swim sessions for each group so that all exercised mice performed the same cumulative effort associated with swimming (i.e., ~695 L of O_2/kg, estimated by time integration of VO_2 during swims). As shown in **Figure 3.2**, the mice achieved similar (P>0.11) total O_2 consumption, whereby mice swam for 120 minutes per day for nine weeks (i.e., ~90 swim sessions), 180 minutes for six weeks (~60 swim sessions), or 240 minutes for only four and a half weeks (~45 swim sessions). Interestingly, the representative VO_2 recordings during swimming revealed the VO_2 levels are higher for all three swim groups in the final week of swimming compared to first week (**Figure 3.3 A and B**). Indeed, **Figure 3.3 C** shows the progressive increase in mean VO_2 during swim sessions as a function of time (in weeks) for the swim groups. These results demonstrate progressive improvement in aerobic conditioning throughout swim training, with the mean VO_2 rising more steeply as a function of the number of weeks, depending on the daily swim duration. Also note that the mean VO_2 levels at the end of training were similar (P=0.36) between the swim groups, suggesting that the conditioning depended directly on the total time spent training. Consistent with this observation, the slope of the relationship between mean VO_2 versus the total hours spent swimming did not differ (P=0.07) between the groups (**Figure 3.3 D**).

Unlike the swim-trained mice, the VO_2 levels for control sedentary mice, who were placed into the tanks for only 10 minutes per session with no current (i.e., not exercising but rather floating), did not change over six weeks. Finally, it is worth noting that when mice enter the tanks, their VO_2 consumption rises quickly and peaks within about 15 minutes, after which the VO_2 declines steadily, suggesting possible progressive fatigue.

Consistent with the progressive improvements in conditioning of the mice associated with the time spent swimming, we found that the mitochondrial COX activity (per milligram of homogenates) in the tibialis anterior and gastrocnemius muscles increased (P<0.04) after swim training compared to controls (**Figure 3.4**). Additionally, no differences (P>0.1) in COX activity were observed between the exercised groups, which aligns with the results in **Figure 3.3** showing similar mean VO_2 levels at the end of the training period for all 3 swim groups.

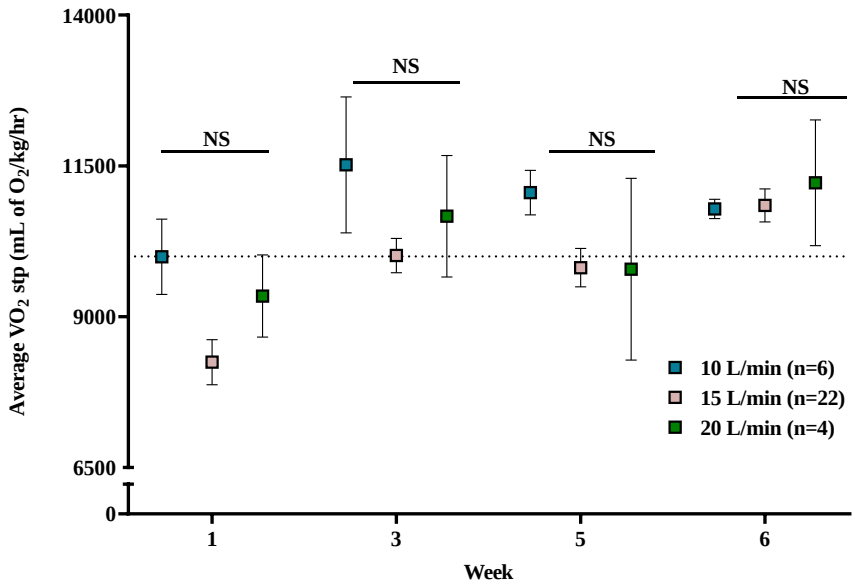

Figure 3.1. Self Regulation Behaviour During Swimming. Pairs of mice were placed in a swim apparatus and O_2 consumption (VO_2) was measured using a modified calorimetry system (Oxymax, Columbus Instruments, Columbus, OH, U.S.A). Swimming behaviour was monitored, and mice swam against a water current provided by a submerged pump. All groups followed the 180 minute training protocol at currents of either 10, 15, or 20 L/min and VO_2 was quantified periodically. Averaged VO_2 for each water current revealed no differences between the groups throughout the training programme. The *n* values indicate the number of mice included. Data are Mean±SEM, **P*<0.05 using two-way ANOVA with Tukey's multiple comparisons tests.

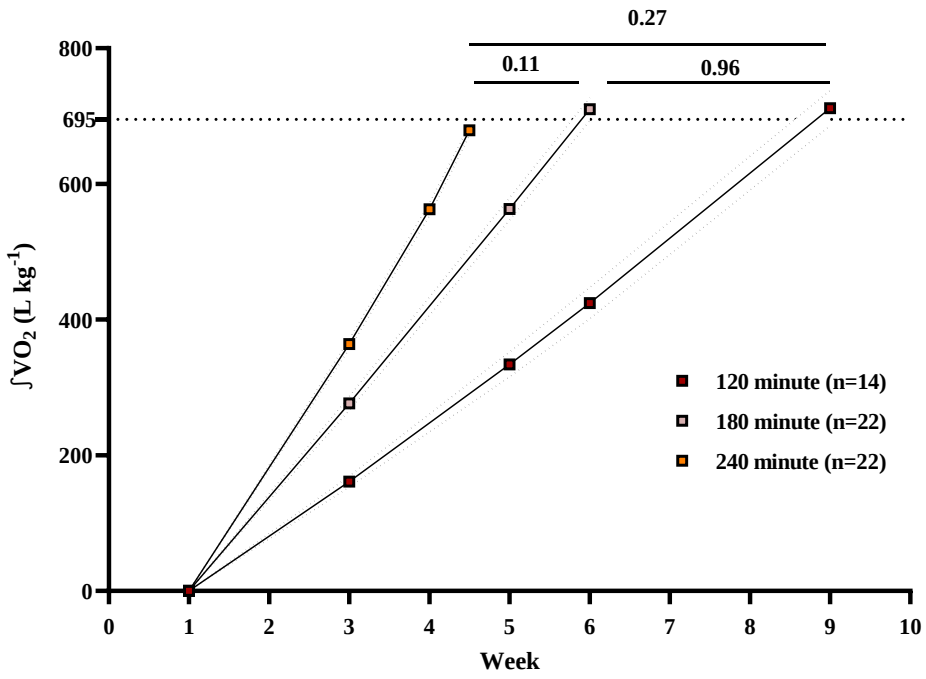

Figure 3.2. Exercise Characterization using a Mouse Swim Model. Mice swam for either 60-, 90- or 120-minute durations twice daily. In contrast, sedentary mice were placed in the swim containers for 10 minutes twice daily with no current. O_2 consumption measurements occurred during swim sessions and were used for titration analysis to ensure each exercise group completed the same cumulative dose. The training was terminated when mice consumed ~695 L of O_2/kg while swimming.

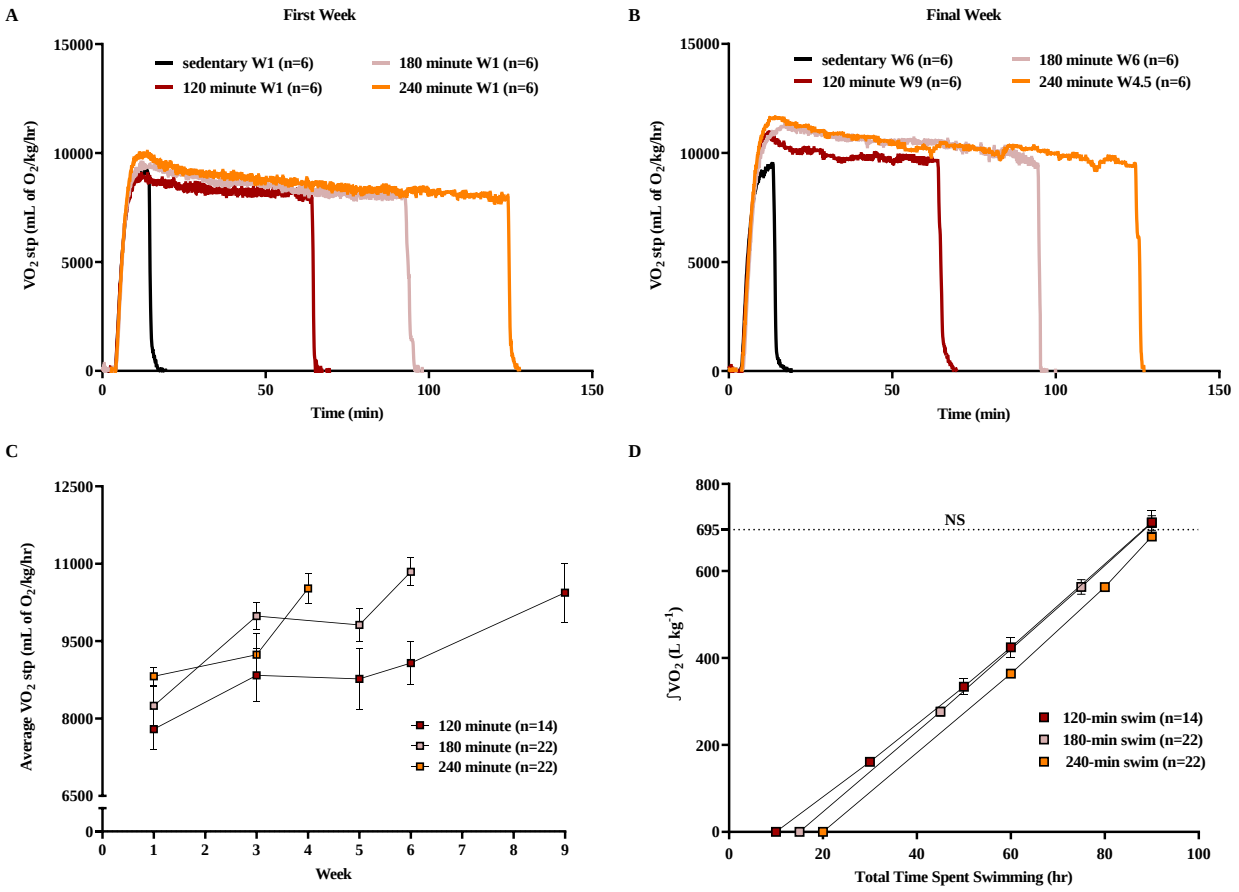

Figure 3.3. VO_2 Measurements During Swimming For Different Durations Each Day. Pairs of mice swam against a water current in the swimming apparatus, exercise behaviour was monitored and O_2 consumption (VO_2) was measured using a modified calorimetry system. (A) Representative VO_2 tracings from the first week of each swimming regime. (B) Representative VO_2 tracings from the final week of each swimming regime. (C) Average VO_2 for each duration swim group throughout the training programs. (D) Cumulative VO_2 while swimming as a function of total hours of exercise. The *n* values indicate the number of mice included. Data are Mean±SEM.

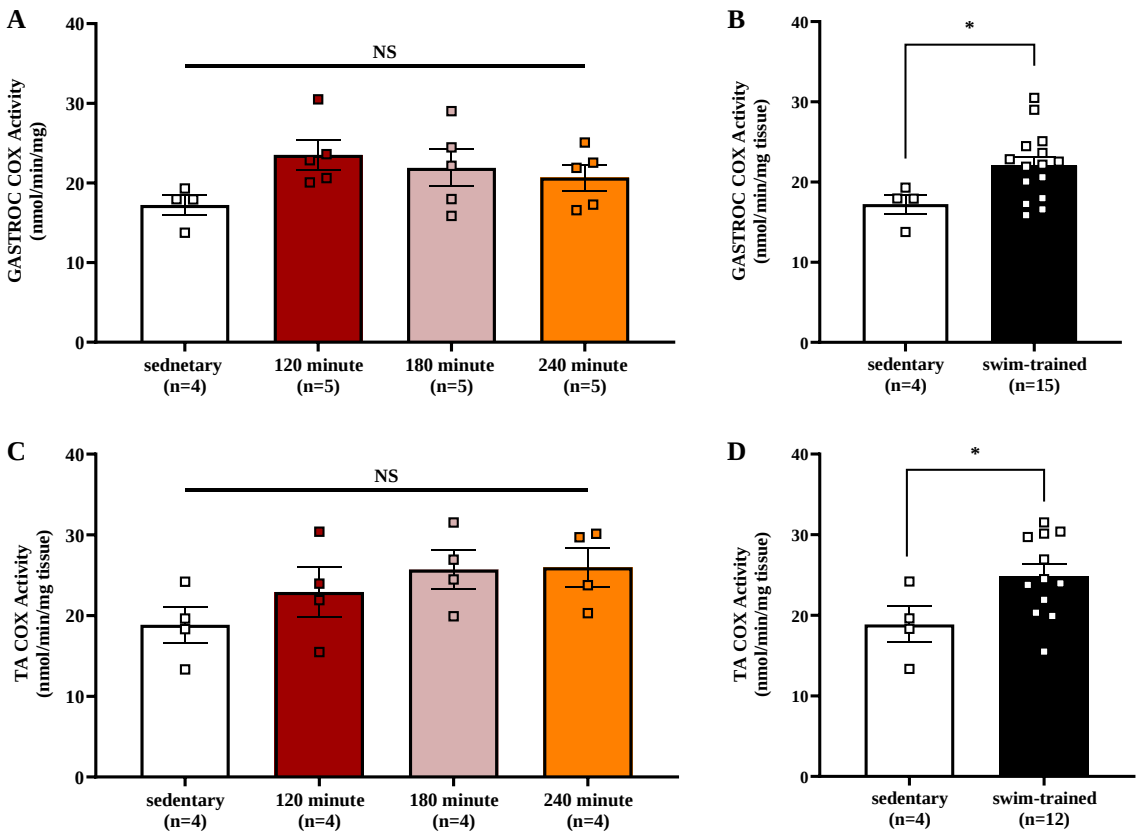

Figure 3.4. Skeletal Muscle Mitochondrial Adaptation. Following swim training termination, skeletal muscle mitochondrial content was assessed using cytochrome c oxidase (COX) activity in (A/B) the gastrocnemius (GASTROC) and (C/D) tibialis anterior (TA), demonstrating significant elevations when swim-trained mice were pooled, yet no differences between swim groups or when sedentary mice were compared to individual swim groups. The *n* values indicate the number of mice included. Data presented as Mean±SEM, **P*<0.05 using a one-way ANOVA with Tukey's multiple comparisons tests (A/C) or Student's t-test (B/D).

3.4.2. Cardiac Adaptations in Swim-Trained Mice

As expected [212], HRs measured in anesthetized mice using surface electrocardiograms were reduced (*P*<0.0001) in all swim-trained mice compared to the non-exercised group (**Table 3.1**). Moreover, linear regression analyses revealed progressive reductions in HR [F(1,28) = 93.62, *P*<0.0001] as daily exercise durations increase (**Figure 3.5 B**). Since autonomic modulation is strongly linked to sinus bradycardia in endurance athletes [213], we examined the effects of parasympathetic and sympathetic autonomic nerve blockade on HR using atropine and propranolol, respectively (**Figure 3.5 C**). Consistent with the prominent role of vagal tone in HR reduction, atropine elevated HRs for all groups with the magnitude of increase (i.e., the atropine-sensitive change in HR) being more pronounced as the swim durations increased, as summarized in **Figure 3.5 D and E.** These results support the conclusion that the

HR reductions on daily swim duration is at least partially mediated by enhanced cardiac vagal activity. Interestingly, after atropine treatment, HR in the exercised mice remained lower (P<0.0001) for all swim groups compared to sedentary controls (ANOVA), with relatively small differences between the exercise groups (**Figure 3.5 C**). To assess whether the lower HRs in the atropine-treated exercised mice were related to differences in cardiac sympathetic inputs, mice were administered propranolol 20 minutes after the atropine treatment. Following complete autonomic blockade, no HR differences (P>0.4, one-way ANOVA) were observed between swim and sedentary mice (**Figure 3.5 C**). The effects of propranolol demonstrate that the HR reductions seen with swim training are mediated partially by decreased cardiac sympathetic activity, which is only marginally influenced by daily exercise dose. Moreover, the absence of HR differences after complete autonomic blockade establishes that HR changes with exercise are not associated with intrinsic SAN alterations, as previously suggested [177].

Table 3.1. Extended Surface Electrocardiogram Heart Rate Data.

	sedentary (control)	**120 minute (60min 2x)**	**180 minute (90min 2x)**	**240 minute (120min 2x)**
Electrocardiography n	*10*	*6*	*7*	*7*
Bl (bpm)	550 ± 9	496 ± 16*	436 ± 9* #	421 ± 10* #
Atr (bpm)	586 ± 10	531 ± 15*	528 ± 13*	500 ± 8*
Atr + Pr (bpm)	434 ± 5	432 ± 5	434 ± 8	422 ± 5

Bl, baseline; Atr, atropine; Pr, propranolol. The *n* values shown presents number of mice included. Data presented as Mean±SEM.
*P<0.05, compared with controls using one-way ANOVA with Tukey's multiple comparisons tests.
#P<0.05, compared with 120-min swim mice using one-way ANOVA with Tukey's multiple comparisons tests.

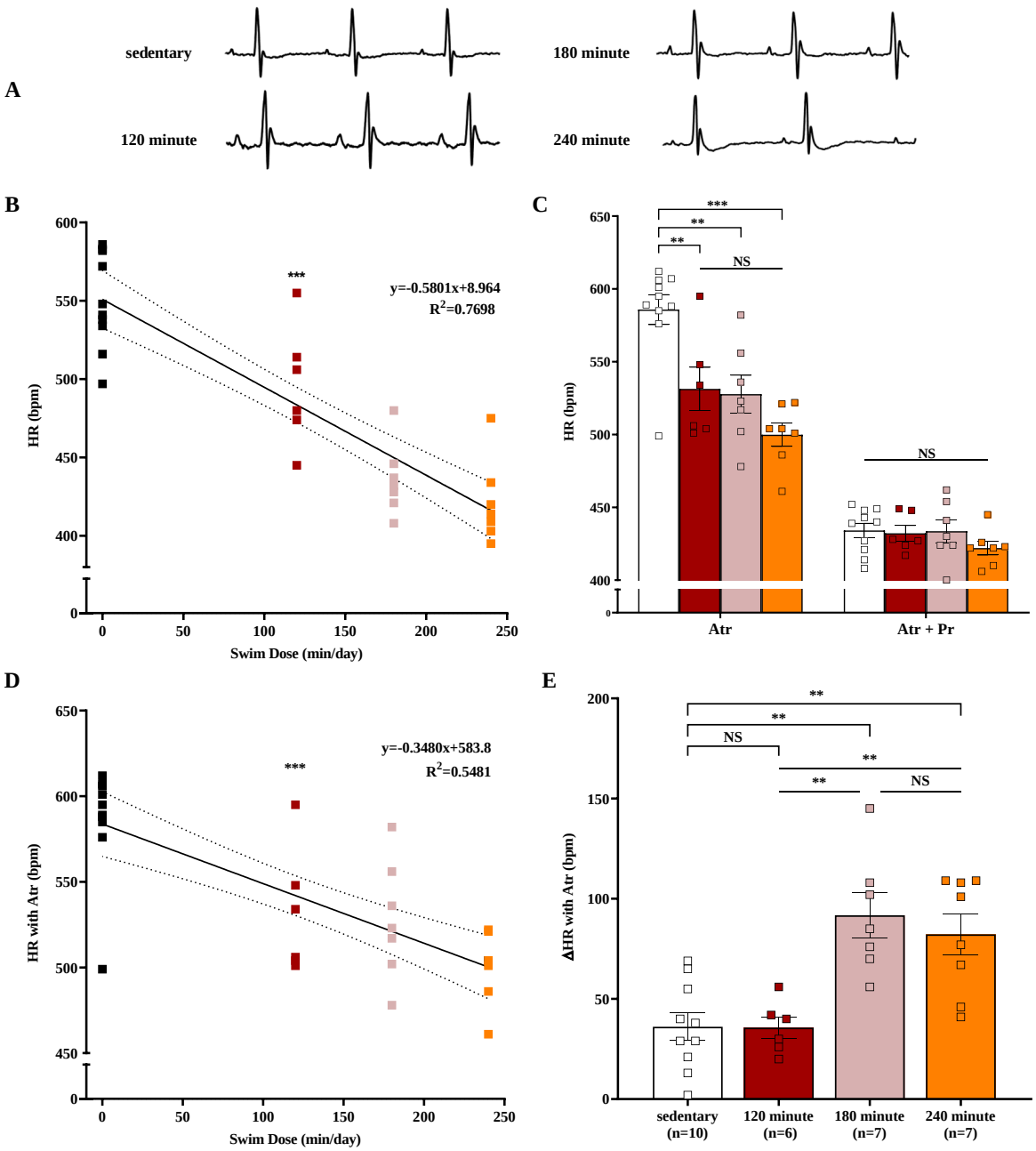

Figure 3.5. Effect of Swim Training on Heart Rates (HRs) and Autonomic Regulation. HR reductions induced by endurance training are associated with cardiac autonomic modulation. Thus, we performed surface ECGs on anesthetized mice before and after atropine (Atr) and propranolol (Pr) administration. (A) Representative 0.2-second ECGs at baseline (Bl) for the control and swim groups. (B) Linear regression analysis of resting HRs as a function of daily swim dose. (C) HRs before and after parasympathetic (atropine) and sympathetic blockade (propranolol). (D) Linear regression analysis following parasympathetic inhibition. (E) Change in HR from baseline to atropine administration. The *n* values in (E) indicate the number of mice used throughout the figure. Data are Mean±SEM., **P*<0.05, ***P*<0.01, ****P*<0.0001, using a one-way ANOVA with Tukey's multiple comparisons tests and simple linear regression analysis.

In addition to the dependence of HR on exercise dose, we also observed using linear regression analyses that ventricle-to-body weight ratios (i.e., VW/BW) increased [R^2= 0.35, F(1,16)= 8.75, P<0.01] with daily swim durations (**Table 3.2**), like the mild physiological hypertrophy seen in endurance athletes [157]. However, the increases in VW/BW with exercise are relatively small and only reach significant increases (P=0.01, unpaired t-test) when comparing sedentary mice to pooled data from the exercised groups (**Figure 3.6 A and B)**. Moreover, when ventricular weights were normalized to tibia lengths (i.e., VW/TL) there were no differences (P=0.12) between groups and a lack of an exercise dose dependency [R^2= 0.14, F(1,16)= 2.67, P<0.12] (**Figure 3.6 C and D**). Nevertheless, echocardiography measurements in anesthetized mice revealed progressive increases (P<0.0001) in both LV end-systolic diameters [R^2=0.49, F(1,61)=59.51] and LV end-diastolic diameters [R^2=0.28, F(1,61)= 24.21] (**Figure 3.7 A and B**) using linear regression analyses. These changes in LV dimensions were also associated with a corresponding clear dose-dependent [R^2=0.32, F(1,60)= 27.96, P<0.0001] reduction in LV wall thickness with exercise duration (**Figure 3.7 C)**. Swim-trained mice also showed reductions (both P<0.0001) in fractional shortening (FS) and ejection fraction (EF) compared to the controls (**Table 3.2**), similar to that seen in athletes [214] and previously reported in exercised mice [189]. However, we observed no differences (P>0.52) between the swim groups using one-way ANOVA with Tukey's multiple comparisons test, despite linear regression revealing an exercise dose dependency for both FS [R^2=0.42, F(1,61)= 44.12, P<0.0001] and EF [R^2=0.43, F(1,61)= 46.18, P<0.0001] (**Figure 3.7 D and E)**. Moreover, in spite of reduced FS, the rate of LV pressure development, with or without dobutamine treatment, was the same (P>0.15) between exercised and sedentary mice (**Table 3.3**).

Table 3.2. Physical Ventricular Parameters of Mice Swim-Trained for Variable Daily Durations.

	sedentary (control)	120 minute (60min 2x)	180 minute (90min 2x)	240 minute (120min 2x)
Body parameters n	*4*	*6*	*3*	*5*
Body Weight (g)	42.6 ±1.5	40.2 ± 1.0	38.0 ± 1.7	38.8 ± 1.2
Tibia Length (mm)	19.3 ± 0.09	19.6 ± 0.16	19.2 ± 0.3	19.3 ± 0.1
Ventricle Weight (mg)	151.7 ± 5.7	169.6 ± 6.0	146.5 ± 3.5	173.1 ± 3.4
Ventricle/Body Weight (mg/g)	3.6 ± 0.1	4.2 ± 0.2	3.9 ± 0.3	4.5 ± 0.2*
Ventricle/Tibia Length (mg/mm)	7.9 ± 0.3	8.7 ± 0.4	7.6 ± 0.1	9.0 ± 0.1
Echocardiography n	*12*	*13*	*17*	*22*
LVDd (mm)	4.28 ± 0.06	4.47 ± 0.05	4.56 ± 0.05*	4.60 ± 0.04*
LVDs (mm)	2.69 ± 0.05	3.03 ± 0.04*	3.09 ± 0.03*	3.16 ± 0.04*
EF (%)	67.4 ± 1.0	60.5 ± 0.8*	60.5 ± 0.6*	59.0 ± 0.8*
FS (%)	37.2 ± 0.8	32.2 ± 0.56*	32.2 ± 0.4*	31.3 ± 0.5*
LVPWTh (mm)	0.79 ± 0.01	0.77 ± 0.01	0.73 ± 0.01*	0.72 ± 0.01*
HR (bpm)	534 ± 8	461 ± 10*	432 ± 5*	423 ± 11*

LVDd, left ventricular diastolic diameter; LVDs, left ventricular systolic diameter; EF, ejection fraction; FS, fractional shortening; LVPWth, left ventricular posterior wall thickness; HR, heart rate. The *n* value shown presents number of mice included. Data presented as Mean±SEM.
*$P<0.05$, compared with sedentary using one-way ANOVA with Tukey's multiple comparisons tests.

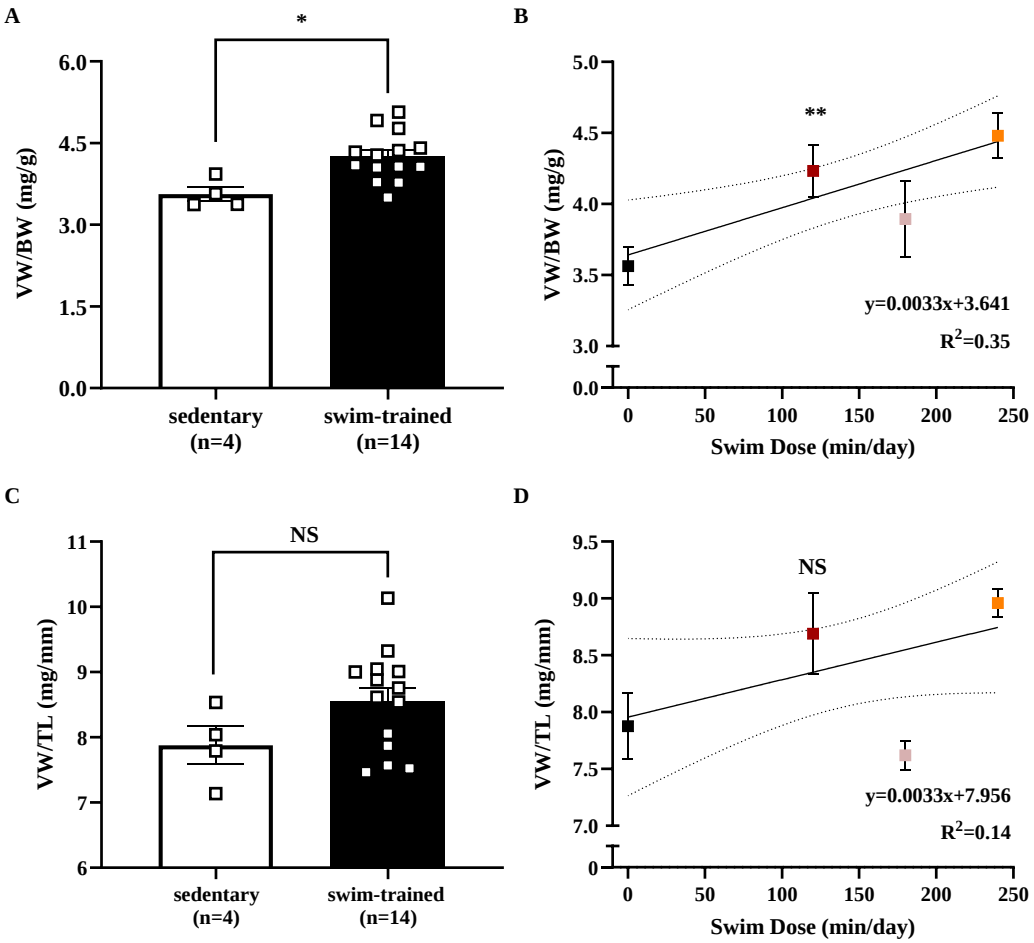

Figure 3.6. Expanded Ventricular Morphometric Data. (A) Ventricular weight (VW) normalized to body weight (BW), and (B) the corresponding linear regression analysis as a function of daily swim dose. (C) VW normalized to tibia length (TL), and (D) the corresponding linear regression analysis as a function of daily swim dose. Data presented as Mean±SEM with **P*<0.05, ***P*<0.01, ****P*<0.0001 using an unpaired student's t-test for A/B; *n*=3 sedentary mice (black), *n*=6 120 minute mice (red), *n*=3 180 minute mice (pink) and *n*=5 240 minute mice (orange).

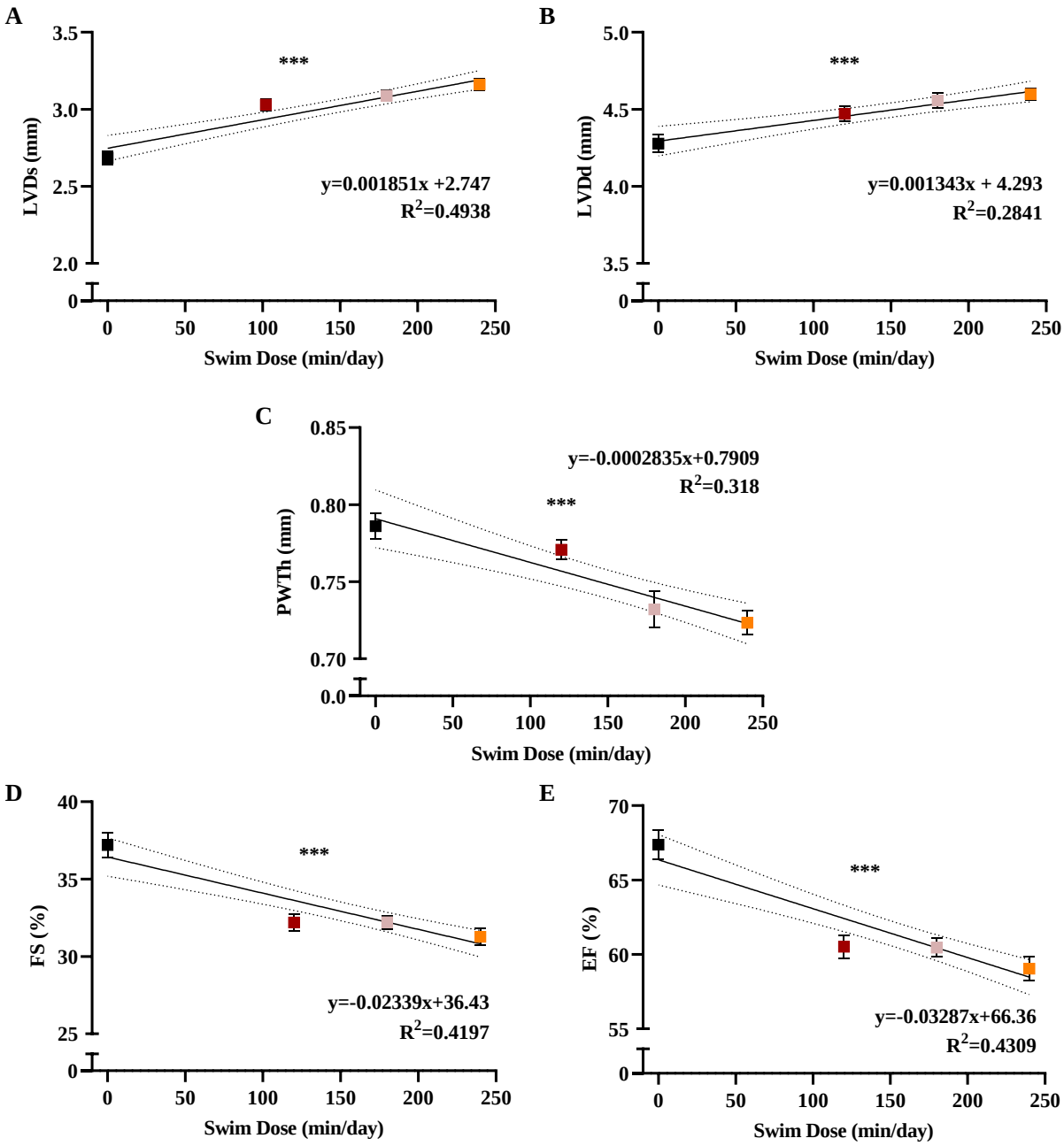

Figure 3.7. Linear Regression of Echocardiographic Measurements. (A) Left ventricular systolic diameter (LVDs), (B) left ventricular diastolic diameter (LVDd), (C) left ventricular posterior wall thickness (PWTh), (D) fractional shortening (FS) and (E) ejection fraction (EF). Data presented as Mean±SEM with ***P<0.0001; n=12 sedentary mice (black), n=13 120 minute mice (red), n=17 180 minute mice (pink) and n=22 240 minute mice (orange).

Table 3.3. Functional Ventricular Parameters of Swim-Trained Mice.

	sedentary (control)	120 minute (60min 2x)	180 minute (90min 2x)	240 minute (120min 2x)
Hemodynamics n	*3*	*3*	*4*	*3*
MAP (mmHg)	82.9 ± 7.7	77.5 ± 3.3	91.4 ± 6.8	93.4 ± 13.5
LVPs (mmHg)	78.2 ± 7.1	72.5 ± 2.2	90.5 ± 6.2	92.0 ± 10.0
LV +dP/dtmax (mmHg/s)	9873 ± 487	8868 ± 692	9945 ± 638	9789 ± 516
LV -dP/dtmin (mmHg/s)	-8848 ± 682	-7829 ± 321	-9810 ± 822	-10114 ± 601
Dob +dP/dtmax (mmHg/s)	10769 ± 611	10195 ± 1144	13363 ± 714	13360 ± 1806

MAP, mean arterial pressure; LVPs, left ventricular systolic pressure; LV +dP/dtmax, maximum rate of left ventricular pressure development; LV -dP/dtmin, minimum rate of left ventricular pressure development; Dob +dP/dtmax, maximum rate of left ventricular pressure development following dobutamine challenge. The *n* values shown presents number of mice included. Data presented as Mean±SEM.
**P*<0.05, compared with sedentary using one-way ANOVA with Tukey's multiple comparisons tests.

3.4.3. Dose-Dependent Arrhythmia Inducibility in Swim-Trained Mice

We next assessed the impact of daily exercise dose on atrial and ventricular arrhythmias following burst pacing, defined as reproducible bouts of chaotic activation lasting >10 seconds. As seen in **Figure 3.8**, AF was not inducible in sedentary control mice. Accordingly, the incidence of sustained atrial arrhythmias (i.e., >10 seconds) was greater (P<0.04) in the swim-trained mice compared to the non-exercised controls. Detailed comparisons revealed that AF inducibility did not differ between the sedentary controls and 120 minute group (P<0.2) or 180 minute group (P=0.07) but increased in the 240 minute group (P=0.01). On the other hand, when sustained AF occurred, the duration was not different (P=0.32 one-way ANOVA) between the exercise groups, as clearly seen in linear regression plots [R^2=0.1, F(1,19)=1.66, P=0.2] (**Figure 3.8 D)**. By contrast, ventricular arrhythmias were not inducible in the sedentary or exercised group (**Figure 3.9**).

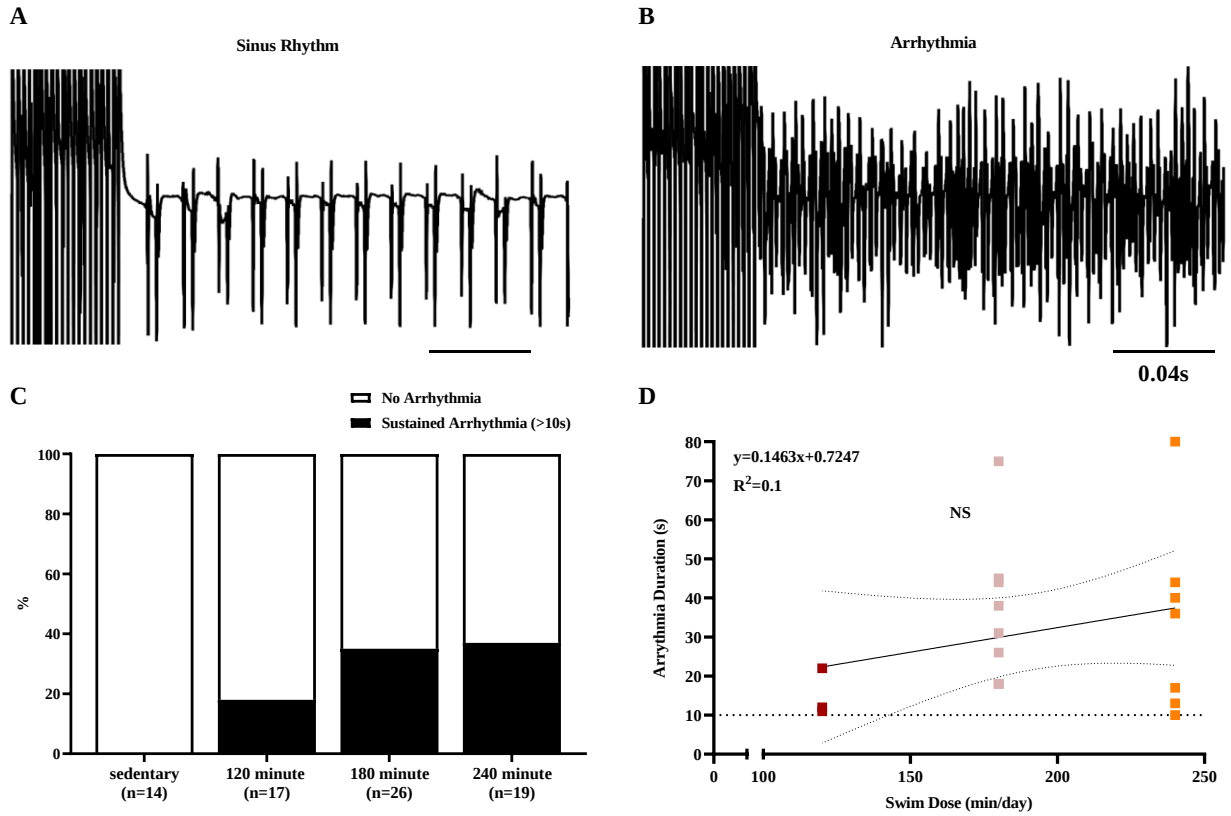

Figure 3.8. Variable Training Duration Increases Atrial Fibrillation Inducibility, Without Refractory or Action Potential Shortening. We delivered rapid atrial burst pacing *in vivo*. Representative electrograms illustrate tracings of (A) sinus rhythm and (B) an atrial fibrillation. (C) Percent of mice that had sustained and reproducible arrythmia inducibility (>10 s). Note the percentage of atrial arrhythmias increases with the prolongation of daily swim duration. (D) Linear regression analyses of the average maximum arrhythmia duration in each group, including only the inducible mice. The dotted line represents the 10 second threshold for classification of a sustained arrythmia. The *n* values indicate the number of mice included. For (D) *n*=3 120 minute mice (red), *n*=6 180 minute mice (pink) and *n*=7 240 minute mice (orange). Data represented as Mean±SEM.

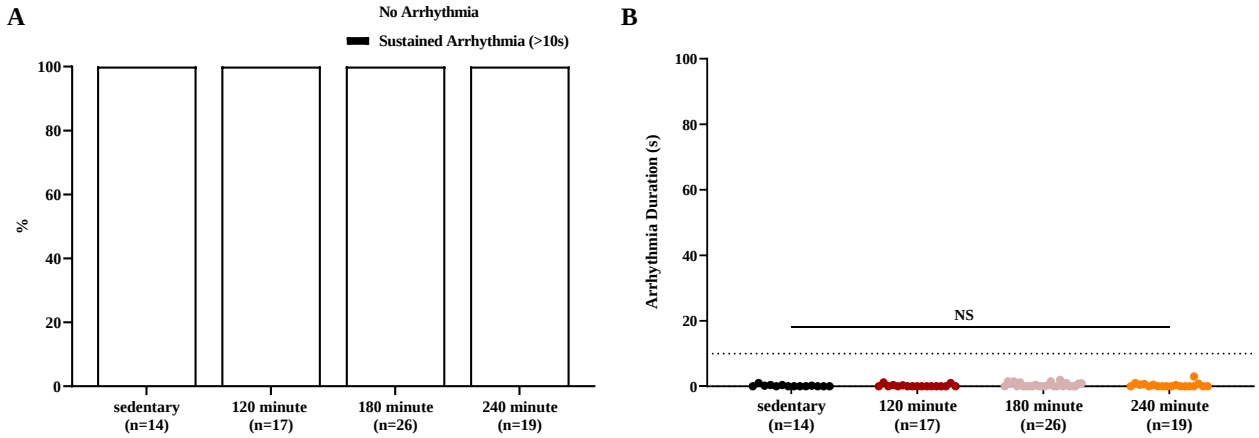

Figure 3.9. Swim-Trained Mice are Not Susceptible to Ventricle Fibrillation (VF). To determine whether training-induced arrhythmogenic remodelling is restricted to atria, stimulations were delivered to the ventricles using distal leads 12. Sustained VF is rapid, irregular ventricular electrical activity lasting >10 s. (A) Ventricular arrhythmia inducibility in control and swim groups. (B) The average maximum VF durations. The *n* values indicate the number of mice included. Together, these suggest atrial-specific arrhythmogenic remodelling in swim-trained mice. Data present as Mean±SEM, using a one-way ANOVA.

To better understand the potential mechanisms for the influence of daily exercise dose on AF vulnerability, we assessed the effects of exercise on atrial electrical refractoriness, hypertrophy and fibrosis since these factors are known to play central roles in AF mechanisms [8,67]. To assess atrial refractoriness on AF vulnerability, we measured effective refractory periods (i.e., AERPs) in anesthetized mice during procedures to interrogate AF vulnerability. Despite the dependence of AF vulnerability on daily exercise dose, AERPs were not different (P>0.42) between the groups (**Figure 3.10 C**). However, after a subset of mice were treated with atropine to block parasympathetic activity we observed, as expected, AERP prolongation (**Figure 3.10 D**), with greater (P<0.0001, one-way ANOVA) durations in swim groups compared to sedentary mice. Also, consistent with the strong influence of the vagus on HR, the AERP prolongation induced by atropine tended to rise as the daily exercise dose increased (**Figure 3.10 E**) and this was associated with reduced AF inducibility in each exercise group (0/17, 2/26 and 2/19 for 120, 180 and 240 minute groups, respectively). Atropine treatment also abbreviated (P<0.02) atrial arrhythmia durations (**Figure 3.10 A and B**). These results establish that, while differences in AERP are not directly contributing to enhanced AF vulnerability induced by elevated exercise dose, parasympathetic nerve activity does influence AF inducibility and durations.

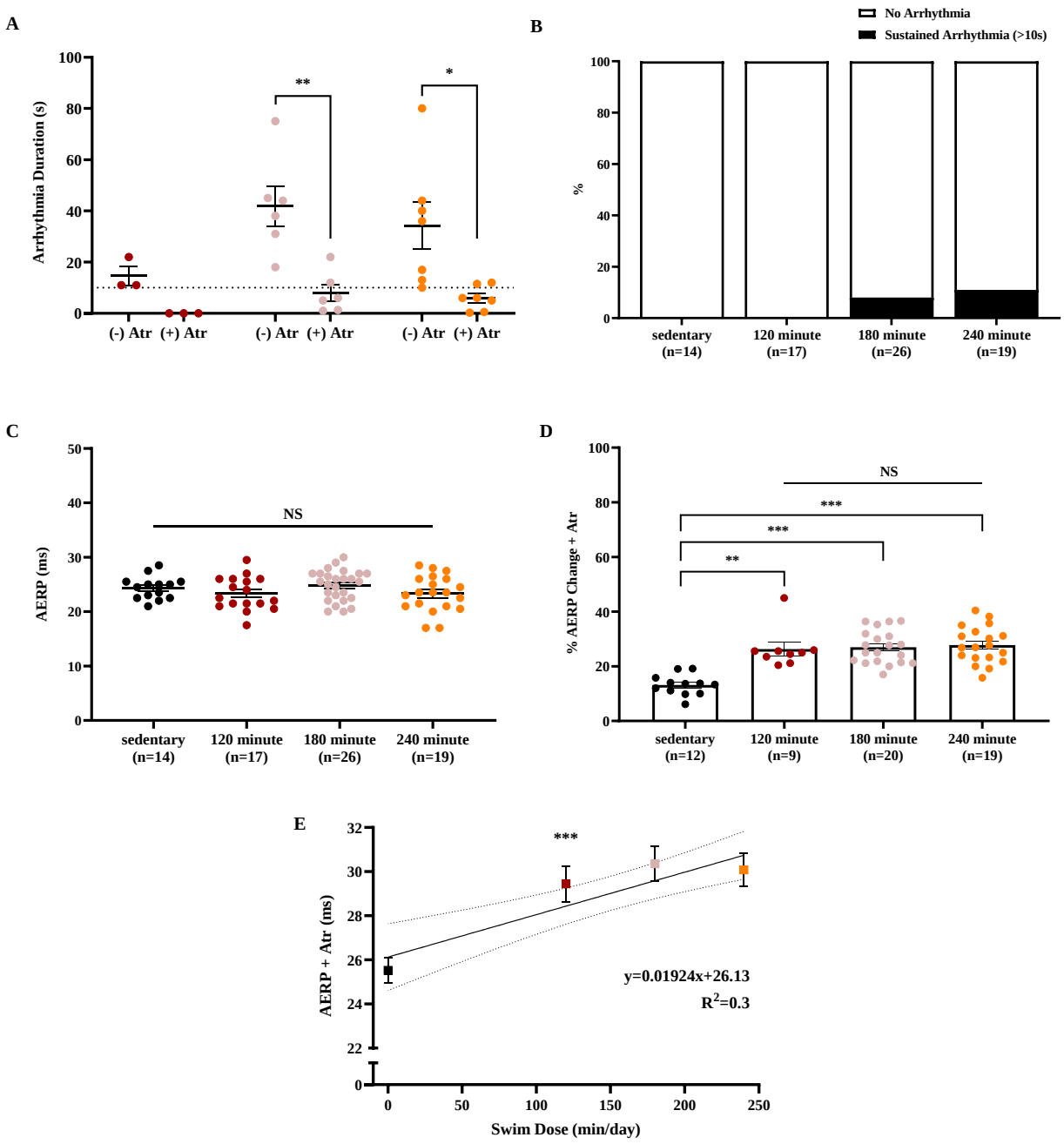

Figure 3.10. Atropine Effects on Atrial Refractoriness and AF Susceptibility in Swim-Trained Mice. To investigate the role of training-induced elevated vagal tone in AF susceptibility, we assessed the refractory periods and AF durations following intraperitoneal injections with 2 mg/kg atropine of anesthetized mice *in vivo*. (A) Arrhythmia durations and (B) arrhythmia contingency following atropine injection. (C) Atrial effective refractory period (AERP) in the right appendage prior to atropine administration. (D) Change in AERP following parasympathetic inhibition. (E) Linear regression analysis of atropine-sensitive AERPs as a function of daily swim dose. The *n* values indicate the number of mice used. For (A) n=3 120 minute mice (red), n=6 180 minute mice (pink) and n=7 240 minute mice (orange), including only the mice that were previously inducible for AF. Data presented as Mean±SEM, *P<0.05, **P<0.01, ***P<0.0001 using a two-way ANOVA with repeated measures (A) or one-way ANOVA with Tukey's multiple comparisons tests (C/D).

Nonetheless, the absence of AERP differences between the groups suggests that other factors must underlie the increased AF vulnerability observed with increasing daily exercise dose. Since fibrosis is seen invariably in AF [211], we assessed atrial collagen content using PSR staining in the left atrial appendages and ventricle. These measurements revealed more atrial fibrosis (P<0.0007, one-way ANOVA) in each swim group compared to sedentary mice, with linear regression analyses establishing a dependence of (P<0.0001) fibrosis on the daily exercise amount [R^2=0.7, F(1,26)=61.8] (**Figure 3.11**). The dose dependency was also observed in both the interstitial [R^2=0.47, F(1,26)=22.97] and pericapsular [R^2=0.7, F(1,26)=61.92] regions of the atria (**Figure 3.12**). However, it should be mentioned that one-way ANOVA analyses did not reveal differences in collagen between the exercised groups (P>0.18 for interstitial and P>0.27 for pericapsular). Interestingly, total collagen content was additionally increased (P=0.02, one-way ANOVA) in the left ventricular free wall for swim groups relative to the controls with linear regression analyses demonstrating a dependence [R^2=0.27, F(1,25)=9.22, P<0.001] on daily exercise dose (**Figure 3.13**). However, it is important to note that the relative amount of fibrosis is considerably smaller in the ventricles compared to left atrial appendages.

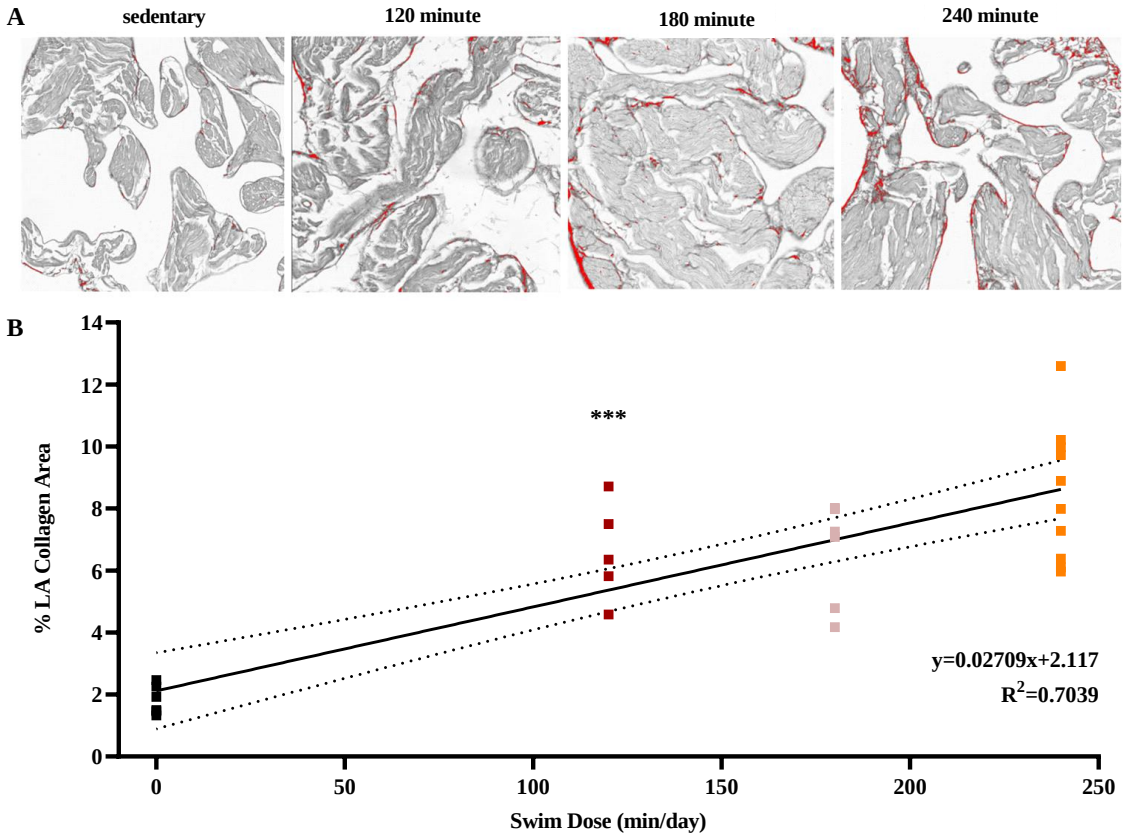

Figure 3.11. Swim Training at Variable Daily Durations Induces Atrial Fibrosis. Left atrial appendage collagen was identified using picrosirius red and imaged using a slide-scanner brightfield microscope at 20x. (A) Representative images suggesting increased collagen deposition with prolonged swim exercise. (B) Quantification of atrial collagen content and simple linear regression analysis based on selecting and counting pixel brightness, standardized to total tissue. Data are Mean±SEM., **P*<0.05, ***P*<0.01, ****P*<0.0001; *n*=7 sedentary mice (black), *n*=5 120 minute mice (red), *n*=6 180 minute mice (pink) and *n*=10 240 minute mice (orange).

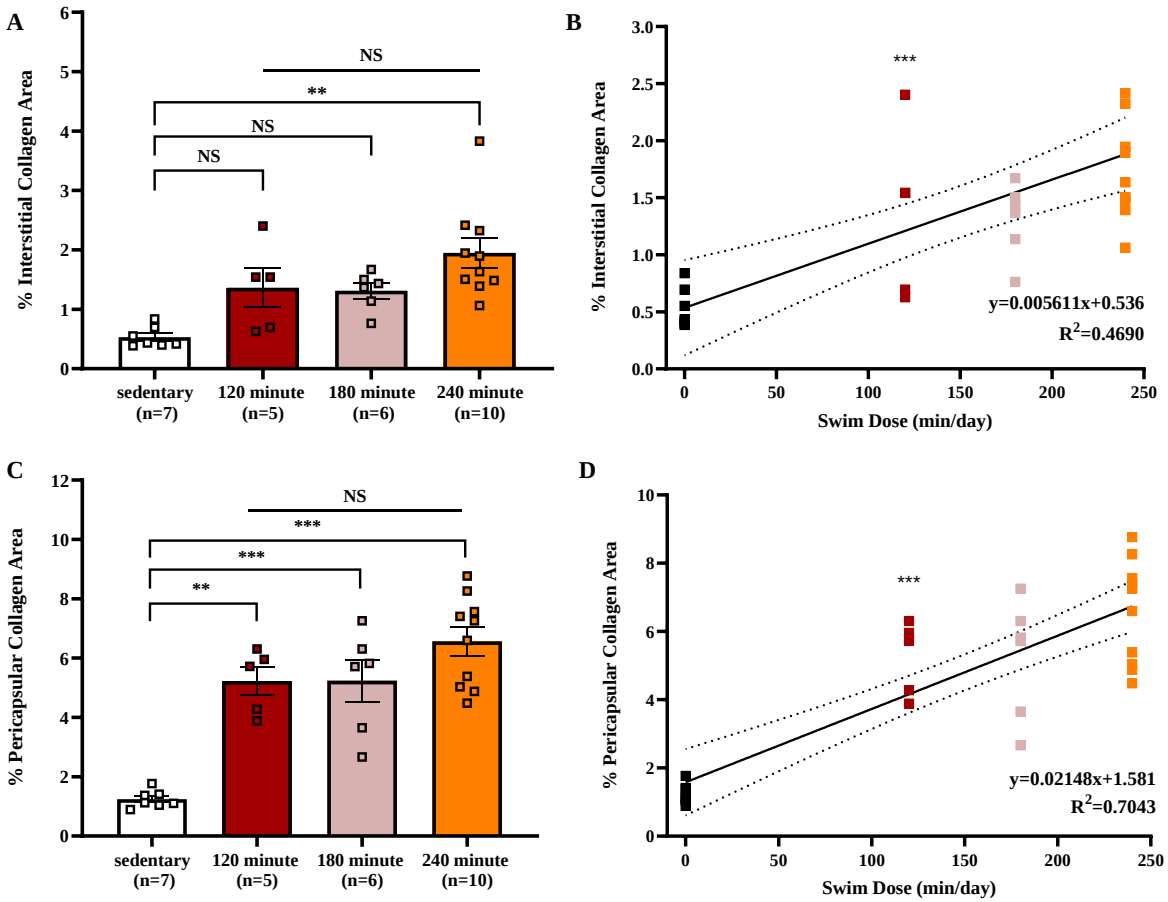

Figure 3.12. Discrimination Between Swim Training Induced Pericapsular and Interstitial Fibrosis. Left atrial appendage collagen was identified using picrosirius red and imaged using a slide-scanner brightfield microscope at 20x. Tissues were separately analyzed for collagen deposition in the pericapsular regions, surrounding blood vessels and the cell exteriors, and interstitial space, between myocyte bundles. (A/B) Quantification and linear regression of the percent interstitial and (C/D) pericapsular collagen deposition based on selecting and counting pixel brightness, standardized to total tissue. The *n* values indicate the number of mice included. Data are Mean±SEM., **P*<0.05, ***P*<0.01, ****P*<0.0001 using a one-way ANOVA with Tukey's multiple comparisons tests or simple linear regression.

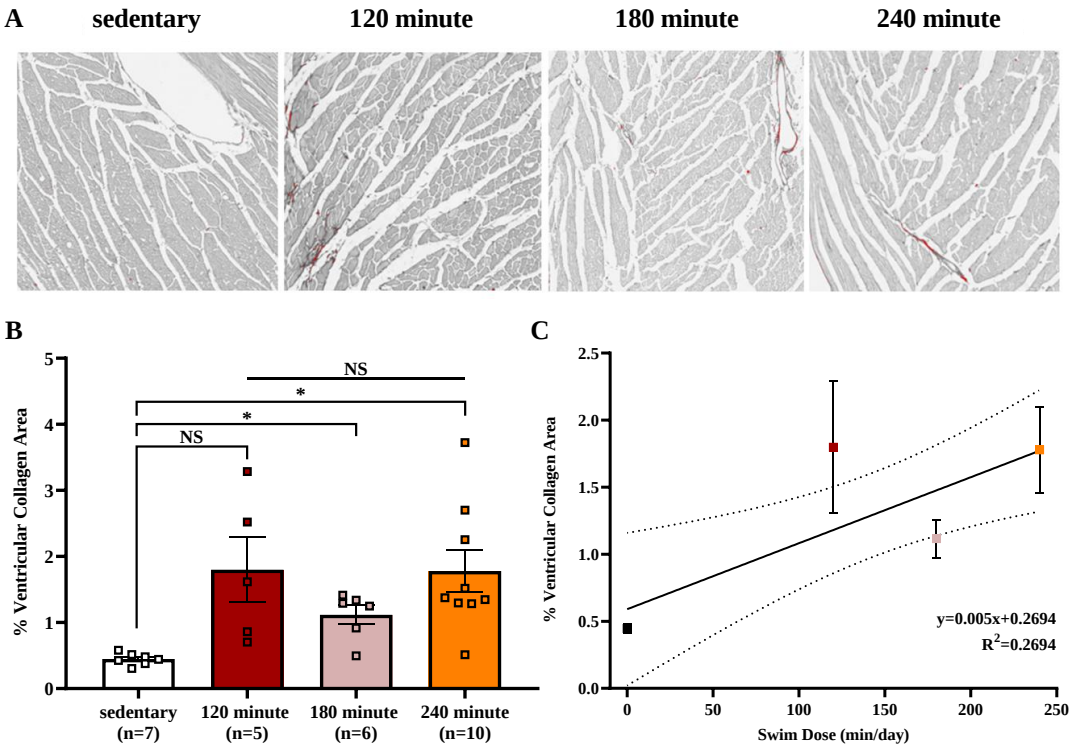

Figure 3.13. Swim Training Induced Minimal Ventricular Fibrosis. Left ventricular collagen content was identified using picrosirius red and imaged using a slide-scanner brightfield microscope at 20x. (A) Representative images of collagen content in the left ventricle. (B) Quantification of ventricular collagen involved selecting and counting pixels based on brightness (i.e., thresholding). (C) Linear regression analysis of swim dose and ventricular collagen data. The *n* values indicate the number of mice included. Data are Mean±SEM, **P*<0.05, using one-way ANOVA with Tukey's multiple comparisons tests (B).

The results above establish that increased AF vulnerability corresponds to differences in fibrosis but not AERP. As such, atrial hypertrophy is another atrial change linked to AF in endurance athletes [215]. We found that as daily exercise durations were prolonged, atrial (wet) weights normalized to either BW (i.e., AW/BW) or TL (i.e., AW/TL) were progressively increased [AW/BW: R^2=0.58, F(1,16)=22.29, *P*=0.0002 and AW/TL: R^2=0.56, F(1,16)=20.29, *P*=0.0004] as summarized in **Table 3.4** and **Figure 3.14.**

Table 3.4. Physical Atrial Parameters of Mice Swim-Trained for Variable Daily Durations.

	sedentary (control)	120 minute (60min 2x)	180 minute (90min 2x)	240 minute (120min 2x)
Body parameters n	*4*	*6*	*3*	*5*
Body Weight (g)	42.6 ±1.5	40.2 ± 1.0	38.0 ± 1.7	38.8 ± 1.2
Tibia Length (mm)	19.3 ± 0.09	19.6 ± 0.16	19.2 ± 0.3	19.3 ± 0.1
Atrial Weight (mg)	14.0 ± 0.6	15.6 ± 0.96	18.1 ± 0.5*	18.7 ± 0.5*
Atria/Body Weight (mg/g)	0.33 ± 0.01	0.39 ± 0.03	0.48 ± 0.03*	0.48 ± 0.02*
Atria/Tibia Length (mg/mm)	0.73 ± 0.03	0.80 ± 0.05	0.94 ± 0.04*	0.97 ± 0.02*
Atria/Ventricle Weight (mg/g)	93.0 ± 5.75	93.0 ± 6.63	123.9 ± 5.10*	108.1 ± 3.07

The *n* value shown presents number of mice included. Data presented as Mean±SEM.
*P<0.05, compared with sedentary using one-way ANOVA with Tukey's multiple comparisons tests.

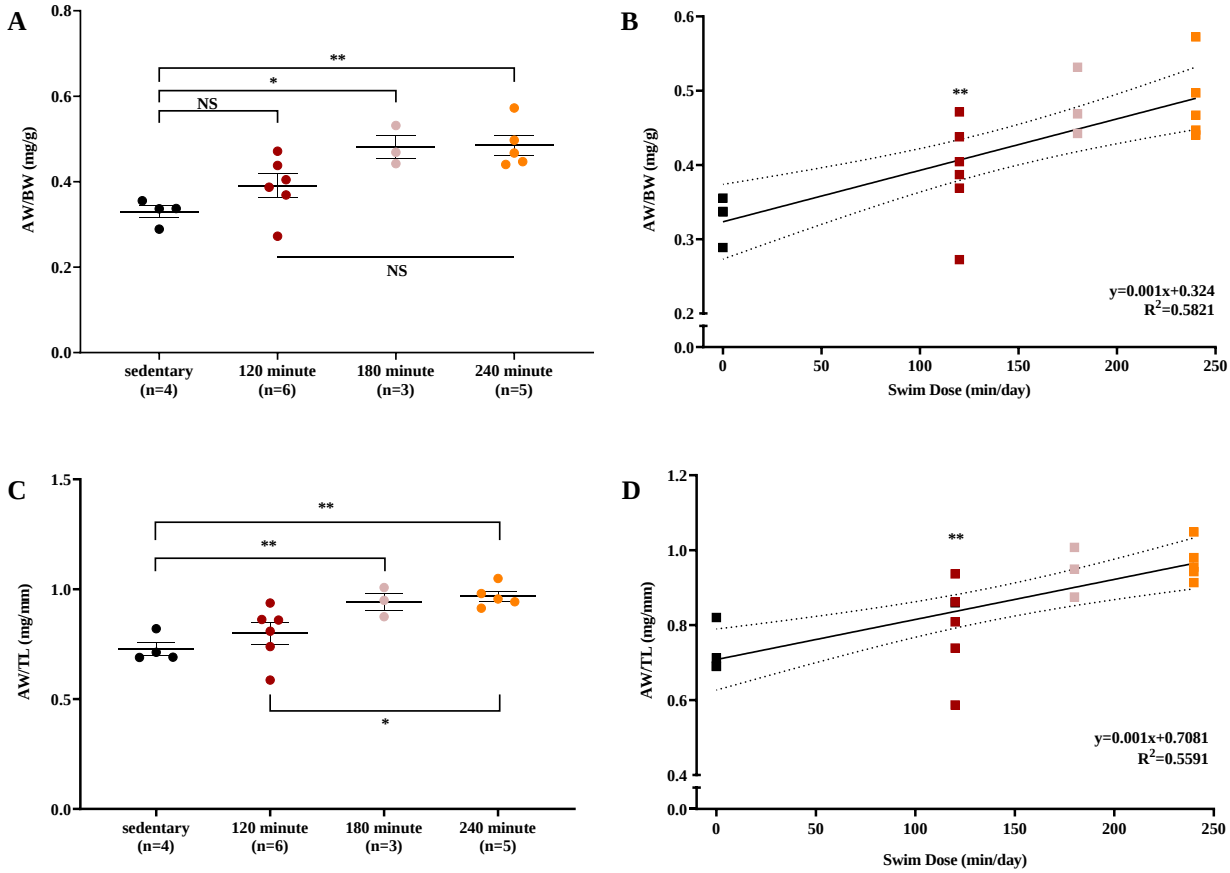

Figure 3.14. Linear Regression of Atrial Hypertrophy Measurements. (A) Atrial weight normalized to body weight (AW/BW) and (B) the corresponding linear regression analysis. (C) Atrial weight normalized to tibia length (AW/TL) and (D) the corresponding linear analysis. Data presented as Mean±SEM with **P<0.01; n=3 sedentary mice (black), n=6 120 minute mice (red), n=3 180 minute mice (pink) and n=5 240 minute mice (orange).

3.4.4. Atrial Macrophage Infiltration in Swim-Trained Mice

As tissue fibrosis is invariably associated with increased immune cell infiltration and inflammation [125], and based on previous findings that macrophages may play a prominent role in the immune response with exercise [189], we also quantified macrophage numbers in histological cardiac sections using F4-80 antibodies. Linear regression analyses showed that total macrophage numbers in the left atrial appendages increased strongly [R^2=0.65, F(1,21) = 38.65, P<0.0001] as daily training duration increased (**Figure 3.15**). By contrast, we found no difference (P=0.91) in macrophage numbers between control and swim groups in the ventricles and no dose dependency following linear regression analysis [R^2=0.24, F(1,10) = 3.19, P=0.1] (**Figure 3.16**).

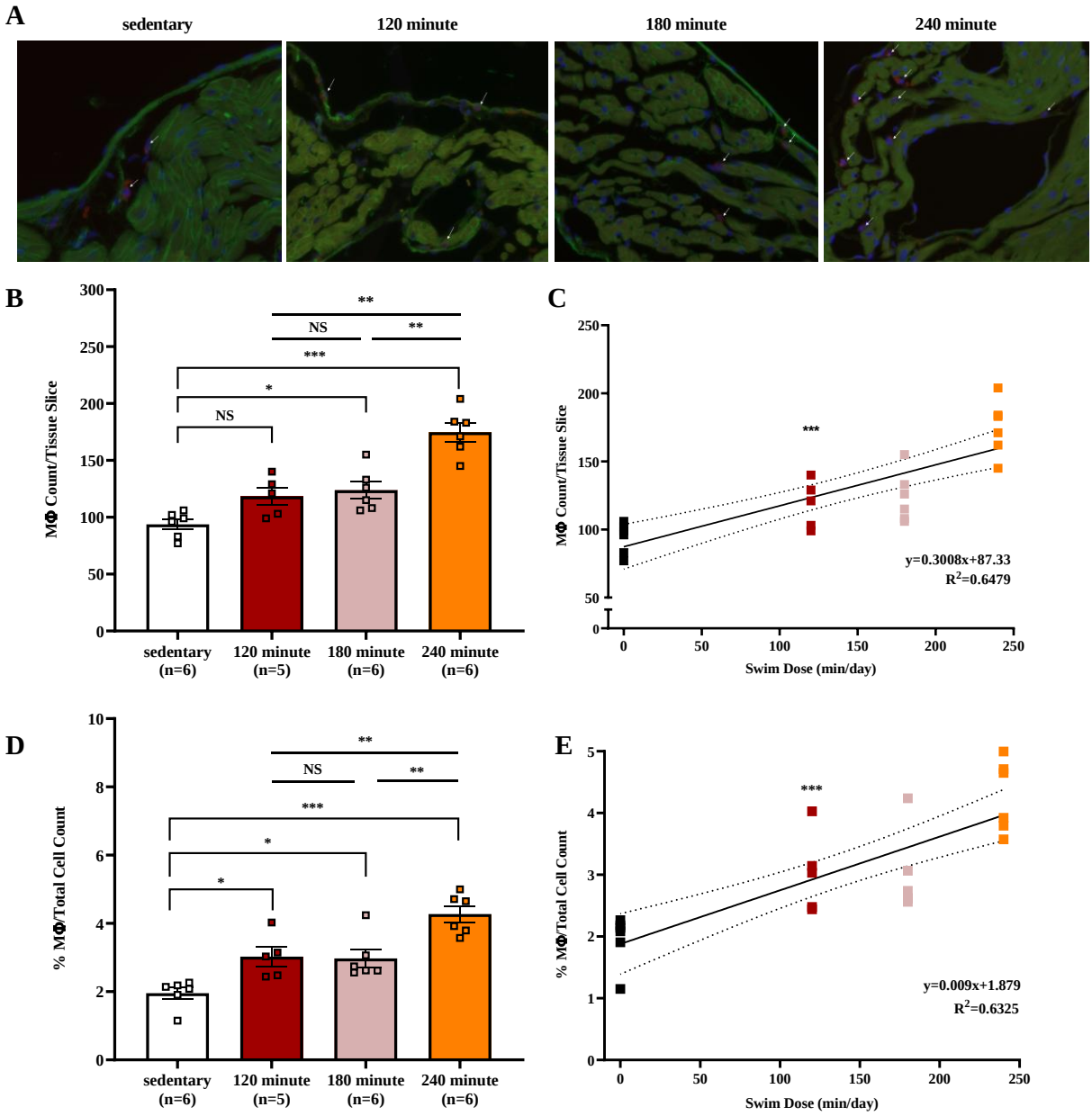

Figure 3.15. Swim Training at Variable Daily Durations Induces Atrial Inflammation. Given our observations of increased atrial collagen induced by swim training, we investigated for the presence of macrophages using immunohistochemistry with F4-80, a mature mouse cell surface glycoprotein expressed by macrophages. (A) Representative images of macrophages in the left atrial appendage. Note the visible increases in positive cells as daily training duration increases, evident by increased numbers of cells that co-stained for DAPI (indicating the nuclei) and F4-80 (macrophage marker). (B) Number of macrophages per tissue slice with (C) linear regression analysis as a function of daily swim dose. (D) Macrophages when normalized to total cell count with (E) linear regression analysis as a function of daily swim dose. The *n* values indicate the number of mice included. Data are Mean±SEM, **P*<0.05, ***P*<0.01, ****P*<0.0001, using one-way ANOVA with Tukey's multiple comparisons tests.

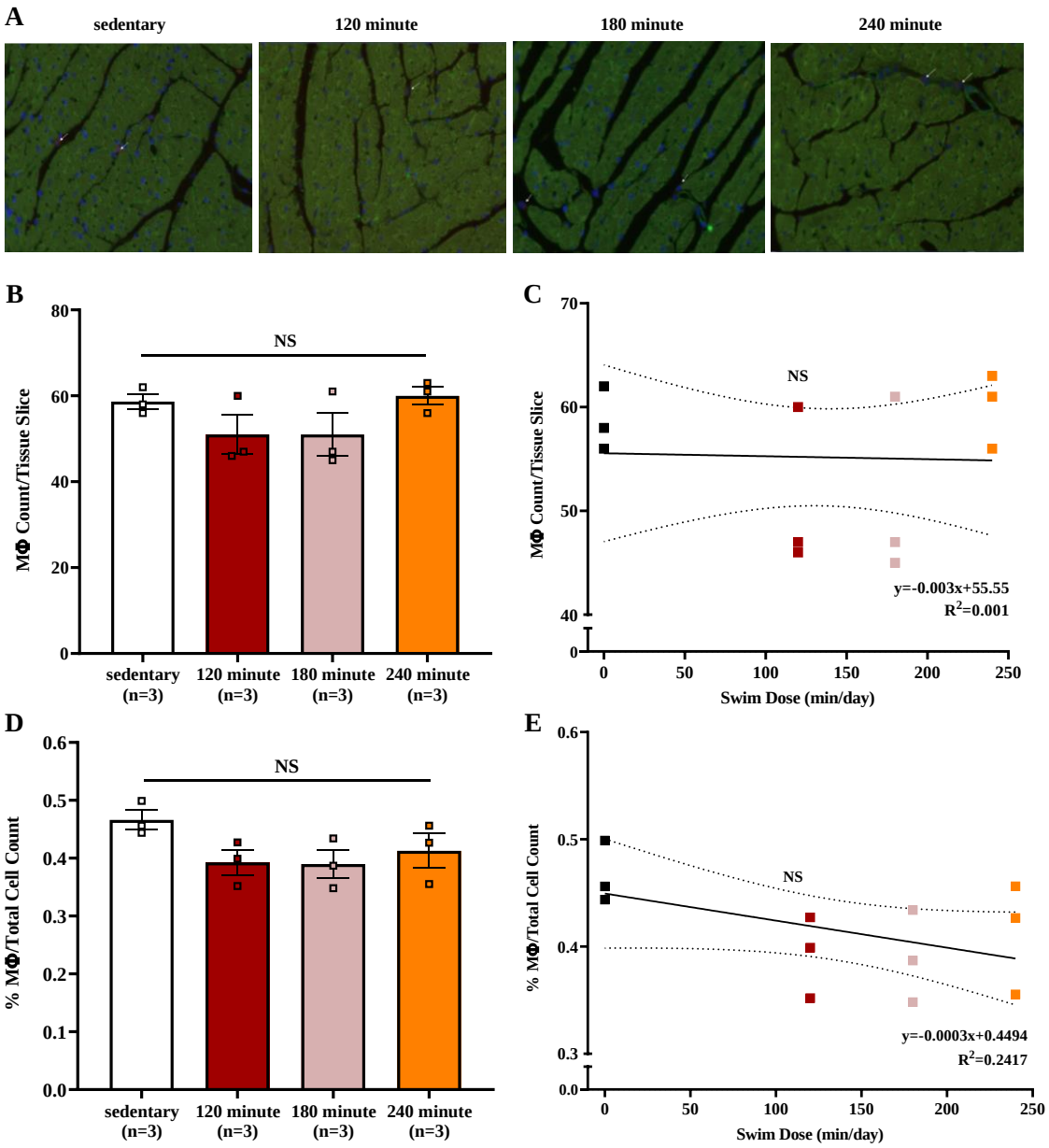

Figure 3.16. Swim Training at Variable Durations Does Not Cause Ventricular Inflammation. The presence of macrophages was examined using immunohistochemistry with F4-80 antibodies, a mature mouse cell surface glycoprotein expressed by macrophages. (A) Representative images of macrophages in the left ventricular free wall. (B/C) Macrophages count per tissue slice and (D/E) when normalized to total cell count. The *n* values indicate the number of mice included. Data are Mean±SEM, using one-way ANOVA with Tukey's multiple comparisons tests or linear regression analysis.

3.5 Discussion

Previous studies concluded that AF incidence shows a J-shaped dependence on exercise [135]. Specifically, individuals with sedentary lifestyles are associated with numerous risk factors for AF, including hypertension, metabolic disorders and obesity, which increase the risk of developing AF [210]. Fortunately, regular PA in the sedentary population can mitigate AF incidence [216]. On the other hand, elite endurance athletes, particularly in the veteran population, are at greater risk of developing AF. While several previous reports have explored the dependence of AF on "exercise dose" in athletes, these studies have relied invariably on self-reporting to quantify exercise [140]. To directly investigate the effects of exercise dose on AF vulnerability, we used a swim model of endurance training in mice, which we showed previously leads to increased AF induction [189]. We initially attempted varying exercise dose by adjusting current velocities (imposing different exercise intensities) but found that the mice self-regulate their swimming effort. Thus, we assessed exercise dose by altering the daily swim duration (i.e., 120, 180 or 240 minutes, divided into two sessions) while maintaining the same absolute work based on the total O_2 consumed during swimming (i.e., ~695 L of O_2/kg). Consequently, all mice swam for a consistent number of hours daily but did so over variable days (i.e., mice swimming for 120 minutes swam for 45 days versus 30 days for the 180 minute groups versus 22.5 days for 240 minute group).

Consistent with equivalent cumulative work during swims, we observed similar increases in skeletal muscle mitochondrial content (i.e., elevated COX enzyme activity) between the exercised groups relative to controls, as expected from previous human studies [217]. Alongside skeletal muscle adaptation, and as typically seen in endurance athletes and rodent exercise models [156,161,188], echocardiographic measurements revealed small, yet dose-dependent, reductions of fractional shortening and progressive ventricular dilation via gradual increases in both end-diastolic and end-systole volumes with lengthened daily swim durations. Linear regression analyses also established a strong dose-dependency of resting heart rate reductions with prolonged daily swim durations linked to enhanced parasympathetic activity and downregulation of sympathetic activity.

The direct impact of daily exercise dose on ventricular dilation and autonomic nerve-dependent HR reductions aligns well with observations that cardiac dilation and bradycardia are most pronounced in athletes engaged in high cardiac output sports [218]. In this regard, a key finding in our studies was the strong influence of daily exercise dose to progressively promote AF inducibility without influencing ventricular arrhythmia risk. Thus, our study shows novel *quantitative* connections between AF vulnerability and daily exercise dose, supporting previous human studies using self-reporting [219]. Moreover, consistent with elevated vagal tone in endurance athletes [213] and the potential links of higher parasympathetic activity to AF [220], especially in athletes [48], parasympathetic blockade using atropine treatment decreased AF susceptibility in association with increased AERP. Presumably, these protective effects are

mediated by blocking vagal-dependent activation of $I_{K,Ach}$ and possible blocking of I_{Ca} inhibition [221]. Experimental and computer models also show elevated parasympathetic activity can increase spatial dispersion and heterogeneity of atrial refractoriness resulting in ERP variability at different atrial sites, possibly caused by inhomogeneous nerve innervation and varying $I_{K,Ach}$ densities, that increase AF susceptibility [222]. More important, although we found clear evidence for elevated parasympathetic nerve activity as daily exercise dose is increased (as seen by the effects of atropine on HR and AERP), no differences in AERP were observed between any groups establishing that the increased AF vulnerability observed as daily exercise dose increased does not depend on variation in electrical refractoriness.

The absence of differences in AERP between the groups (despite alterations of vagal tone with exercise dose) suggests that the increased AF vulnerability is related to tissue factors such as atrial hypertrophy and fibrosis [168]. Consistent with the literature, we observed atrial hypertrophic remodelling in each swim group (measured by atrial weight normalized to body weight and tibia length) that increased with daily training duration. These findings are presumably caused by sustained preload elevations experienced during exercise [68] and are likewise observed in humans following exhaustive training [170]. Atrial hypertrophy thus permits an increased capacity to accommodate elevated workload through an amplified atrial ejection volume [168], yet excessive endurance exercise may cause severe atrial overload of the particularly vulnerable thin walls, modulating adverse remodelling [86,98]. Moreover, due to high atrial compliance, elevations in filling pressures may activate stretch-mediated pathways involving angiotensin II, tumour necrosis factor (TNF) and other pro-inflammatory and pro-fibrotic markers [86,222].

Thus, consistent with human studies showing that chronic endurance training may promote atrial fibrosis remodelling [191], we observed increased fibrosis in the atria, primarily in pericapsular regions, as daily exercise dose increased (based on linear regression analysis), with minimal to no effect on the ventricles. Direct evidence for the role of exercise-induced atrial fibrosis in AF pathogenesis has also been identified in several rodent studies [188,189] with the presumed intent to preserve structural integrity following hemodynamic stress. Furthermore, fibrotic remodelling remains an invariable hallmark of AF, regardless of the patient population [84].

Correspondingly, knowing the link between cardiac fibrosis, inflammation and arrhythmia susceptibility [83], we and others [224] hypothesized that atrial inflammation is also an integral feature of AF in athletes by recruiting circulating monocytes [225] and regulating resident tissue macrophages [226]. Accordingly, we found a significant increase in normalized macrophage numbers compared to controls, with considerable elevations as the daily exercise dose increased. Our observations are also consistent in human and rodent models, wherein macrophages are one of the primary immune cells that accumulate throughout the atria with AF [227]. Moreover, Oishi and colleagues [199] found that mechanical stretch *in vitro* and transverse aortic constriction *in vivo* induced atrial macrophage accumulation via extracellular

ATP-dependent recruitment through pannexin-2 channels in a mice model, further strengthening the association between atrial stretch and adverse remodelling. As such, our study is the first to demonstrate that exercise-induced inflammation in athletes has a dose dependency on daily training duration that increases with prolonged swimming periods, and we suspect that sustained atrial volume overload and stretch may contribute to the macrophage accumulation seen with strenuous endurance training.

Together, our results support the conclusion that a dose-dependent relationship exists between endurance training and AF, whereby the degree of sinus bradycardia and adverse atrial is contingent on daily swim duration, independent of intensity, frequency and total cumulative exercise. Notably, we found AF arising from excessive daily swimming shares comparable adverse remodelling seen in patients with CVD [228] and obesity [210], suggesting our study provides insightful implications on AF pathology irrespective of the patient population.

3.5.1 Limitations

Despite similar atrial remodelling and AF vulnerability, the extrapolation of murine findings to human athletes requires caution [8]. Note also that our training protocol is not voluntary. Nevertheless, we minimized stress by swimming the mice in their thermoneutral range, avoiding floating preventions that promote drowning (i.e., tail weights and bubbling) and maintaining water depth slightly above the vertical body length of a mouse for ground awareness. Also note that although swim groups were not age-matched at the time of endpoint assessments, due to the varying number of swim sessions required to achieve the same cumulative dose, the sedentary and 180 minute mice were identical, and controls were only 2.5 weeks younger than the 120 minute group and 1.5 weeks older than the 240 minute group.

Moreover, despite the concern that exercise intensity will decline with exposure to the same current (due to repetitive training adaptation), the mice gradually increase their engagement with the water current as the training programme progresses (i.e., continuously moving towards the perimeter of the bucket where the water current is most forceful).

Lastly, caution should be applied when comparing the results of the one-way ANOVA/Tukey multiple comparisons tests and the linear regression analysis. We included both as they provide insightful information regarding the relationship of daily exercise dose with each investigated parameter yet provide slightly varying interpretations of the data.

3.5.2. Conclusion

To our knowledge, this study is the first to employ a controlled swim model in mice that quantitatively assessed the influence of daily exercise dose on AF pathogenesis. As mentioned above, we propose that prolonged participation in excessive endurance activity imposes repetitive hemodynamic stress on the atria causing stretch and subsequent AF-related remodelling. In particular, mice demonstrate abrupt

increases in LV systolic pressure (LVSP), LV end-diastolic pressure (LVEDP) and HRs with swim onset, as expected with endurance exercise [68], whereby elevated LVSP remains throughout the swimming period alongside a continuous rise in LVEDP beyond ~45 minutes. Since the atria are highly compliant relative to ventricles, LVEDP elevations for extended periods can cause considerable volume overload in the atria [229], known to activate adverse remodelling pathways [86]. Thus, prolonged exposure could exacerbate the atrial response to exercise, acting as the primary driver of AF with extended swim durations that does not promote ventricular pathology or arrhythmia risk. Our results are consistent with this interpretation, as we observed progressive increases in vagal tone and adverse atrial-specific remodelling, including hypertrophy, fibrosis, macrophage accumulation and resultant AF inducibility with prolonged daily exercise bouts. Thus, increased AF risk in elite athletes can reflect over-recruitment of this stretch response, causing dose-dependent structural reinforcement at the cost of electrical perturbation.

3.5.3. Future Directions

Despite observing increased atrial macrophages with prolonged swim durations, characterization of the subtypes and the complex temporal and spatial relationship in response to endurance training has not been explored. As such, future studies should aim to elucidate the inflammatory response occurring with variable exercise doses and determine the specific role played in exercise-induced AF.

Furthermore, having established a quantitative relationship between daily training duration and AF susceptibility, atrial responses when mice swim for 240 minutes divided into shorter bouts (i.e., reducing the extent of continual atrial volume challenge) would be insightful. It would also be interesting to assess the effects of increasing the total cumulative dose achieved by the 240 minute subgroup. We suspect extended weeks of exposure will promote further adverse autonomic and atrial structural remodelling. To this end, we are investigating whether increasing the 240 minute training regime from 4.5 weeks to 6 weeks would support these hypotheses.

Chapter 4: Extended Discussion

This thesis sought to investigate the relationship between training-induced cardiac remodelling and AF vulnerability using a mouse swim model, with a particular focus on examining the effects of varying daily exercise dose. As such, we utilized a novel swim apparatus for training CD1 mice that mimicked chronic adaptations observed in endurance athletes and whereby training was quantified by measuring O_2 consumption during swims. Together, this allowed us to prospectively study the link between daily exercise dose and AF susceptibility under highly-controlled conditions of constant intensity, frequency and total cumulative work. The primary objectives were to characterize the dose-dependent relationship between daily training duration and AF and determine the pathophysiological mechanisms underlying arrhythmogenesis in swim-trained mice. As such, this model utilized techniques, including surface ECGs, echocardiography, *in vivo* electrophysiological studies, histology and immunohistochemistry, non-invasive hemodynamics and morphometry, to comprehensively assess the triggers, modulators and substrates mediating atrial arrhythmogenesis. I hypothesized that endurance training and AF vulnerability would demonstrate a dose-dependent relationship, and the adverse atrial remodelling (or extreme physiological response) underlying AF in swim-trained mice would depend on daily exercise dose. Indeed, the results quantitatively revealed that increasing daily swim dose (i.e., duration) caused progressive increases in AF inducibility, corresponding with gradual increases in bradycardia and cardiac vagal tone as well as atrial hypertrophy, fibrosis and inflammation. By contrast, the ventricles showed evidence of physiological remodelling consistent with the athlete's heart phenotype [152]. The lack of a similar atrial phenotype in the sedentary group and the increasing degrees of remodelling seen with extending daily swim duration suggests the prolonged nature of exercise bouts mediates this phenotype, supported by continuous elevations in preload throughout the swim.

4.2 Possible Pathways Between AF Remodelling with Exercise versus CVD

Our results support the conclusion that a quantitative dose-dependent relationship exists between daily exercise duration and AF, wherein cardiac responses observed with excessive endurance training share similar features with pathological remodelling seen in CVD [7]. However, AF manifestation with exercise versus CVD may involve somewhat distinct pathways. For example, physiological cardiac hypertrophy leads to enhanced cardiac function and metabolic activity, as observed in our swim mice. By contrast, pathological hypertrophy with CVD causes impaired contractile function, apoptosis and upregulated fetal gene expression [230]. Mechanistically, physiological hypertrophy requires proportional angiogenesis to expand the coronary vasculature and ensure adequate oxygen and nutrients for cardiomyocyte growth, whereas diseased states lack coronary expansion causing cardiac underperfusion and hypoxia [231]. Comparisons of different "athletic" (e.g., hare or wild rat) and sedentary (e.g., rabbit or

laboratory rat) animals reveal that cardiac capillary density is inversely related to heart rate [232]. Thus, in contrast to most CVDs associated with increased resting HRs [233], bradycardia with endurance training may improve cardiac perfusion by favouring diastolic filling (and thus coronary perfusion), shown to induce angiogenesis in normal hearts [234]. As such, our swim mice are consistent with the description of physiological, rather than pathological, cardiac hypertrophy, showing progressive reductions in HR with increased daily exercise and similar increases regarding atrial hypertrophy measurements.

Moreover, while fibrosis is typically an indicator of pathological remodelling in CVD, our laboratory has also recently shown that the increased atrial fibrosis associated with exercise occurs in the absence of increased collagen synthesis or upregulation of the TGF-β pathway [235], inconsistent with fibrosis seen in most cardiac conditions such as hypertension, HF and cardiomyopathies [236]. As shown in **Chapter 3**, we also found atrial fibrosis predominantly in the pericapsular regions rather than interstitial, inconsistent with myocardial damage seen in CVD [237]. Interestingly, the lack of elevated collagen mRNA in fibrotic exercised atria is similar to the discordant pattern with age-related fibrosis [238]. In this regard, a possible alternative explanation for the increased atrial collagen observed with exercise in our mice (and possibly age) may relate to lysyl oxidases (LOXs). In particular, LOX physiologically cross-links collagen, facilitating collagen fibril stability and digestion resistance by the action of the matrix metalloproteinases [239]. Moreover, given that (1) we previously showed no change in neutrophil, mast cell and myofibroblast counts with exercise [189], (2) chronic volume overload models show significant macrophage infiltrations (Barnes *et al*., 2014) and (3) preliminary data reveals co-localization of LOXL3 with macrophages in the swim exercise model (unpublished data), this may suggest the potential involvement of macrophages in the upregulation of LOX and LOXL enzymes promoting atrial collagen increases. In other words, the increase in atrial fibrosis observed in exercised mice may reflect increased collagen stability, rather than increased collagen deposition. These findings are also consistent with the progressive rise in both atrial fibrosis and macrophage accumulation we observed with increased daily swim durations and may suggest an alternative pathway whereby increased collagen intends to preserve structural integrity, representing an extreme manifestation of a physiological response.

4.3 Scaling of Exercise Dose and Response from Mouse Models to Humans

The task of precisely estimating how our swim protocols translate into human activity is difficult, as briefly discussed in **Chapter 3**. For example, our training protocol is not voluntary. Nevertheless, we believe that stress had minimal to no effects on atrial remodelling for several reasons. In addition to the rationale in **Chapter 3**, our swim-trained mice developed HR reductions, whereas mice subjected to psychosocial stress have chronic HR elevations [240]. Second, our laboratory previously collected fecal corticosterone levels from swim-trained groups, revealing no significant differences when compared to

sedentary mice. In fact, only slight increases in fecal corticosterone levels were observed in the exercised mice [189], similar to what has been reported in human endurance athletes [241].

Another factor to consider when comparing between species is how mice and humans augment CO during exercise. In addition to having much smaller hearts, mice intrinsically possess a resting HR of 500 to 600 bpm, whereas humans typically range from 60 to 100 bpm [8]. As such, HRs in humans can jump 3-4 times above baseline values with exercise stress, whereas mice demonstrate only ~50% elevations with exercise due to their already high resting HRs restricting further modulation [242]. As a result, exercise-induced CO can increase 5- to 10-fold in humans (via a combination of HR and SV) but only 1.3- to 2-fold in mice, with a greater reliance on stroke volume to augment function [242]. Thus, differences in CO augmentation could impact the exercise dose-response relationship in mice, with increases in preload predicted to invoke a more potent volume overload and stimulus for remodelling compared to humans. These species differences might also explain the appearance of atrial fibrosis, hypertrophy and an arrhythmogenic substrate after only 4.5-weeks of 240 minutes of swimming per day, yet the lack of prospective studies makes it difficult to estimate a theoretical period for the development of a similar phenotype in humans. Using a rough approximate established by Benito *et al*. [190] and considering a typical mouse life expectancy is 1 to 1.5 years, our 6- to 10-week exercise protocol (including the variable number of acclimation swims plus training periods) would be equivalent to ≈7.4 to 12.3 years of daily exercise training in humans, based on an average Canadian lifespan of 82 years. However, this estimate is incomplete and dependent on numerous assumptions, making it challenging to translate the workload of any animal training regime to that of a professional athlete. Nonetheless, the ability of our mouse swim model to recapitulate many of the phenotypic characteristics of the exercise-induced proarrhythmic phenotype on a much shorter timescale, suggests these findings will be invaluable moving forward to understand the factors and mechanisms that determine AF predisposition in endurance athletes and the exercise dose dependency. Moreover, previous studies have showed that atrial filling pressures during exercise are remarkedly similar between humans [170] and mice [189], implying a comparable exercise remodelling stimuli.

4.4 Dose-Response Relationship and Heterogeneous Cardiac Remodelling in Athletes

The exercise dose-response curve has only been partially delineated in humans. The optimal and minimal amounts of PA needed to achieve cardiovascular health benefits remain unresolved, with endurance athletes often exercising at levels 5-to-10-fold greater than the recommended guidelines [139] and requiring a sustained increase in CO that puts considerable hemodynamic stress on the heart, with particular burden on the atria [98]. As such, there appears to be a tipping point between adaptive and (potentially) maladaptive or extreme physiological phenotypes, yet it is clear that exercise is not a binary intervention as significant phenotypic inter-individual variability exists amongst athletes regarding the

exercise dose-response relationship that are not solely related to previous training [243]. For example, the same mutation that causes heart failure and arrhythmogenesis in one patient, can remain asymptomatic in another [244], with minority groups of non-responders and super-responders [245]. Additional factors likely account for this phenotypic variability, with the interaction between genetic and environmental determining the threshold for phenotypic expression. The complexity of inter-individual variability was also evident in our study whereby only a subset of mice from each swim group displayed atrial arrhythmia inducibility, despite completing the same daily exercise.

Taken together, we propose that prolonged participation in excessive endurance activity, as most elite athletes utilize, increases repetitive volume overload and causes subsequent remodelling that promotes AF. Importantly, the remodelling we observed in our swim-trained mice may reflect a protective process that reinforces the atrial myocardium in the face of hemodynamic stress. Thus, increased AF in elite athletes may represent the over-recruitment of this response, leading to structural reinforcement at the cost of electrical perturbation and is dependent on daily exercise dose.

4.4 Future Directions

While we have established an association between daily swim training and proarrhythmic atrial remodelling in mice, it is unknown whether this represents a permanent structural change or is reversible with deconditioning. In particular, Guasch *et al*. [100] observed fully reversed AF susceptibility in exercised rats without a reversal in atrial fibrosis. Thus, although important, atrial fibrosis is likely not the sole mechanism involved in exercise-induced AF susceptibility, yet monitoring detraining would allow us to confirm whether aspects of cardiac remodelling (i.e., hypertrophy, immune cell infiltration) and arrhythmia vulnerability are reversible, shedding light on whether this represents a pathological phenotype or the manifestation of an extreme physiological cardiac responses to excessive exercise. Moreover, although there exists some research in animal models, human studies are required to confirm the reversibility of underlying mechanisms and how athletes receive such recommendations.

Another critical factor is that only male mice were assessed, despite females reportedly having lower AF incidence regardless of the risk factors involved [246], and demonstrating reduced susceptibility with strenuous endurance training compared to men [247]. Thus, additional work regarding the influence of sex on exercise-induced AF remodelling, and whether females display an exercise dose-dependency with AF, in human athlete populations would be of great interest.

Furthermore, despite alluding to the potential role of LOX with exercised-induced atrial fibrosis, the relationship remains predominately unexplored and undoubtedly requires further investigation. For example, if LOX/LOXLs are involved in endurance training remodelling, what LOX and LOXL isoforms

are modulating collagen turnover, as well as their relative cellular origins and upstream regulators and downstream effectors? These questions are currently being investigated by Dr. Backx.

Lastly, as suggested in **Chapter 3**, it would also be compelling to assess the effects of increasing the total cumulative dose achieved by the 240 minute subgroup, as we suspect extended exposure will promote further adverse remodelling. As such, we briefly investigated whether prolonging the 240 minute training regime from 4.5 weeks to 6 weeks would support these conclusions. Remarkedly, we observed AF inducibility in 57% (4/7) of these mice (**Appendix Figure A.1**). However, unexpectedly, our preliminary results showed no significant differences between the sedentary and extended 240 minute mice regarding HRs at rest, following parasympathetic inhibition or with complete autonomic blockade, while also demonstrating considerable variability between mice (**Appendix Figure A.2**). One possible explanation is cardiac autonomic dysfunction, as seen with extreme overtraining [139]. AERPs for the extended 240 minute mice were also similar to sedentary mice, yet trended further towards reduction and had the highest percent change in durations following atropine administration (**Appendix Figure A.3**). Lastly, total atrial collagen notably increased in the extended 240 minute group compared to controls yet was similar to the other swim groups (**Appendix Figure A.4**). Thus, these findings help support a dose-dependency regarding cumulative dose on AF inducibility, suggesting modulation of all exercise parameters is likely required for achieving an optimal exercise dose without promoting AF.

Chapter 5: References

[1] M. Rienstra *et al.*, "Symptoms and functional status of patients with atrial fibrillation: state of the art and future research opportunities.," *Circulation*, vol. 125, no. 23, pp. 2933–43, Jun. 2012, doi: 10.1161/CIRCULATIONAHA.111.069450.

[2] C. R. Vasamreddy *et al.*, "Symptomatic and Asymptomatic Atrial Fibrillation in Patients Undergoing Radiofrequency Catheter Ablation," *J. Cardiovasc. Electrophysiol.*, vol. 17, no. 2, pp. 134–139, Feb. 2006, doi: 10.1111/j.1540-8167.2006.00359.x.

[3] D. M. Bers, "Cardiac excitation–contraction coupling," *Nature*, vol. 415, no. 6868, pp. 198–205, Jan. 2002, doi: 10.1038/415198a.

[4] D. C. Bartos, E. Grandi, and C. M. Ripplinger, "Ion Channels in the Heart," in *Comprehensive Physiology*, Wiley, 2015, pp. 1423–1464. doi: 10.1002/cphy.c140069.

[5] E. Carmeliet, "Cardiac Ionic Currents and Acute Ischemia: From Channels to Arrhythmias," *Physiol. Rev.*, vol. 79, no. 3, pp. 917–1017, Jul. 1999, doi: 10.1152/physrev.1999.79.3.917.

[6] C. L.-H. Huang, "Murine Electrophysiological Models of Cardiac Arrhythmogenesis," *Physiol. Rev.*, vol. 97, no. 1, pp. 283–409, Jan. 2017, doi: 10.1152/physrev.00007.2016.

[7] U. Schotten, S. Verheule, P. Kirchhof, and A. Goette, "Pathophysiological Mechanisms of Atrial Fibrillation: A Translational Appraisal," *Physiol. Rev.*, vol. 91, no. 1, pp. 265–325, Jan. 2011, doi: 10.1152/physrev.00031.2009.

[8] A. Varró *et al.*, "Cardiac transmembrane ion channels and action potentials: cellular physiology and arrhythmogenic behavior," *Physiol. Rev.*, vol. 101, no. 3, pp. 1083–1176, Jul. 2021, doi: 10.1152/physrev.00024.2019.

[9] A. Varró, D. A. Lathrop, S. B. Hester, P. P. Nánási, and J. G. Y. Papp, "Ionic currents and action potentials in rabbit, rat, and guinea pig ventricular myocytes," *Basic Res. Cardiol.*, vol. 88, no. 2, pp. 93–102, Mar. 1993, doi: 10.1007/BF00798257.

[10] D. Zipes, J. Jalife, and W. Stevenson, *Cardiac Electrophysiology: From Cell to Bedside* , Seventh Edition. 2017.

[11] S. Nattel, A. Maguy, S. Le Bouter, and Y.-H. Yeh, "Arrhythmogenic Ion-Channel Remodeling in the Heart: Heart Failure, Myocardial Infarction, and Atrial Fibrillation," *Physiol. Rev.*, vol. 87, no. 2, pp. 425–456, Apr. 2007, doi: 10.1152/physrev.00014.2006.

[12] L. Skibsbye and U. Ravens, "Mechanism of Proarrhythmic Effects of Potassium Channel Blockers," *Card. Electrophysiol. Clin.*, vol. 8, no. 2, pp. 395–410, Jun. 2016, doi: 10.1016/j.ccep.2016.02.004.

[13] C. Antzelevitch and A. Burashnikov, "Overview of Basic Mechanisms of Cardiac Arrhythmia," *Card. Electrophysiol. Clin.*, vol. 3, no. 1, pp. 23–45, Mar. 2011, doi: 10.1016/j.ccep.2010.10.012.

[14] E. Marban, S. W. Robinson, and W. G. Wier, "Mechanisms of arrhythmogenic delayed and early afterdepolarizations in ferret ventricular muscle.," *J. Clin. Invest.*, vol. 78, no. 5, pp. 1185–1192, Nov. 1986, doi: 10.1172/JCI112701.

[15] C. H. Luo and Y. Rudy, "A dynamic model of the cardiac ventricular action potential. I. Simulations of ionic currents and concentration changes.," *Circ. Res.*, vol. 74, no. 6, pp. 1071–1096, Jun. 1994, doi: 10.1161/01.RES.74.6.1071.

[16] B. Szabo, T. Kovacs, and R. Lazzara, "Role of Calcium Loading in Early Afterdepolarizations Generated by Cs^+ in Canine and Guinea Pig Purkinje Fibers," *J. Cardiovasc. Electrophysiol.*, vol. 6, no. 10, pp. 796–812, Oct. 1995, doi: 10.1111/j.1540-8167.1995.tb00356.x.

[17] H. Uchinoumi *et al.*, “CaMKII-dependent phosphorylation of RyR2 promotes targetable pathological RyR2 conformational shift,” *J. Mol. Cell. Cardiol.*, vol. 98, pp. 62–72, Sep. 2016, doi: 10.1016/j.yjmcc.2016.06.007.

[18] M. B. Liu, C. Y. Ko, Z. Song, A. Garfinkel, J. N. Weiss, and Z. Qu, “A Dynamical Threshold for Cardiac Delayed Afterdepolarization-Mediated Triggered Activity,” *Biophys. J.*, vol. 111, no. 11, pp. 2523–2533, Dec. 2016, doi: 10.1016/j.bpj.2016.10.009.

[19] G. R. Mines, “Further experiments on the action of the vagus on the electrogram of the frog’s heart,” *J. Physiol.*, vol. 47, no. 6, pp. 419–430, Feb. 1914, doi: 10.1113/jphysiol.1914.sp001634.

[20] N. Wiener and A. Rosenblueth, “The mathematical formulation of the problem of conduction of impulses in a network of connected excitable elements, specifically in cardiac muscle.,” *Arch. Inst. Cardiol. Mex.*, vol. 16, no. 3, pp. 205–65, Jul. 1946.

[21] E. G. Daoud *et al.*, “Effect of Atrial Fibrillation on Atrial Refractoriness in Humans,” *Circulation*, vol. 94, no. 7, pp. 1600–1606, Oct. 1996, doi: 10.1161/01.CIR.94.7.1600.

[22] M. Boutjdir *et al.*, “Inhomogeneity of Cellular Refractoriness in Human Atrium: Factor of Arrhythmia?.,” *Pacing Clin. Electrophysiol.*, vol. 9, no. 6, pp. 1095–1100, Nov. 1986, doi: 10.1111/j.1540-8159.1986.tb06676.x.

[23] J. A. Abildskov and R. L. Lux, “Spiral Waves in a Computer Model of Cardiac Excitation,” *Pacing Clin. Electrophysiol.*, vol. 17, no. 5, pp. 944–952, May 1994, doi: 10.1111/j.1540-8159.1994.tb01437.x.

[24] R. Coronel, F. J. G. Wilms-Schopman, T. Opthof, and M. J. Janse, “Dispersion of repolarization and arrhythmogenesis,” *Hear. Rhythm*, vol. 6, no. 4, pp. 537–543, Apr. 2009, doi: 10.1016/j.hrthm.2009.01.013.

[25] J. Heijman, N. Voigt, S. Nattel, and D. Dobrev, “Cellular and Molecular Electrophysiology of Atrial Fibrillation Initiation, Maintenance, and Progression,” *Circ. Res.*, vol. 114, no. 9, pp. 1483–1499, Apr. 2014, doi: 10.1161/CIRCRESAHA.114.302226.

[26] A. S. McGuirt, D. C. Schmacht, and J. L. Ardell, “Autonomic interactions for control of atrial rate are maintained after SA nodal parasympathectomy,” *Am. J. Physiol. Circ. Physiol.*, vol. 272, no. 6, pp. H2525–H2533, Jun. 1997, doi: 10.1152/ajpheart.1997.272.6.H2525.

[27] T. Kawashima, “The autonomic nervous system of the human heart with special reference to its origin, course, and peripheral distribution,” *Anat. Embryol. (Berl).*, vol. 209, no. 6, pp. 425–438, Jul. 2005, doi: 10.1007/s00429-005-0462-1.

[28] G. M. Mawe, E. K. Talmage, K. P. Lee, and R. L. Parsons, “Expression of choline acetyltransferase immunoreactivity in guinea pig cardiac ganglia,” *Cell Tissue Res.*, vol. 285, no. 2, pp. 281–286, Jul. 1996, doi: 10.1007/s004410050645.

[29] D. A. Hopkins and J. Andrew Armour, “Ganglionic distribution of afferent neurons innervating the canine heart and cardiopulmonary nerves,” *J. Auton. Nerv. Syst.*, vol. 26, no. 3, pp. 213–222, Apr. 1989, doi: 10.1016/0165-1838(89)90170-7.

[30] R. B. Schuessler, T. M. Grayson, B. I. Bromberg, J. L. Cox, and J. P. Boineau, “Cholinergically mediated tachyarrhythmias induced by a single extrastimulus in the isolated canine right atrium.,” *Circ. Res.*, vol. 71, no. 5, pp. 1254–1267, Nov. 1992, doi: 10.1161/01.RES.71.5.1254.

[31] Y.-J. Chen *et al.*, “Role of atrial electrophysiology and autonomic nervous system in patients with supraventricular tachycardia and paroxysmal atrial fibrillation,” *J. Am. Coll. Cardiol.*, vol. 32, no. 3, pp. 732–738, Sep. 1998, doi: 10.1016/S0735-1097(98)00305-2.

[32] R. K. Kharbanda, W. F. B. van der Does, L. N. van Staveren, Y. J. H. J. Taverne, A. J. J. C. Bogers, and N. M. S. de Groot, “Vagus Nerve Stimulation and Atrial Fibrillation: Revealing the

Paradox," *Neuromodulation Technol. Neural Interface*, vol. 25, no. 3, pp. 356–365, Apr. 2022, doi: 10.1016/j.neurom.2022.01.008.

[33] H. Dobrzynski *et al.*, "Distribution of the Muscarinic K+ Channel Proteins Kir3.1 and Kir3.4 in the Ventricle, Atrium, and Sinoatrial Node of Heart," *J. Histochem. Cytochem.*, vol. 49, no. 10, pp. 1221–1234, Oct. 2001, doi: 10.1177/002215540104901004.

[34] J. L. Smeets, M. A. Allessie, W. J. Lammers, F. I. Bonke, and J. Hollen, "The wavelength of the cardiac impulse and reentrant arrhythmias in isolated rabbit atrium. The role of heart rate, autonomic transmitters, temperature, and potassium.," *Circ. Res.*, vol. 58, no. 1, pp. 96–108, Jan. 1986, doi: 10.1161/01.RES.58.1.96.

[35] T. Tomita *et al.*, "Role of Autonomic Tone in the Initiation and Termination of Paroxysmal Atrial Fibrillation in Patients Without Structural Heart Disease," *J. Cardiovasc. Electrophysiol.*, vol. 14, no. 6, pp. 559–564, Jun. 2003, doi: 10.1046/j.1540-8167.2003.02462.x.

[36] R. B. Schnabel *et al.*, "50 year trends in atrial fibrillation prevalence, incidence, risk factors, and mortality in the Framingham Heart Study: a cohort study," *Lancet*, vol. 386, no. 9989, pp. 154–162, Jul. 2015, doi: 10.1016/S0140-6736(14)61774-8.

[37] E. J. Benjamin *et al.*, "Heart Disease and Stroke Statistics—2019 Update: A Report From the American Heart Association," *Circulation*, vol. 139, no. 10, Mar. 2019, doi: 10.1161/CIR.0000000000000659.

[38] L. Mou *et al.*, "Lifetime Risk of Atrial Fibrillation by Race and Socioeconomic Status," *Circ. Arrhythmia Electrophysiol.*, vol. 11, no. 7, Jul. 2018, doi: 10.1161/CIRCEP.118.006350.

[39] J. G. Andrade *et al.*, "The 2020 Canadian Cardiovascular Society/Canadian Heart Rhythm Society Comprehensive Guidelines for the Management of Atrial Fibrillation," *Can. J. Cardiol.*, vol. 36, no. 12, pp. 1847–1948, Dec. 2020, doi: 10.1016/j.cjca.2020.09.001.

[40] B. P. Krijthe *et al.*, "Projections on the number of individuals with atrial fibrillation in the European Union, from 2000 to 2060," *Eur. Heart J.*, vol. 34, no. 35, pp. 2746–2751, Sep. 2013, doi: 10.1093/eurheartj/eht280.

[41] C.-E. Chiang, K.-L. Wang, and G. Y. H. Lip, "Stroke prevention in atrial fibrillation: An Asian perspective," *Thromb. Haemost.*, vol. 111, no. 05, pp. 789–797, Nov. 2014, doi: 10.1160/TH13-11-0948.

[42] J. Kornej, C. S. Börschel, E. J. Benjamin, and R. B. Schnabel, "Epidemiology of Atrial Fibrillation in the 21st Century," *Circ. Res.*, vol. 127, no. 1, pp. 4–20, Jun. 2020, doi: 10.1161/CIRCRESAHA.120.316340.

[43] N.-H. Pan, H.-M. Tsao, N.-C. Chang, Y.-J. Chen, and S.-A. Chen, "Aging Dilates Atrium and Pulmonary Veins," *Chest*, vol. 133, no. 1, pp. 190–196, Jan. 2008, doi: 10.1378/chest.07-1769.

[44] W. Wongcharoen, Y.-C. Chen, Y.-J. Chen, C.-I. Lin, and S.-A. Chen, "Effects of Aging and Ouabain on Left Atrial Arrhythmogenicity," *J. Cardiovasc. Electrophysiol.*, vol. 18, no. 5, pp. 526–531, May 2007, doi: 10.1111/j.1540-8167.2007.00781.x.

[45] K. E. Odening *et al.*, "Mechanisms of sex differences in atrial fibrillation: role of hormones and differences in electrophysiology, structure, function, and remodelling," *EP Eur.*, vol. 21, no. 3, pp. 366–376, Mar. 2019, doi: 10.1093/europace/euy215.

[46] A. S. Volgman, M. F. Manankil, D. Mookherjee, and R. G. Trohman, "Women with atrial fibrillation: Greater risk, less attention," *Gend. Med.*, vol. 6, no. 3, pp. 419–432, Sep. 2009, doi: 10.1016/j.genm.2009.09.008.

[47] J. G. Andrade, M. W. Deyell, A. Y. K. Lee, and L. Macle, "Sex Differences in Atrial Fibrillation," *Can. J. Cardiol.*, vol. 34, no. 4, pp. 429–436, Apr. 2018, doi: 10.1016/j.cjca.2017.11.022.

[48] S. Saba *et al.*, "Effects of Estrogen on Cardiac Electrophysiology in Female Mice," *J. Cardiovasc. Electrophysiol.*, vol. 13, no. 3, pp. 276–280, Mar. 2002, doi: 10.1046/j.1540-8167.2002.00276.x.

[49] G. M. . Rosano *et al.*, "Acute electrophysiologic effect of estradiol 17β in menopausal women," *Am. J. Cardiol.*, vol. 86, no. 12, pp. 1385–1387, Dec. 2000, doi: 10.1016/S0002-9149(00)01251-0.

[50] H. Cochet *et al.*, "Age, Atrial Fibrillation, and Structural Heart Disease Are the Main Determinants of Left Atrial Fibrosis Detected by Delayed-Enhanced Magnetic Resonance Imaging in a General Cardiology Population," *J. Cardiovasc. Electrophysiol.*, vol. 26, no. 5, pp. 484–492, May 2015, doi: 10.1111/jce.12651.

[51] C. J. Rodriguez *et al.*, "Atrial fibrillation incidence and risk factors in relation to race-ethnicity and the population attributable fraction of atrial fibrillation risk factors: the Multi-Ethnic Study of Atherosclerosis," *Ann. Epidemiol.*, vol. 25, no. 2, pp. 71-76.e1, Feb. 2015, doi: 10.1016/j.annepidem.2014.11.024.

[52] G. M. Marcus *et al.*, "Racial Differences in Atrial Fibrillation Prevalence and Left Atrial Size," *Am. J. Med.*, vol. 123, no. 4, pp. 375.e1-375.e7, Apr. 2010, doi: 10.1016/j.amjmed.2009.05.019.

[53] J. D. Roberts *et al.*, "Genetic Investigation Into the Differential Risk of Atrial Fibrillation Among Black and White Individuals," *JAMA Cardiol.*, vol. 1, no. 4, p. 442, Jul. 2016, doi: 10.1001/jamacardio.2016.1185.

[54] K. K. Poppe *et al.*, "Ethnic-Specific Normative Reference Values for Echocardiographic LA and LV Size, LV Mass, and Systolic Function," *JACC Cardiovasc. Imaging*, vol. 8, no. 6, pp. 656–665, Jun. 2015, doi: 10.1016/j.jcmg.2015.02.014.

[55] M. J. Ackerman *et al.*, "Spectrum and prevalence of cardiac sodium channel variants among black, white, Asian, and Hispanic individuals: Implications for arrhythmogenic susceptibility and Brugada/long QT syndrome genetic testing," *Hear. Rhythm*, vol. 1, no. 5, pp. 600–607, Nov. 2004, doi: 10.1016/j.hrthm.2004.07.013.

[56] E. J. Benjamin, D. Levy, S. M. Vaziri, R. B. D'Agostino, A. J. Belanger, and P. A. Wolf, "Independent risk factors for atrial fibrillation in a population-based cohort. The Framingham Heart Study.," *JAMA*, vol. 271, no. 11, pp. 840–4, Mar. 1994.

[57] Y.-F. Lau, K.-H. Yiu, C.-W. Siu, and H.-F. Tse, "Hypertension and atrial fibrillation: epidemiology, pathophysiology and therapeutic implications," *J. Hum. Hypertens.*, vol. 26, no. 10, pp. 563–569, Oct. 2012, doi: 10.1038/jhh.2011.105.

[58] M. S. Dzeshka, G. Y. H. Lip, V. Snezhitskiy, and E. Shantsila, "Cardiac Fibrosis in Patients With Atrial Fibrillation," *J. Am. Coll. Cardiol.*, vol. 66, no. 8, pp. 943–959, Aug. 2015, doi: 10.1016/j.jacc.2015.06.1313.

[59] A. O. Odegaard, D. R. Jacobs, O. A. Sanchez, D. C. Goff, A. P. Reiner, and M. D. Gross, "Oxidative stress, inflammation, endothelial dysfunction and incidence of type 2 diabetes," *Cardiovasc. Diabetol.*, vol. 15, no. 1, p. 51, Dec. 2016, doi: 10.1186/s12933-016-0369-6.

[60] H. Shan *et al.*, "Downregulation of miR-133 and miR-590 contributes to nicotine-induced atrial remodelling in canines," *Cardiovasc. Res.*, vol. 83, no. 3, pp. 465–472, Aug. 2009, doi: 10.1093/cvr/cvp130.

[61] H. Wang *et al.*, "Nicotine Is a Potent Blocker of the Cardiac A-Type K^+ Channels," *Circulation*, vol. 102, no. 10, pp. 1165–1171, Sep. 2000, doi: 10.1161/01.CIR.102.10.1165.

[62] A. Hruby and F. B. Hu, "The Epidemiology of Obesity: A Big Picture," *Pharmacoeconomics*, vol. 33, no. 7, pp. 673–689, Jul. 2015, doi: 10.1007/s40273-014-0243-x.

[63] M. Kubala, C. de Chillou, Y. Bohbot, P. Lancellotti, M. Enriquez-Sarano, and C. Tribouilloy, "Arrhythmias in Patients With Valvular Heart Disease: Gaps in Knowledge and the Way

Forward," *Front. Cardiovasc. Med.*, vol. 9, Feb. 2022, doi: 10.3389/fcvm.2022.792559.

[64] K. S. Dujardin, M. Enriquez-Sarano, H. V. Schaff, K. R. Bailey, J. B. Seward, and A. J. Tajik, "Mortality and Morbidity of Aortic Regurgitation in Clinical Practice," *Circulation*, vol. 99, no. 14, pp. 1851–1857, Apr. 1999, doi: 10.1161/01.CIR.99.14.1851.

[65] A. Banerjee *et al.*, "Subtypes of atrial fibrillation with concomitant valvular heart disease derived from electronic health records: phenotypes, population prevalence, trends and prognosis," *EP Eur.*, vol. 21, no. 12, pp. 1776–1784, Dec. 2019, doi: 10.1093/europace/euz220.

[66] S. M. Vaziri, M. G. Larson, E. J. Benjamin, and D. Levy, "Echocardiographic predictors of nonrheumatic atrial fibrillation. The Framingham Heart Study.," *Circulation*, vol. 89, no. 2, pp. 724–730, Feb. 1994, doi: 10.1161/01.CIR.89.2.724.

[67] Y. C. Chen, A. Voskoboinik, A. La Gerche, T. H. Marwick, and J. R. McMullen, "Prevention of Pathological Atrial Remodeling and Atrial Fibrillation," *J. Am. Coll. Cardiol.*, vol. 77, no. 22, pp. 2846–2864, Jun. 2021, doi: 10.1016/j.jacc.2021.04.012.

[68] R. Lakin, R. Debi, N. Polidovitch, W. Chen, S. Yakobov, and P. Backx, "Atrial Stretch-Dependent Tumor Necrosis Factor-Mediated Adverse Atrial Remodeling and Atrial Arrhythmia Inducibility in a Mouse Model of Aortic Regurgitation," *Can. J. Cardiol.*, vol. 37, no. 10, p. S3, Oct. 2021, doi: 10.1016/j.cjca.2021.07.023.

[69] K. A. L. Mueller *et al.*, "Histopathological and Immunological Characteristics of Tachycardia-Induced Cardiomyopathy," *J. Am. Coll. Cardiol.*, vol. 69, no. 17, pp. 2160–2172, May 2017, doi: 10.1016/j.jacc.2017.02.049.

[70] S. S. Rathore *et al.*, "Acute Myocardial Infarction Complicated by Atrial Fibrillation in the Elderly," *Circulation*, vol. 101, no. 9, pp. 969–974, Mar. 2000, doi: 10.1161/01.CIR.101.9.969.

[71] M. Daccarett *et al.*, "Association of Left Atrial Fibrosis Detected by Delayed-Enhancement Magnetic Resonance Imaging and the Risk of Stroke in Patients With Atrial Fibrillation," *J. Am. Coll. Cardiol.*, vol. 57, no. 7, pp. 831–838, Feb. 2011, doi: 10.1016/j.jacc.2010.09.049.

[72] E. J. Benjamin, R. B. D'Agostino, A. J. Belanger, P. A. Wolf, and D. Levy, "Left Atrial Size and the Risk of Stroke and Death," *Circulation*, vol. 92, no. 4, pp. 835–841, Aug. 1995, doi: 10.1161/01.CIR.92.4.835.

[73] E. Wettwer *et al.*, "Role of IKur in Controlling Action Potential Shape and Contractility in the Human Atrium," *Circulation*, vol. 110, no. 16, pp. 2299–2306, Oct. 2004, doi: 10.1161/01.CIR.0000145155.60288.71.

[74] M. C. E. F. Wijffels, C. J. H. J. Kirchhof, R. Dorland, and M. A. Allessie, "Atrial Fibrillation Begets Atrial Fibrillation," *Circulation*, vol. 92, no. 7, pp. 1954–1968, Oct. 1995, doi: 10.1161/01.CIR.92.7.1954.

[75] B. Liang *et al.*, "G-protein-coupled inward rectifier potassium current contributes to ventricular repolarization," *Cardiovasc. Res.*, vol. 101, no. 1, pp. 175–184, Jan. 2014, doi: 10.1093/cvr/cvt240.

[76] D. Dobrev *et al.*, "The G Protein–Gated Potassium Current $I_{K,ACh}$ Is Constitutively Active in Patients With Chronic Atrial Fibrillation," *Circulation*, vol. 112, no. 24, pp. 3697–3706, Dec. 2005, doi: 10.1161/CIRCULATIONAHA.105.575332.

[77] J. Heijman *et al.*, "Muscarinic type-1 receptors contribute to I K,ACh in human atrial cardiomyocytes and are upregulated in patients with chronic atrial fibrillation," *Int. J. Cardiol.*, vol. 255, pp. 61–68, Mar. 2018, doi: 10.1016/j.ijcard.2017.12.050.

[78] D. Dobrev, "Atrial Ca2+/calmodulin-dependent protein kinase II: A druggable master switch of atrial fibrillation-associated atrial remodeling?," *Hear. Rhythm*, vol. 16, no. 7, pp. 1089–1090, Jul.

2019, doi: 10.1016/j.hrthm.2019.02.002.

[79] N. Voigt *et al.*, "Enhanced Sarcoplasmic Reticulum Ca $^{2+}$ Leak and Increased Na $^{+}$ -Ca $^{2+}$ Exchanger Function Underlie Delayed Afterdepolarizations in Patients With Chronic Atrial Fibrillation," *Circulation*, vol. 125, no. 17, pp. 2059–2070, May 2012, doi: 10.1161/CIRCULATIONAHA.111.067306.

[80] S. Nattel, J. Heijman, L. Zhou, and D. Dobrev, "Molecular Basis of Atrial Fibrillation Pathophysiology and Therapy," *Circ. Res.*, vol. 127, no. 1, pp. 51–72, Jun. 2020, doi: 10.1161/CIRCRESAHA.120.316363.

[81] J. Gemel *et al.*, "Connexin40 abnormalities and atrial fibrillation in the human heart," *J. Mol. Cell. Cardiol.*, vol. 76, pp. 159–168, Nov. 2014, doi: 10.1016/j.yjmcc.2014.08.021.

[82] H. M. W. VELDEN *et al.*, "Altered Pattern of Connexin40 Distribution in Persistent Atrial Fibrillation in the Goat," *J. Cardiovasc. Electrophysiol.*, vol. 9, no. 6, pp. 596–607, Jun. 1998, doi: 10.1111/j.1540-8167.1998.tb00940.x.

[83] A. Frustaci, C. Chimenti, F. Bellocci, E. Morgante, M. A. Russo, and A. Maseri, "Histological Substrate of Atrial Biopsies in Patients With Lone Atrial Fibrillation," *Circulation*, vol. 96, no. 4, pp. 1180–1184, Aug. 1997, doi: 10.1161/01.CIR.96.4.1180.

[84] A. Y. Tan and P. Zimetbaum, "Atrial Fibrillation and Atrial Fibrosis," *J. Cardiovasc. Pharmacol.*, vol. 57, no. 6, pp. 625–629, Jun. 2011, doi: 10.1097/FJC.0b013e3182073c78.

[85] M. D. Flannery, J. M. Kalman, P. Sanders, and A. La Gerche, "State of the Art Review: Atrial Fibrillation in Athletes," *Hear. Lung Circ.*, vol. 26, no. 9, pp. 983–989, Sep. 2017, doi: 10.1016/j.hlc.2017.05.132.

[86] A. M. De Jong, A. H. Maass, S. U. Oberdorf-Maass, D. J. Van Veldhuisen, W. H. Van Gilst, and I. C. Van Gelder, "Mechanisms of atrial structural changes caused by stretch occurring before and during early atrial fibrillation," *Cardiovasc. Res.*, vol. 89, no. 4, pp. 754–765, Mar. 2011, doi: 10.1093/cvr/cvq357.

[87] D. A. Patel, C. J. Lavie, R. V Milani, S. Shah, and Y. Gilliland, "Clinical implications of left atrial enlargement: a review.," *Ochsner J.*, vol. 9, no. 4, pp. 191–6, 2009.

[88] H. R. L. Fraser and R. Turner, "Electrocardiography in Mitral Vavular Disease," *Heart*, vol. 17, no. 4, pp. 459–483, Oct. 1955, doi: 10.1136/hrt.17.4.459.

[89] W. L. Henry *et al.*, "Relation between echocardiographically determined left atrial size and atrial fibrillation.," *Circulation*, vol. 53, no. 2, pp. 273–279, Feb. 1976, doi: 10.1161/01.CIR.53.2.273.

[90] R. Khatib, P. Joseph, M. Briel, S. Yusuf, and J. Healey, "Blockade of the renin–angiotensin–aldosterone system (RAAS) for primary prevention of non-valvular atrial fibrillation: A systematic review and meta analysis of randomized controlled trials," *Int. J. Cardiol.*, vol. 165, no. 1, pp. 17–24, Apr. 2013, doi: 10.1016/j.ijcard.2012.02.009.

[91] F. Ravelli and M. Allessie, "Effects of Atrial Dilatation on Refractory Period and Vulnerability to Atrial Fibrillation in the Isolated Langendorff-Perfused Rabbit Heart," *Circulation*, vol. 96, no. 5, pp. 1686–1695, Sep. 1997, doi: 10.1161/01.CIR.96.5.1686.

[92] F. Bode, A. Katchman, R. L. Woosley, and M. R. Franz, "Gadolinium Decreases Stretch-Induced Vulnerability to Atrial Fibrillation," *Circulation*, vol. 101, no. 18, pp. 2200–2205, May 2000, doi: 10.1161/01.CIR.101.18.2200.

[93] S. C. M. Eijsbouts, M. Majidi, M. van Zandvoort, and M. A. Allessie, "Effects of Acute Atrial Dilation on Heterogeneity in Conduction in the Isolated Rabbit Heart," *J. Cardiovasc. Electrophysiol.*, vol. 14, no. 3, pp. 269–278, Mar. 2003, doi: 10.1046/j.1540-8167.2003.02280.x.

[94] J. Kalifa *et al.*, “Intra-Atrial Pressure Increases Rate and Organization of Waves Emanating From the Superior Pulmonary Veins During Atrial Fibrillation,” *Circulation*, vol. 108, no. 6, pp. 668–671, Aug. 2003, doi: 10.1161/01.CIR.0000086979.39843.7B.

[95] J. Eckstein, S. Verheule, N. de Groot, M. Allessie, and U. Schotten, “Mechanisms of perpetuation of atrial fibrillation in chronically dilated atria,” *Prog. Biophys. Mol. Biol.*, vol. 97, no. 2–3, pp. 435–451, Jun. 2008, doi: 10.1016/j.pbiomolbio.2008.02.019.

[96] M. J. Janse, R. Coronel, F. J. . Wilms-Schopman, and J. R. de Groot, “Mechanical effects on arrhythmogenesis: from pipette to patient,” *Prog. Biophys. Mol. Biol.*, vol. 82, no. 1–3, pp. 187–195, May 2003, doi: 10.1016/S0079-6107(03)00015-4.

[97] Y. Chen *et al.*, “Tumor necrosis factor-α produced in cardiomyocytes mediates a predominant myocardial inflammatory response to stretch in early volume overload,” *J. Mol. Cell. Cardiol.*, vol. 49, no. 1, pp. 70–78, Jul. 2010, doi: 10.1016/j.yjmcc.2009.12.013.

[98] D. R. Hamilton, R. S. Dani, R. A. Semlacher, E. R. Smith, T. M. Kieser, and J. V Tyberg, “Right atrial and right ventricular transmural pressures in dogs and humans. Effects of the pericardium.,” *Circulation*, vol. 90, no. 5, pp. 2492–2500, Nov. 1994, doi: 10.1161/01.CIR.90.5.2492.

[99] C. Chimenti, M. A. Russo, A. Carpi, and A. Frustaci, “Histological substrate of human atrial fibrillation,” *Biomed. Pharmacother.*, vol. 64, no. 3, pp. 177–183, Mar. 2010, doi: 10.1016/j.biopha.2009.09.017.

[100] E. Guasch *et al.*, “Atrial Fibrillation Promotion by Endurance Exercise,” *J. Am. Coll. Cardiol.*, vol. 62, no. 1, pp. 68–77, Jul. 2013, doi: 10.1016/j.jacc.2013.01.091.

[101] M. A. Rossi, “Connective tissue skeleton in the normal left ventricle and in hypertensive left ventricular hypertrophy and chronic chagasic myocarditis.,” *Med. Sci. Monit.*, vol. 7, no. 4, pp. 820–32, 2001.

[102] F. G. Spinale, “Myocardial Matrix Remodeling and the Matrix Metalloproteinases: Influence on Cardiac Form and Function,” *Physiol. Rev.*, vol. 87, no. 4, pp. 1285–1342, Oct. 2007, doi: 10.1152/physrev.00012.2007.

[103] M. H. Luo, Y. S. Li, and K. P. Yang, “Fibrosis of Collagen I and Remodeling of Connexin 43 in Atrial Myocardium of Patients with Atrial Fibrillation,” *Cardiology*, vol. 107, no. 4, pp. 248–253, 2007, doi: 10.1159/000095501.

[104] P. Kong, P. Christia, and N. G. Frangogiannis, “The pathogenesis of cardiac fibrosis,” *Cell. Mol. Life Sci.*, vol. 71, no. 4, pp. 549–574, Feb. 2014, doi: 10.1007/s00018-013-1349-6.

[105] T. Nagai *et al.*, “Decreased Myocardial Dendritic Cells is Associated With Impaired Reparative Fibrosis and Development of Cardiac Rupture After Myocardial Infarction in Humans,” *J. Am. Heart Assoc.*, vol. 3, no. 3, May 2014, doi: 10.1161/JAHA.114.000839.

[106] K. Schimmel, K. Ichimura, S. Reddy, F. Haddad, and E. Spiekerkoetter, “Cardiac Fibrosis in the Pressure Overloaded Left and Right Ventricle as a Therapeutic Target,” *Front. Cardiovasc. Med.*, vol. 9, May 2022, doi: 10.3389/fcvm.2022.886553.

[107] M. S. Spach and J. P. Boineau, “Microfibrosis Produces Electrical Load Variations Due to Loss of Side-to-Side Cell Connections; A Major Mechanism of Structural Heart Disease Arrhythmias,” *Pacing Clin. Electrophysiol.*, vol. 20, no. 2, pp. 397–413, Feb. 1997, doi: 10.1111/j.1540-8159.1997.tb06199.x.

[108] T. Kawara *et al.*, “Activation Delay After Premature Stimulation in Chronically Diseased Human Myocardium Relates to the Architecture of Interstitial Fibrosis,” *Circulation*, vol. 104, no. 25, pp. 3069–3075, Dec. 2001, doi: 10.1161/hc5001.100833.

[109] J. M. de Bakker *et al.*, “Slow conduction in the infarcted human heart. ‘Zigzag’ course of

activation.," *Circulation*, vol. 88, no. 3, pp. 915–926, Sep. 1993, doi: 10.1161/01.CIR.88.3.915.

[110] G. Sygitowicz, A. Maciejak-Jastrzębska, and D. Sitkiewicz, "A Review of the Molecular Mechanisms Underlying Cardiac Fibrosis and Atrial Fibrillation," *J. Clin. Med.*, vol. 10, no. 19, p. 4430, Sep. 2021, doi: 10.3390/jcm10194430.

[111] V. V. Petrov, R. H. Fagard, and P. J. Lijnen, "Stimulation of Collagen Production by Transforming Growth Factor-β 1 During Differentiation of Cardiac Fibroblasts to Myofibroblasts," *Hypertension*, vol. 39, no. 2, pp. 258–263, Feb. 2002, doi: 10.1161/hy0202.103268.

[112] A. Leask, "Potential Therapeutic Targets for Cardiac Fibrosis," *Circ. Res.*, vol. 106, no. 11, pp. 1675–1680, Jun. 2010, doi: 10.1161/CIRCRESAHA.110.217737.

[113] H. Nakajima *et al.*, "Atrial but Not Ventricular Fibrosis in Mice Expressing a Mutant Transforming Growth Factor-β 1 Transgene in the Heart," *Circ. Res.*, vol. 86, no. 5, pp. 571–579, Mar. 2000, doi: 10.1161/01.RES.86.5.571.

[114] E. Anter, "Limitations and Pitfalls of Substrate Mapping for Ventricular Tachycardia," *JACC Clin. Electrophysiol.*, vol. 7, no. 4, pp. 542–560, Apr. 2021, doi: 10.1016/j.jacep.2021.02.007.

[115] S. Xiao *et al.*, "Uncovering potential novel biomarkers and immune infiltration characteristics in persistent atrial fibrillation using integrated bioinformatics analysis," *Math. Biosci. Eng.*, vol. 18, no. 4, pp. 4696–4712, 2021, doi: 10.3934/mbe.2021238.

[116] S. Sirisinha, "Insight into the mechanisms regulating immune homeostasis in health and disease.," *Asian Pacific J. allergy Immunol.*, vol. 29, no. 1, pp. 1–14, Mar. 2011.

[117] M.-C. Chen *et al.*, "Increased Inflammatory Cell Infiltration in the Atrial Myocardium of Patients With Atrial Fibrillation," *Am. J. Cardiol.*, vol. 102, no. 7, pp. 861–865, Oct. 2008, doi: 10.1016/j.amjcard.2008.05.038.

[118] D. R. Van Wagoner, "Oxidative Stress and Inflammation in Atrial Fibrillation: Role in Pathogenesis and Potential as a Therapeutic Target," *J. Cardiovasc. Pharmacol.*, vol. 52, no. 4, pp. 306–313, Oct. 2008, doi: 10.1097/FJC.0b013e31817f9398.

[119] Y. Yao, M. Yang, D. Liu, and Q. Zhao, "Immune remodeling and atrial fibrillation," *Front. Physiol.*, vol. 13, Jul. 2022, doi: 10.3389/fphys.2022.927221.

[120] T. Schober *et al.*, "Myofilament Ca Sensitization Increases Cytosolic Ca Binding Affinity, Alters Intracellular Ca Homeostasis, and Causes Pause-Dependent Ca-Triggered Arrhythmia," *Circ. Res.*, vol. 111, no. 2, pp. 170–179, Jul. 2012, doi: 10.1161/CIRCRESAHA.112.270041.

[121] Z. Sun *et al.*, "Cross-talk between macrophages and atrial myocytes in atrial fibrillation," *Basic Res. Cardiol.*, vol. 111, no. 6, p. 63, Nov. 2016, doi: 10.1007/s00395-016-0584-z.

[122] M. K. Chung *et al.*, "C-Reactive Protein Elevation in Patients With Atrial Arrhythmias," *Circulation*, vol. 104, no. 24, pp. 2886–2891, Dec. 2001, doi: 10.1161/hc4901.101760.

[123] R. J. Aviles *et al.*, "Inflammation as a Risk Factor for Atrial Fibrillation," *Circulation*, vol. 108, no. 24, pp. 3006–3010, Dec. 2003, doi: 10.1161/01.CIR.0000103131.70301.4F.

[124] Y.-H. Kao, Y.-C. Chen, C.-C. Cheng, T.-I. Lee, Y.-J. Chen, and S.-A. Chen, "Tumor necrosis factor-α decreases sarcoplasmic reticulum Ca2+-ATPase expressions via the promoter methylation in cardiomyocytes*," *Crit. Care Med.*, vol. 38, no. 1, pp. 217–222, Jan. 2010, doi: 10.1097/CCM.0b013e3181b4a854.

[125] M. D. M. Engelmann and J. H. Svendsen, "Inflammation in the genesis and perpetuation of atrial fibrillation," *Eur. Heart J.*, vol. 26, no. 20, pp. 2083–2092, Oct. 2005, doi: 10.1093/eurheartj/ehi350.

[126] H. Deng, Y. Xue, X. Zhan, H. Liao, H. Guo, and S. Wu, "Role of tumor necrosis factor-alpha in

the pathogenesis of atrial fibrillation.," *Chin. Med. J. (Engl).*, vol. 124, no. 13, pp. 1976–82, Jul. 2011.

[127] V. A. Fadok, D. L. Bratton, A. Konowal, P. W. Freed, J. Y. Westcott, and P. M. Henson, "Macrophages that have ingested apoptotic cells in vitro inhibit proinflammatory cytokine production through autocrine/paracrine mechanisms involving TGF-beta, PGE2, and PAF.," *J. Clin. Invest.*, vol. 101, no. 4, pp. 890–898, Feb. 1998, doi: 10.1172/JCI1112.

[128] Y. Wang and K. Ashokan, "Physical Exercise: An Overview of Benefits From Psychological Level to Genetics and Beyond," *Front. Physiol.*, vol. 12, Aug. 2021, doi: 10.3389/fphys.2021.731858.

[129] R. Ross *et al.*, "Canadian 24-Hour Movement Guidelines for Adults aged 18–64 years and Adults aged 65 years or older: an integration of physical activity, sedentary behaviour, and sleep," *Appl. Physiol. Nutr. Metab.*, vol. 45, no. 10 (Suppl. 2), pp. S57–S102, Oct. 2020, doi: 10.1139/apnm-2020-0467.

[130] S. Carbone, M. G. Del Buono, C. Ozemek, and C. J. Lavie, "Obesity, risk of diabetes and role of physical activity, exercise training and cardiorespiratory fitness," *Prog. Cardiovasc. Dis.*, vol. 62, no. 4, pp. 327–333, Jul. 2019, doi: 10.1016/j.pcad.2019.08.004.

[131] L. F. M. de Rezende *et al.*, "Physical activity and cancer: an umbrella review of the literature including 22 major anatomical sites and 770 000 cancer cases," *Br. J. Sports Med.*, vol. 52, no. 13, pp. 826–833, Jul. 2018, doi: 10.1136/bjsports-2017-098391.

[132] C. Fiuza-Luces *et al.*, "Exercise benefits in cardiovascular disease: beyond attenuation of traditional risk factors," *Nat. Rev. Cardiol.*, vol. 15, no. 12, pp. 731–743, Dec. 2018, doi: 10.1038/s41569-018-0065-1.

[133] L. E. Garnvik *et al.*, "Physical activity, cardiorespiratory fitness, and cardiovascular outcomes in individuals with atrial fibrillation: the HUNT study," *Eur. Heart J.*, vol. 41, no. 15, pp. 1467–1475, Apr. 2020, doi: 10.1093/eurheartj/ehaa032.

[134] T. M. H. Eijsvogels, A. B. Fernandez, and P. D. Thompson, "Are There Deleterious Cardiac Effects of Acute and Chronic Endurance Exercise?," *Physiol. Rev.*, vol. 96, no. 1, pp. 99–125, Jan. 2016, doi: 10.1152/physrev.00029.2014.

[135] B. J. R. Buckley, G. Y. H. Lip, and D. H. J. Thijssen, "The counterintuitive role of exercise in the prevention and cause of atrial fibrillation," *Am. J. Physiol. Circ. Physiol.*, vol. 319, no. 5, pp. H1051–H1058, Nov. 2020, doi: 10.1152/ajpheart.00509.2020.

[136] A. Coelho *et al.*, "Tachyarrhythmias in young athletes," *J. Am. Coll. Cardiol.*, vol. 7, no. 1, pp. 237–243, Jan. 1986, doi: 10.1016/S0735-1097(86)80287-X.

[137] L. Mont, "Long-lasting sport practice and lone atrial fibrillation," *Eur. Heart J.*, vol. 23, no. 6, pp. 477–482, Mar. 2002, doi: 10.1053/euhj.2001.2802.

[138] M. Myrstad *et al.*, "Increased risk of atrial fibrillation among elderly Norwegian men with a history of long-term endurance sport practice," *Scand. J. Med. Sci. Sports*, vol. 24, no. 4, Aug. 2014, doi: 10.1111/sms.12150.

[139] L. E. Armstrong, M. F. Bergeron, E. C. Lee, J. E. Mershon, and E. M. Armstrong, "Overtraining Syndrome as a Complex Systems Phenomenon," *Front. Netw. Physiol.*, vol. 1, Jan. 2022, doi: 10.3389/fnetp.2021.794392.

[140] A. L. Gerche and C. M. Schmied, "Atrial fibrillation in athletes and the interplay between exercise and health," *Eur. Heart J.*, vol. 34, no. 47, pp. 3599–3602, Dec. 2013, doi: 10.1093/eurheartj/eht265.

[141] K. Andersen *et al.*, "Risk of arrhythmias in 52 755 long-distance cross-country skiers: a cohort

study," *Eur. Heart J.*, vol. 34, no. 47, pp. 3624–3631, Dec. 2013, doi: 10.1093/eurheartj/eht188.

[142] R. Elosua *et al.*, "Sport practice and the risk of lone atrial fibrillation: A case–control study," *Int. J. Cardiol.*, vol. 108, no. 3, pp. 332–337, Apr. 2006, doi: 10.1016/j.ijcard.2005.05.020.

[143] A. Aizer, J. M. Gaziano, N. R. Cook, J. E. Manson, J. E. Buring, and C. M. Albert, "Relation of Vigorous Exercise to Risk of Atrial Fibrillation," *Am. J. Cardiol.*, vol. 103, no. 11, pp. 1572–1577, Jun. 2009, doi: 10.1016/j.amjcard.2009.01.374.

[144] M.-N. Jin *et al.*, "Physical Activity and Risk of Atrial Fibrillation: A Nationwide Cohort Study in General Population," *Sci. Rep.*, vol. 9, no. 1, p. 13270, Sep. 2019, doi: 10.1038/s41598-019-49686-w.

[145] C. S. Kwok, S. G. Anderson, P. K. Myint, M. A. Mamas, and Y. K. Loke, "Physical activity and incidence of atrial fibrillation: A systematic review and meta-analysis," *Int. J. Cardiol.*, vol. 177, no. 2, pp. 467–476, Dec. 2014, doi: 10.1016/j.ijcard.2014.09.104.

[146] J. Karjalainen, U. M. Kujala, J. Kaprio, S. Sarna, and M. Viitasalo, "Lone atrial fibrillation in vigorously exercising middle aged men: case-control study," *BMJ*, vol. 316, no. 7147, pp. 1784–1785, Jun. 1998, doi: 10.1136/bmj.316.7147.1784.

[147] G. D. Sanna, E. Gabrielli, E. De Vito, G. Nusdeo, D. Prisco, and G. Parodi, "Atrial fibrillation in athletes: From epidemiology to treatment in the novel oral anticoagulants era," *J. Cardiol.*, vol. 72, no. 4, pp. 269–276, Oct. 2018, doi: 10.1016/j.jjcc.2018.04.011.

[148] F. Sanchis-Gomar *et al.*, "Atrial fibrillation in highly trained endurance athletes — Description of a syndrome," *Int. J. Cardiol.*, vol. 226, pp. 11–20, Jan. 2017, doi: 10.1016/j.ijcard.2016.10.047.

[149] A. La Gerche *et al.*, "The Athlete's Heart—Challenges and Controversies," *J. Am. Coll. Cardiol.*, vol. 80, no. 14, pp. 1346–1362, Oct. 2022, doi: 10.1016/j.jacc.2022.07.014.

[150] J. H. Mitchell, "Task Force 8: classification of sports. In: Maron BJ, Zipes DP, eds. 36th Bethesda Conference: eligibility recommendations for competitive athletes with cardiovascular abnormalities. ," *J. Am. Coll. Cardiol.*, vol. 45, no. 8, pp. 1313–1315, Apr. 2005, doi: 10.1016/j.jacc.2005.02.004.

[151] B. J. Maron and A. Pelliccia, "The Heart of Trained Athletes," *Circulation*, vol. 114, no. 15, pp. 1633–1644, Oct. 2006, doi: 10.1161/CIRCULATIONAHA.106.613562.

[152] R. Fagard, C. Van Den Broeke, and A. Amery, "Left ventricular dynamics during exercise in elite marathon runners," *J. Am. Coll. Cardiol.*, vol. 14, no. 1, pp. 112–118, Jul. 1989, doi: 10.1016/0735-1097(89)90060-0.

[153] A. La Gerche and D. L. Prior, "Exercise—Is it Possible to Have Too Much of a Good Thing?," *Hear. Lung Circ.*, vol. 16, pp. S102–S104, Jan. 2007, doi: 10.1016/j.hlc.2007.03.014.

[154] A. Merghani, A. Malhotra, and S. Sharma, "The U-shaped relationship between exercise and cardiac morbidity," *Trends Cardiovasc. Med.*, vol. 26, no. 3, pp. 232–240, Apr. 2016, doi: 10.1016/j.tcm.2015.06.005.

[155] S. Sharma, A. Merghani, and L. Mont, "Exercise and the heart: the good, the bad, and the ugly," *Eur. Heart J.*, vol. 36, no. 23, pp. 1445–1453, Jun. 2015, doi: 10.1093/eurheartj/ehv090.

[156] R. Fagard, "Athlete's heart.," *Heart*, vol. 89, no. 12, pp. 1455–61, Dec. 2003, doi: 10.1136/heart.89.12.1455.

[157] J. Morganroth, "Comparative Left Ventricular Dimensions in Trained Athletes," *Ann. Intern. Med.*, vol. 82, no. 4, p. 521, Apr. 1975, doi: 10.7326/0003-4819-82-4-521.

[158] J. Scharhag, G. Schneider, A. Urhausen, V. Rochette, B. Kramann, and W. Kindermann, "Athlete's heart," *J. Am. Coll. Cardiol.*, vol. 40, no. 10, pp. 1856–1863, Nov. 2002, doi:

10.1016/S0735-1097(02)02478-6.

[159] D. Oxborough *et al.*, "The Right Ventricle of the Endurance Athlete: The Relationship between Morphology and Deformation," *J. Am. Soc. Echocardiogr.*, vol. 25, no. 3, pp. 263–271, Mar. 2012, doi: 10.1016/j.echo.2011.11.017.

[160] R. Jurcut, S. Giusca, A. La Gerche, S. Vasile, C. Ginghina, and J.-U. Voigt, "The echocardiographic assessment of the right ventricle: what to do in 2010?," *Eur. J. Echocardiogr.*, vol. 11, no. 2, pp. 81–96, Mar. 2010, doi: 10.1093/ejechocard/jep234.

[161] L. Banks, Z. Sasson, M. Busato, and J. M. Goodman, "Impaired left and right ventricular function following prolonged exercise in young athletes: influence of exercise intensity and responses to dobutamine stress," *J. Appl. Physiol.*, vol. 108, no. 1, pp. 112–119, Jan. 2010, doi: 10.1152/japplphysiol.00898.2009.

[162] R. Fagard, "Athlete's Heart: A Meta-Analysis of the Echocardiographic Experience," *Int. J. Sports Med.*, vol. 17, no. S 3, pp. S140–S144, Nov. 1996, doi: 10.1055/s-2007-972915.

[163] S. D. Colan, S. P. Sanders, and K. M. Borow, "Physiologie hypertrophy: Effects on left ventricular systolic mechanics in athletes," *J. Am. Coll. Cardiol.*, vol. 9, no. 4, pp. 776–783, Apr. 1987, doi: 10.1016/S0735-1097(87)80232-2.

[164] Y. Seko *et al.*, "Association between atrial fibrillation, atrial enlargement, and left ventricular geometric remodeling," *Sci. Rep.*, vol. 8, no. 1, p. 6366, Apr. 2018, doi: 10.1038/s41598-018-24875-1.

[165] C. J. Lavie, A. Pandey, D. H. Lau, M. A. Alpert, and P. Sanders, "Obesity and Atrial Fibrillation Prevalence, Pathogenesis, and Prognosis," *J. Am. Coll. Cardiol.*, vol. 70, no. 16, pp. 2022–2035, Oct. 2017, doi: 10.1016/j.jacc.2017.09.002.

[166] A. M. Hauser, R. H. Dressendorfer, M. Vos, T. Hashimoto, S. Gordon, and G. C. Timmis, "Symmetric cardiac enlargement in highly trained endurance athletes: A two-dimensional echocardiographic study," *Am. Heart J.*, vol. 109, no. 5, pp. 1038–1044, May 1985, doi: 10.1016/0002-8703(85)90247-9.

[167] C. Höglund, "Enlarged Left Atrial Dimension in Former Endurance Athletes: An Echocardiographic Study," *Int. J. Sports Med.*, vol. 07, no. 03, pp. 133–136, Jun. 1986, doi: 10.1055/s-2008-1025750.

[168] A. Pelliccia *et al.*, "Prevalence and Clinical Significance of Left Atrial Remodeling in Competitive Athletes," *J. Am. Coll. Cardiol.*, vol. 46, no. 4, pp. 690–696, Aug. 2005, doi: 10.1016/j.jacc.2005.04.052.

[169] L. G. Rudski *et al.*, "Guidelines for the Echocardiographic Assessment of the Right Heart in Adults: A Report from the American Society of Echocardiography," *J. Am. Soc. Echocardiogr.*, vol. 23, no. 7, pp. 685–713, Jul. 2010, doi: 10.1016/j.echo.2010.05.010.

[170] J. T. Reeves *et al.*, "Operation Everest II: Cardiac filling pressures during cycle exercise at sea level," *Respir. Physiol.*, vol. 80, no. 2–3, pp. 147–154, May 1990, doi: 10.1016/0034-5687(90)90078-D.

[171] S. Sharma *et al.*, "Electrocardiographic changes in 1000 highly trained junior elite athletes," *Br. J. Sports Med.*, vol. 33, no. 5, pp. 319–324, Oct. 1999, doi: 10.1136/bjsm.33.5.319.

[172] N. A. M. Estes, M. S. Link, M. Homoud, P. J. Wang, and P. D. Thompson, "ECG Findings in Active Patients," *Phys. Sportsmed.*, vol. 29, no. 3, pp. 67–74, Mar. 2001, doi: 10.3810/psm.2001.03.675.

[173] P. Luthi *et al.*, "Echocardiographic findings in former professional cyclists after long-term deconditioning of more than 30years," *Eur. J. Echocardiogr.*, Apr. 2007, doi:

10.1016/j.euje.2007.03.001.

[174] A. Carpenter, A. Frontera, R. Bond, E. Duncan, and G. Thomas, "Vagal atrial fibrillation: What is it and should we treat it?," *Int. J. Cardiol.*, vol. 201, pp. 415–421, Dec. 2015, doi: 10.1016/j.ijcard.2015.08.108.

[175] T. Ashira *et al.*, "Differences in sympathetic and vagal effects on paroxysmal atrial fibrillation: a simulation study," *Biomed. Pharmacother.*, vol. 56, pp. 359–363, Nov. 2002, doi: 10.1016/S0753-3322(02)00317-7.

[176] A. E. Lomax, R. A. Rose, and W. R. Giles, "Electrophysiological evidence for a gradient of G protein-gated K^+ current in adult mouse atria," *Br. J. Pharmacol.*, vol. 140, no. 3, pp. 576–584, Oct. 2003, doi: 10.1038/sj.bjp.0705474.

[177] R. Stein, C. M. Medeiros, G. A. Rosito, L. I. Zimerman, and J. P. Ribeiro, "Intrinsic sinus and atrioventricular node electrophysiologic adaptations in endurance athletes," *J. Am. Coll. Cardiol.*, vol. 39, no. 6, pp. 1033–1038, Mar. 2002, doi: 10.1016/S0735-1097(02)01722-9.

[178] M. H. Laughlin *et al.*, "Peripheral Circulation," in *Comprehensive Physiology*, Wiley, 2012, pp. 321–447. doi: 10.1002/cphy.c100048.

[179] D. A. Hood, J. M. Memme, A. N. Oliveira, and M. Triolo, "Maintenance of Skeletal Muscle Mitochondria in Health, Exercise, and Aging," *Annu. Rev. Physiol.*, vol. 81, no. 1, pp. 19–41, Feb. 2019, doi: 10.1146/annurev-physiol-020518-114310.

[180] J. O. Holloszy, "Biochemical adaptations in muscle. Effects of exercise on mitochondrial oxygen uptake and respiratory enzyme activity in skeletal muscle.," *J. Biol. Chem.*, vol. 242, no. 9, pp. 2278–82, May 1967.

[181] C. G. R. Perry, J. Lally, G. P. Holloway, G. J. F. Heigenhauser, A. Bonen, and L. L. Spriet, "Repeated transient mRNA bursts precede increases in transcriptional and mitochondrial proteins during training in human skeletal muscle," *J. Physiol.*, vol. 588, no. 23, pp. 4795–4810, Dec. 2010, doi: 10.1113/jphysiol.2010.199448.

[182] H. Hoppeler *et al.*, "Endurance training in humans: aerobic capacity and structure of skeletal muscle," *J. Appl. Physiol.*, vol. 59, no. 2, pp. 320–327, Aug. 1985, doi: 10.1152/jappl.1985.59.2.320.

[183] F. N. Daussin *et al.*, "Effect of interval versus continuous training on cardiorespiratory and mitochondrial functions: relationship to aerobic performance improvements in sedentary subjects," *Am. J. Physiol. Integr. Comp. Physiol.*, vol. 295, no. 1, pp. R264–R272, Jul. 2008, doi: 10.1152/ajpregu.00875.2007.

[184] R. J. Youle and A. M. van der Bliek, "Mitochondrial Fission, Fusion, and Stress," *Science (80-.).*, vol. 337, no. 6098, pp. 1062–1065, Aug. 2012, doi: 10.1126/science.1219855.

[185] S. Campello, F. Strappazzon, and F. Cecconi, "Mitochondrial dismissal in mammals, from protein degradation to mitophagy," *Biochim. Biophys. Acta - Bioenerg.*, vol. 1837, no. 4, pp. 451–460, Apr. 2014, doi: 10.1016/j.bbabio.2013.11.010.

[186] M. Flockhart, L. C. Nilsson, S. Tais, B. Ekblom, W. Apró, and F. J. Larsen, "Excessive exercise training causes mitochondrial functional impairment and decreases glucose tolerance in healthy volunteers," *Cell Metab.*, vol. 33, no. 5, pp. 957-970.e6, May 2021, doi: 10.1016/j.cmet.2021.02.017.

[187] R. Shave *et al.*, "Exercise-Induced Cardiac Troponin Elevation," *J. Am. Coll. Cardiol.*, vol. 56, no. 3, pp. 169–176, Jul. 2010, doi: 10.1016/j.jacc.2010.03.037.

[188] R. Shave *et al.*, "Exercise-Induced Cardiac Troponin T Release," *Med. Sci. Sport. Exerc.*, vol. 39, no. 12, pp. 2099–2106, Dec. 2007, doi: 10.1249/mss.0b013e318153ff78.

[189] R. Aschar-Sobbi *et al.*, “Increased atrial arrhythmia susceptibility induced by intense endurance exercise in mice requires TNFα,” *Nat. Commun.*, vol. 6, no. 1, p. 6018, Jan. 2015, doi: 10.1038/ncomms7018.

[190] B. Benito *et al.*, “Cardiac Arrhythmogenic Remodeling in a Rat Model of Long-Term Intensive Exercise Training,” *Circulation*, vol. 123, no. 1, pp. 13–22, Jan. 2011, doi: 10.1161/CIRCULATIONAHA.110.938282.

[191] D. C. Peritz *et al.*, “High-intensity endurance training is associated with left atrial fibrosis,” *Am. Heart J.*, vol. 226, pp. 206–213, Aug. 2020, doi: 10.1016/j.ahj.2020.05.015.

[192] É. Cerqueira, D. A. Marinho, H. P. Neiva, and O. Lourenço, “Inflammatory Effects of High and Moderate Intensity Exercise—A Systematic Review,” *Front. Physiol.*, vol. 10, Jan. 2020, doi: 10.3389/fphys.2019.01550.

[193] L. S. Silveira, B. de M. M. Antunes, A. L. A. Minari, R. V. T. dos Santos, J. C. R. Neto, and F. S. Lira, “Macrophage Polarization: Implications on Metabolic Diseases and the Role of Exercise,” *Crit. Rev. Eukaryot. Gene Expr.*, vol. 26, no. 2, pp. 115–132, 2016, doi: 10.1615/CritRevEukaryotGeneExpr.2016015920.

[194] A. I. Moldoveanu, R. J. Shephard, and P. N. Shek, “The Cytokine Response to Physical Activity and Training,” *Sport. Med.*, vol. 31, no. 2, pp. 115–144, 2001, doi: 10.2165/00007256-200131020-00004.

[195] M. Gleeson, N. C. Bishop, D. J. Stensel, M. R. Lindley, S. S. Mastana, and M. A. Nimmo, “The anti-inflammatory effects of exercise: mechanisms and implications for the prevention and treatment of disease,” *Nat. Rev. Immunol.*, vol. 11, no. 9, pp. 607–615, Sep. 2011, doi: 10.1038/nri3041.

[196] Y. Oishi and I. Manabe, “Macrophages in inflammation, repair and regeneration,” *Int. Immunol.*, vol. 30, no. 11, pp. 511–528, Oct. 2018, doi: 10.1093/intimm/dxy054.

[197] J. M. Peake, O. Neubauer, N. P. Walsh, and R. J. Simpson, “Recovery of the immune system after exercise,” *J. Appl. Physiol.*, vol. 122, no. 5, pp. 1077–1087, May 2017, doi: 10.1152/japplphysiol.00622.2016.

[198] T. A. Butterfield, T. M. Best, and M. A. Merrick, “The dual roles of neutrophils and macrophages in inflammation: a critical balance between tissue damage and repair.,” *J. Athl. Train.*, vol. 41, no. 4, pp. 457–65, 2006.

[199] S. Oishi, T. Sasano, Y. Tateishi, N. Tamura, M. Isobe, and T. Furukawa, “Stretch of Atrial Myocytes Stimulates Recruitment of Macrophages via ATP Released Through Gap-Junction Channels,” *J. Pharmacol. Sci.*, vol. 120, no. 4, pp. 296–304, 2012, doi: 10.1254/jphs.12202FP.

[200] S. M. Ulven *et al.*, “An acute bout of exercise modulate the inflammatory response in peripheral blood mononuclear cells in healthy young men,” *Arch. Physiol. Biochem.*, vol. 121, no. 2, pp. 41–49, Mar. 2015, doi: 10.3109/13813455.2014.1003566.

[201] A. Oláh *et al.*, “Sex Differences in Morphological and Functional Aspects of Exercise-Induced Cardiac Hypertrophy in a Rat Model,” *Front. Physiol.*, vol. 10, Jul. 2019, doi: 10.3389/fphys.2019.00889.

[202] D. Lee, R. R. Pate, C. J. Lavie, X. Sui, T. S. Church, and S. N. Blair, “Leisure-Time Running Reduces All-Cause and Cardiovascular Mortality Risk,” *J. Am. Coll. Cardiol.*, vol. 64, no. 5, pp. 472–481, Aug. 2014, doi: 10.1016/j.jacc.2014.04.058.

[203] H. Khan, D. Kella, R. Rauramaa, K. Savonen, M. S. Lloyd, and J. A. Laukkanen, “Cardiorespiratory fitness and atrial fibrillation: A population-based follow-up study,” *Hear. Rhythm*, vol. 12, no. 7, pp. 1424–1430, Jul. 2015, doi: 10.1016/j.hrthm.2015.03.024.

[204] J. R. Speakman, “Measuring Energy Metabolism in the Mouse – Theoretical, Practical, and Analytical Considerations,” *Front. Physiol.*, vol. 4, 2013, doi: 10.3389/fphys.2013.00034.

[205] J. H. O’Keefe, H. R. Patil, C. J. Lavie, A. Magalski, R. A. Vogel, and P. A. McCullough, “Potential Adverse Cardiovascular Effects From Excessive Endurance Exercise,” *Mayo Clin. Proc.*, vol. 87, no. 6, pp. 587–595, Jun. 2012, doi: 10.1016/j.mayocp.2012.04.005.

[206] T. K. Kontro, S. Sarna, J. Kaprio, and U. M. Kujala, “Mortality and health-related habits in 900 Finnish former elite athletes and their brothers,” *Br. J. Sports Med.*, vol. 52, no. 2, pp. 89–95, Jan. 2018, doi: 10.1136/bjsports-2017-098206.

[207] A. M. Al-Kaisey and J. M. Kalman, “Obesity and Atrial Fibrillation: Epidemiology, Pathogenesis and Effect of Weight Loss,” *Arrhythmia Electrophysiol. Rev.*, vol. 10, no. 3, pp. 159–164, Oct. 2021, doi: 10.15420/aer.2021.36.

[208] L. J. Bohne, D. Johnson, R. A. Rose, S. B. Wilton, and A. M. Gillis, “The Association Between Diabetes Mellitus and Atrial Fibrillation: Clinical and Mechanistic Insights,” *Front. Physiol.*, vol. 10, Feb. 2019, doi: 10.3389/fphys.2019.00135.

[209] N. A. M. Estes and C. Madias, “Atrial Fibrillation in Athletes,” *JACC Clin. Electrophysiol.*, vol. 3, no. 9, pp. 921–928, Sep. 2017, doi: 10.1016/j.jacep.2017.03.019.

[210] K. A. Bizhanov, K. B. Abzaliyev, A. K. Baimbetov, A. B. Sarsenbayeva, and E. Lyan, “Atrial fibrillation: Epidemiology, pathophysiology, and clinical complications (literature review),” *J. Cardiovasc. Electrophysiol.*, vol. 34, no. 1, pp. 153–165, Jan. 2023, doi: 10.1111/jce.15759.

[211] C. Sohns and N. F. Marrouche, “Atrial fibrillation and cardiac fibrosis,” *Eur. Heart J.*, vol. 41, no. 10, pp. 1123–1131, Mar. 2020, doi: 10.1093/eurheartj/ehz786.

[212] R. L. Goldsmith, D. M. Bloomfield, and E. T. Rosenwinkel, “Exercise and autonomic function,” *Coron. Artery Dis.*, vol. 11, no. 2, pp. 129–135, Mar. 2000, doi: 10.1097/00019501-200003000-00007.

[213] M. Wilhelm *et al.*, “Early Repolarization, Left Ventricular Diastolic Function, and Left Atrial Size in Professional Soccer Players,” *Am. J. Cardiol.*, vol. 106, no. 4, pp. 569–574, Aug. 2010, doi: 10.1016/j.amjcard.2010.03.072.

[214] V. Conti *et al.*, “Right heart exercise-training-adaptation and remodelling in endurance athletes,” *Sci. Rep.*, vol. 11, no. 1, p. 22532, Nov. 2021, doi: 10.1038/s41598-021-02028-1.

[215] M. K. Turagam, G. C. Flaker, P. Velagapudi, S. Vadali, and M. A. Alpert, “Atrial Fibrillation In Athletes: Pathophysiology, Clinical Presentation, Evaluation and Management.,” *J. Atr. Fibrillation*, vol. 8, no. 4, p. 1309, Dec. 2015, doi: 10.4022/jafib.1309.

[216] R. K. Pathak *et al.*, “Impact of CARDIOrespiratory FITness on Arrhythmia Recurrence in Obese Individuals With Atrial Fibrillation,” *J. Am. Coll. Cardiol.*, vol. 66, no. 9, pp. 985–996, Sep. 2015, doi: 10.1016/j.jacc.2015.06.488.

[217] C. L. Dumke *et al.*, “Successive bouts of cycling stimulates genes associated with mitochondrial biogenesis,” *Eur. J. Appl. Physiol.*, vol. 107, no. 4, pp. 419–427, Nov. 2009, doi: 10.1007/s00421-009-1143-1.

[218] M. A. Nystoriak and A. Bhatnagar, “Cardiovascular Effects and Benefits of Exercise,” *Front. Cardiovasc. Med.*, vol. 5, Sep. 2018, doi: 10.3389/fcvm.2018.00135.

[219] B. Morseth *et al.*, “Physical activity, resting heart rate, and atrial fibrillation: the Tromsø Study,” *Eur. Heart J.*, vol. 37, no. 29, pp. 2307–2313, Aug. 2016, doi: 10.1093/eurheartj/ehw059.

[220] M. J. Shen and D. P. Zipes, “Role of the Autonomic Nervous System in Modulating Cardiac Arrhythmias,” *Circ. Res.*, vol. 114, no. 6, pp. 1004–1021, Mar. 2014, doi:

10.1161/CIRCRESAHA.113.302549.

[221] M. Rebecchi *et al.*, “Atrial fibrillation and autonomic nervous system: A translational approach to guide therapeutic goals,” *J. Arrhythmia*, vol. 37, no. 2, pp. 320–330, Apr. 2021, doi: 10.1002/joa3.12512.

[222] Yung-Hsin Yeh, Kristina Lemola, and Stanley Nattel, “Vagal Atrial Fibrillation,” *Acta Cardiol Sin*, vol. 23, no. 1г12, 2007.

[223] B. Burstein and S. Nattel, “Atrial Fibrosis: Mechanisms and Clinical Relevance in Atrial Fibrillation,” *J. Am. Coll. Cardiol.*, vol. 51, no. 8, pp. 802–809, Feb. 2008, doi: 10.1016/j.jacc.2007.09.064.

[224] D. R. Swanson, “Atrial fibrillation in athletes: Implicit literature-based connections suggest that overtraining and subsequent inflammation may be a contributory mechanism,” *Med. Hypotheses*, vol. 66, no. 6, pp. 1085–1092, Jan. 2006, doi: 10.1016/j.mehy.2006.01.006.

[225] D. Venkatesh *et al.*, “Endothelial TNF Receptor 2 Induces IRF1 Transcription Factor-Dependent Interferon-β Autocrine Signaling to Promote Monocyte Recruitment,” *Immunity*, vol. 38, no. 5, pp. 1025–1037, May 2013, doi: 10.1016/j.immuni.2013.01.012.

[226] P. J. Hohensinner *et al.*, “Macrophage colony stimulating factor expression in human cardiac cells is upregulated by tumor necrosis factor-α via an NF-κB dependent mechanism,” *J. Thromb. Haemost.*, vol. 5, no. 12, pp. 2520–2528, Dec. 2007, doi: 10.1111/j.1538-7836.2007.02784.x.

[227] T. Yamashita *et al.*, “Recruitment of Immune Cells Across Atrial Endocardium in Human Atrial Fibrillation,” *Circ. J.*, vol. 74, no. 2, pp. 262–270, 2010, doi: 10.1253/circj.CJ-09-0644.

[228] D. Qiu, L. Peng, D. N. Ghista, and K. K. L. Wong, “Left Atrial Remodeling Mechanisms Associated with Atrial Fibrillation,” *Cardiovasc. Eng. Technol.*, vol. 12, no. 3, pp. 361–372, Jun. 2021, doi: 10.1007/s13239-021-00527-w.

[229] M. A. Rosenberg and W. J. Manning, “Diastolic Dysfunction and Risk of Atrial Fibrillation,” *Circulation*, vol. 126, no. 19, pp. 2353–2362, Nov. 2012, doi: 10.1161/CIRCULATIONAHA.112.113233.

[230] J. H. van Berlo, M. Maillet, and J. D. Molkentin, “Signaling effectors underlying pathologic growth and remodeling of the heart,” *J. Clin. Invest.*, vol. 123, no. 1, pp. 37–45, Jan. 2013, doi: 10.1172/JCI62839.

[231] K. A. Hemanthakumar and R. Kivelä, “Angiogenesis and angiocrines regulating heart growth,” *Vasc. Biol.*, vol. 2, no. 1, pp. R93–R104, Jul. 2020, doi: 10.1530/VB-20-0006.

[232] O. Hudlicka, M. Brown, and S. Egginton, “Angiogenesis in skeletal and cardiac muscle,” *Physiol. Rev.*, vol. 72, no. 2, pp. 369–417, Apr. 1992, doi: 10.1152/physrev.1992.72.2.369.

[233] D. Zhang, X. Shen, and X. Qi, “Resting heart rate and all-cause and cardiovascular mortality in the general population: a meta-analysis,” *Can. Med. Assoc. J.*, vol. 188, no. 3, pp. E53–E63, Feb. 2016, doi: 10.1503/cmaj.150535.

[234] R. Gogiraju, M. L. Bochenek, and K. Schäfer, “Angiogenic Endothelial Cell Signaling in Cardiac Hypertrophy and Heart Failure,” *Front. Cardiovasc. Med.*, vol. 6, Mar. 2019, doi: 10.3389/fcvm.2019.00020.

[235] Y. Oh *et al.*, “Transcriptomic Bioinformatic Analyses of Atria Uncover Involvement of Pathways Related to Strain and Post-translational Modification of Collagen in Increased Atrial Fibrillation Vulnerability in Intensely Exercised Mice,” *Front. Physiol.*, vol. 11, Dec. 2020, doi: 10.3389/fphys.2020.605671.

[236] N. G. Frangogiannis, “Cardiac fibrosis: Cell biological mechanisms, molecular pathways and

therapeutic opportunities," *Mol. Aspects Med.*, vol. 65, pp. 70–99, Feb. 2019, doi: 10.1016/j.mam.2018.07.001.

[237] A. González, E. B. Schelbert, J. Díez, and J. Butler, "Myocardial Interstitial Fibrosis in Heart Failure," *J. Am. Coll. Cardiol.*, vol. 71, no. 15, pp. 1696–1706, Apr. 2018, doi: 10.1016/j.jacc.2018.02.021.

[238] M. J. Podolsky *et al.*, "Age-dependent regulation of cell-mediated collagen turnover," *JCI Insight*, vol. 5, no. 10, May 2020, doi: 10.1172/jci.insight.137519.

[239] X. Bi *et al.*, "Collagen Cross-Linking Is Associated With Cardiac Remodeling in Hypertrophic Obstructive Cardiomyopathy," *J. Am. Heart Assoc.*, vol. 10, no. 1, Jan. 2021, doi: 10.1161/JAHA.120.017752.

[240] A. Bartolomucci *et al.*, "Chronic psychosocial stress persistently alters autonomic function and physical activity in mice," *Physiol. Behav.*, vol. 80, no. 1, pp. 57–67, Oct. 2003, doi: 10.1016/S0031-9384(03)00209-9.

[241] N. Skoluda, L. Dettenborn, T. Stalder, and C. Kirschbaum, "Elevated hair cortisol concentrations in endurance athletes," *Psychoneuroendocrinology*, vol. 37, no. 5, pp. 611–617, May 2012, doi: 10.1016/j.psyneuen.2011.09.001.

[242] P. M. L. Janssen, B. J. Biesiadecki, M. T. Ziolo, and J. P. Davis, "The Need for Speed: Mice, Men, and Myocardial Kinetic Reserve," *Circ. Res.*, vol. 119, no. 3, pp. 418–421, Jul. 2016, doi: 10.1161/CIRCRESAHA.116.309126.

[243] V. Gaudreault *et al.*, "Transient Myocardial Tissue and Function Changes During a Marathon in Less Fit Marathon Runners," *Can. J. Cardiol.*, vol. 29, no. 10, pp. 1269–1276, Oct. 2013, doi: 10.1016/j.cjca.2013.04.022.

[244] D. Corrado, M. S. Link, and H. Calkins, "Arrhythmogenic Right Ventricular Cardiomyopathy," *N. Engl. J. Med.*, vol. 376, no. 1, pp. 61–72, Jan. 2017, doi: 10.1056/NEJMra1509267.

[245] C. Bouchard, T. Rankinen, and J. A. Timmons, "Genomics and Genetics in the Biology of Adaptation to Exercise," in *Comprehensive Physiology*, Wiley, 2011, pp. 1603–1648. doi: 10.1002/cphy.c100059.

[246] S. Mohanty *et al.*, "Differential Association of Exercise Intensity With Risk of Atrial Fibrillation in Men and Women: Evidence from a Meta-Analysis," *J. Cardiovasc. Electrophysiol.*, vol. 27, no. 9, pp. 1021–1029, Sep. 2016, doi: 10.1111/jce.13023.

[247] N. Svedberg, J. Sundström, S. James, U. Hållmarker, K. Hambraeus, and K. Andersen, "Long-Term Incidence of Atrial Fibrillation and Stroke Among Cross-Country Skiers: Cohort Study of Endurance-Trained Male and Female Athletes," *Circulation*, p. CIRCULATIONAHA.118.039461, Aug. 2019, doi: 10.1161/CIRCULATIONAHA.118.039461.

Appendix

A.1 Swim O_2 Calculation Corrections

A.1.1 Calibration

As with most technological equipment, values observed and expected do not always align. Thus, a two-point calibration is performed using dry room air at 20.95%O_2 as the upper limit (according to the Oxymax manual) and 20.5%O_2, 5000 ppm CO_2 & N_2 balanced gas (Custom, Praxair, Inc., CT, U.S.A) as the lower limit. These calibration gases are passed throughout the apparatus to simulate experimental conditions. Based on previous O_2 calibrations, the measured %O_2 is allowed to equilibrate for a minimum of 5 minutes, and an average %O_2 over 1 minute is registered as observed %O_2. Therefore, a calibration curve is be plotted as expected %O_2 vs. observed %O_2 such that:

$$yi = m * xi + c$$

Where yi is the observed %O_2, xi is the expected %O_2, m is the gain and c is the offset of the calibration curve. Each data point collected during the swims is then calibrated using the generated standard curve and referred as xi onwards.

A.1.2 Pressure Compensation

The Oxymax sensor consists of an electrochemical fuel cell that measures O_2 content using reduction chemical reactions whereby the produced electricity is directly proportional to the O_2 content in the sampled gas. As such, the cell depends on the diffusion of gas and is intrinsically dependent on the partial pressure of O_2 (P_{O_2}), according to Fick's Law of Diffusion. Thus, pressure is measured simultaneously with air inflow, using a pressure sensor (Adafruit BME280 I2C or SPI Temperature Humidity Pressure Sensor, Bosch Sensortec, Kusterdingen, Germany) connected to a custom beagle board (Texas Instruments Incorporated, TX, U.S.A) and Python software. According to Dalton's Law, the P_{O_2} is assumed directly proportional to P_{atm}, with pressure corrections completed according to:

$$xi,p = xi * (P_{atm\ i}/P_{atm\ c})$$

Where, xi,p = calibrated, pressure compensated %O_2, xi = calibrated %O_2, $P_{atm\ i}$ = atmospheric pressure at point i and $P_{atm\ c}$ = atmospheric pressure at calibration.

A.1.3 Baselining

Intrinsic to the oxygen sensor is fluctuation in the recorded %O_2 despite the lack of real changes. Thus, corrections were made by adjusting all recorded values based on fluctuations in the measured data of a known calibration gas using the following equation:

$$xi,b = xi + (\%O_2\ known,expected - \%O_2\ known,observed)$$

Where, xi,b = baselined $\%O_2$, xi = raw $\%O_2$ at point i, $\%O_2$known,expected = $\%O_2$ content of the known calibration gas and $\%O_2$known,observed = the measured $\%O_2$ content of calibration gas. For example, given one of the calibration points is dried room air (20.95 $\%O_2$), it's easily used as $\%O_2$known,expected by measuring oxygen content before and after swim completion. Points used for baselining also need to be calibrated and pressure compensated, similar to the aforementioned individual VO_2 points. Correspondingly, a standard linear curve is derived from the two baseline points (b1,i,p and b2,i,p) for estimating any value of bn,i,p– the baseline point at time n throughout the swim. Finally, to complete baselining, the calibrated and pressure compensated $\%O_2$ was adjusted according to the following:

$$xi,p,b = xi,p + (20.95\% - bn,i,p)$$

Where xi,p,b is the calibrated, pressure compensated and baselined observed $\%O_2$, xi,p is the value before baselining, and bn,i,b is the estimated baseline point at the time i.

A.1.4 Conversion to Molarity and Volume

VO_2 is often presented at Standard Conditions of Pressure and Temperature (STP), which allows experimental data to be easily compared across various studies. Thus, the STP correction can be modelled according to the following equation, where the VO_2 units are measured as volume:

$$VO_{2\,STP} = \frac{\frac{20.95\%}{100} * \frac{P_{atm}}{RT_{in}} * F - \frac{xi,p,b}{100} * \frac{P_{atm}}{RT_{out}} * F}{\text{mass animals}} * \frac{RT_{STP}}{P_{STP}}$$

Aside: at STP, Patm is 1atm (or 101.325kPa) and Temperature is 0°C (or 273.15K).

A.1.5 Humidity Compensation

The final correction is humidity compensation. All values recorded experimentally are desiccated and therefore lack the effects of humidity. As such, xi,p,b must be corrected for the lack of water (H_2O) upon recording. To do this, we calculate the following value:

$$P_{bucket} = P_{atm} - P_{H2O}.$$

As such, the value of (P_{atm}- P_{H2O}) is always less than P_{atm}, decreasing the recorded $\%O_2$ entering and leaving the apparatus. Despite this, inflow and outflow recordings have different water contents as water in the atmosphere fluctuates greatly and rapidly. In contrast, the water content in the swimming apparatus is always at 100% due to vapour from the swimming water. Given $P_{H2O\ in} < P_{H2O\ out}$, as excess water *must exit the bucket,* $F1_{(inflow)} < F2_{(outflow)}$. In this regard, there are no means to measure F2, implying it must be calculated. Assuming no mice in the bucket, $\%O_{2inflow\ dry} = \%O_{2outflow}$ and therefore, xi,p,b=20.95%. Part of the above equation thus becomes:

$$F=\frac{\frac{P_{atm}-P_{H2O\ in}}{RT_{in}}}{\frac{P_{atm}-P_{H2O\ out}}{RT_{out}}}*F1$$

Using the derived F, VO_2 now becomes:

$$VO2_{STP\ i}=\frac{\frac{20.95\%}{100}-\frac{xi,p,b}{100}*\frac{P_{atm}-P_{H2O\ in}}{RT_{in}}*F1}{\text{mass animals}}*\frac{RT_{STP}}{P_{STP}}$$

and $P_{H2O\ in}$ is measured using the Magnus equation:

$$P_{H2O}=\frac{\%H2O}{100}*6.1094*\frac{e^{\frac{17.625xtemp\ c}{temp\ c+243.04}}}{10}$$

Where temp c= temperature of inflow air in Celsius. This is the same temperature used in the VO_2 calculation. Atmospheric $\%H_2O$ and temp c are measured using the BME280 pressure and humidity sensor.

A.2 Oxygen Consumption and Total Exercise Dose Calculations

The grand VO_2 of the swim bout is then calculated as:

$$\text{avg } VO2=\frac{\sum_i N\ \ VO2_{STP\ i}}{N}$$

Where N is the number of data points selected to analyze from each swim bout.

Lastly, the total exercise dose is defined as the total volume of O_2 consumed throughout the exercise regime. Total exercise dose can not be hypothetically structured and must be empirically determined by monitoring O_2 consumption during swims throughout each training protocol. For our study, previous experiments were conducted on mice that swam for six weeks, twice daily in 90 minute bouts (Aschar-Sobbi *et al*., 2015). As such, this group swam first, and all other doses were titrated relative to this value (i.e., ~695 L of O_2/kg). Finally, integration analysis is performed to ensure appropriate swim equivalents between each swim group. To achieve this titration, we estimated an average work conducted per swim (measured as the volume of O_2 consumed per swim) according to:

approximate work per bout (mL of O_2/swim bout)= VO_2 estimated * time.

Lastly, total exercise dose was calculated using this value for each subgroup:

current dose achieved (mL of O_2/kg)= approximate work per bout * total number of swims completed.

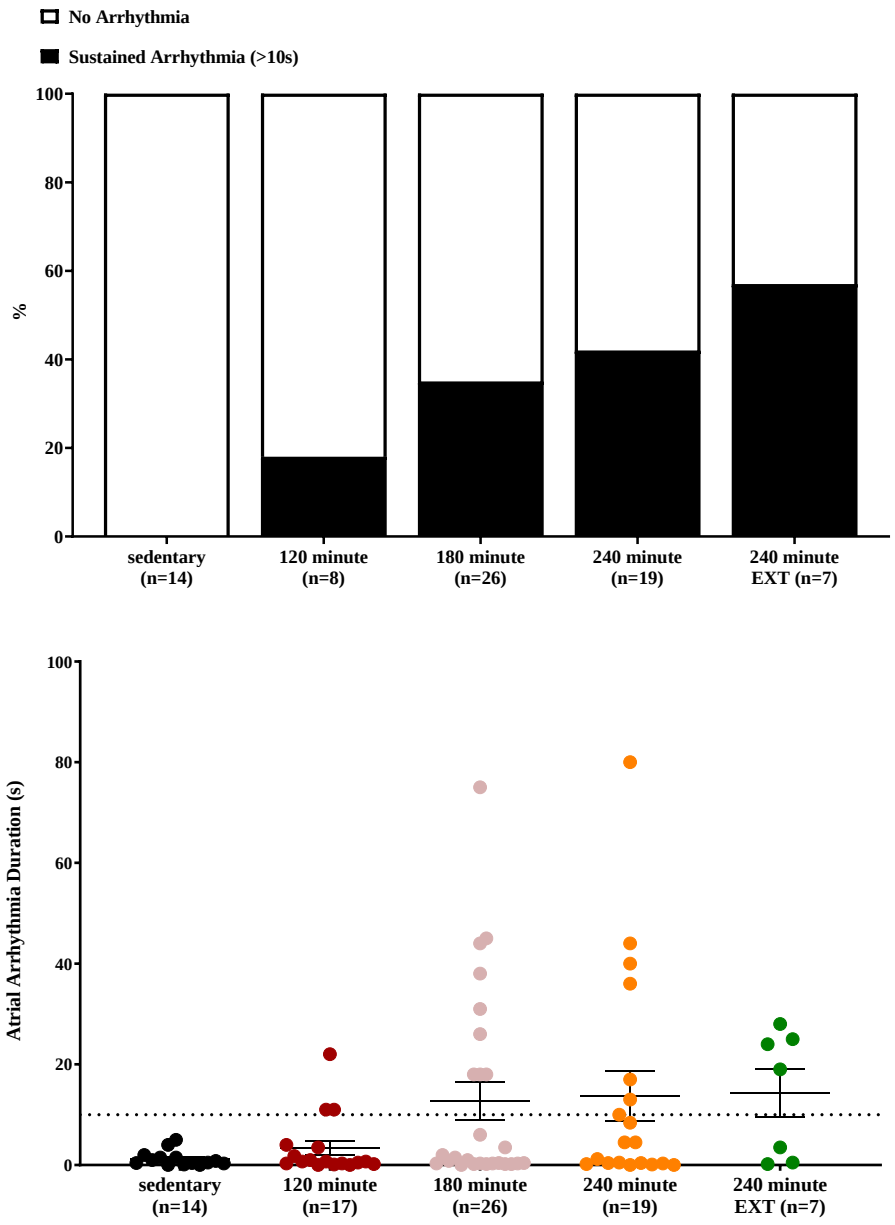

Appendix Figure A.1. Dose-Dependent AF Susceptibility in Swim-Trained Mice (Extended). An octapolar EP recording/stimulation catheter was inserted into the right jugular vein and guided into the right ventricle of anesthetized mice to investigate *in vivo* AF vulnerability. The top panel shows the percent of mice that had sustained AF inducibility (>10 s) in each group. The *bottom panel* reveals the average maximum AF duration. The *n* values indicate the number of mice included. Summary data are Mean±SEM.

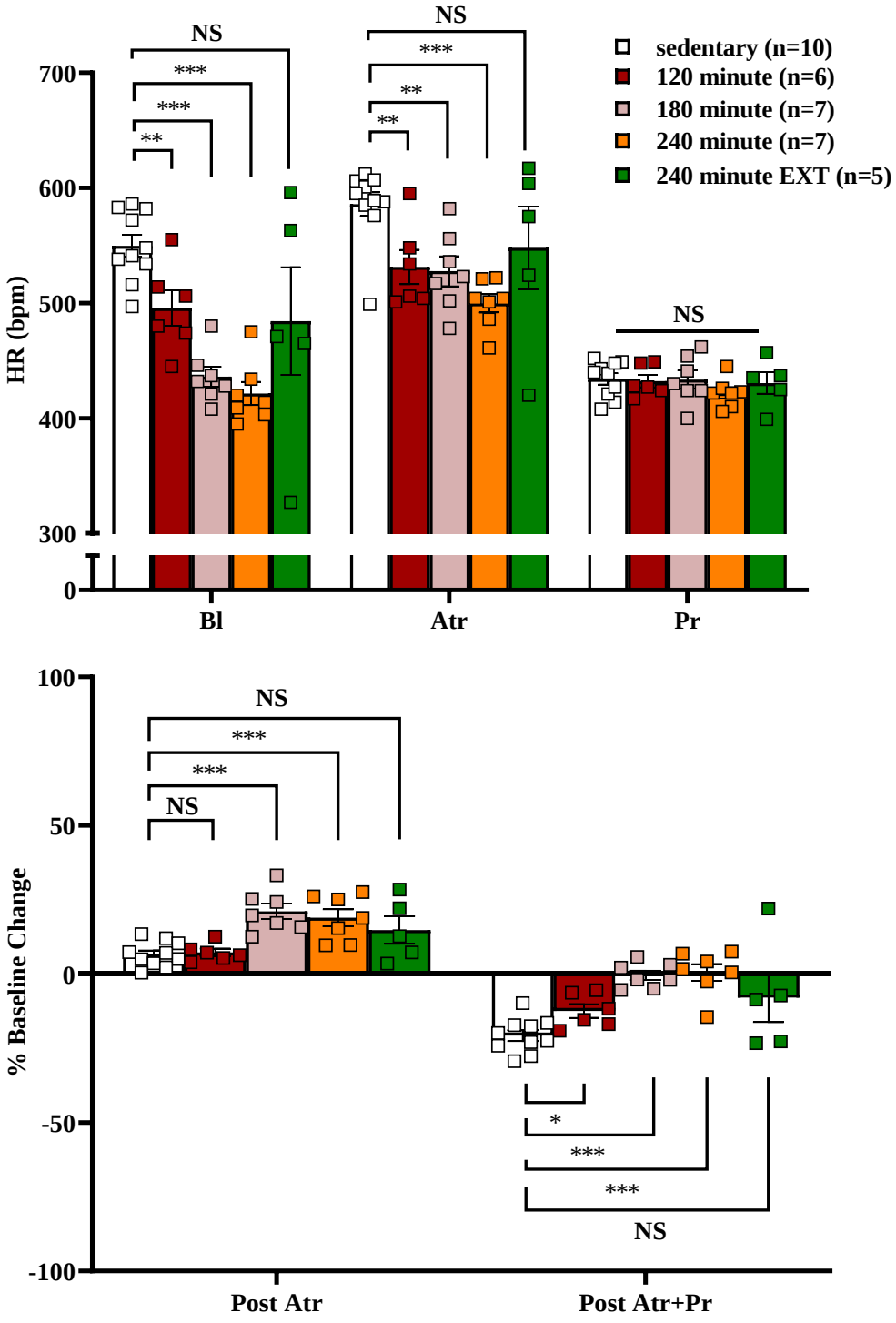

Appendix Figure A.2. Effect of Swim Training on Heart Rates (HRs) and Autonomic Regulation (Extended). The *top panel* demonstrates HRs from surface ECG recordings before and after parasympathetic blockade (atropine) and followed by sympathetic blockade (propranolol). The *bottom panel* shows % HR change from baseline with a complete autonomic blockade. Bl, baseline. The *n* values indicate the number of mice included. Data presented as Mean±SEM, **P*<0.05, ***P*<0.01, ****P*<0.0001 using a one-way ANOVA with Tukey's multiple comparisons tests.

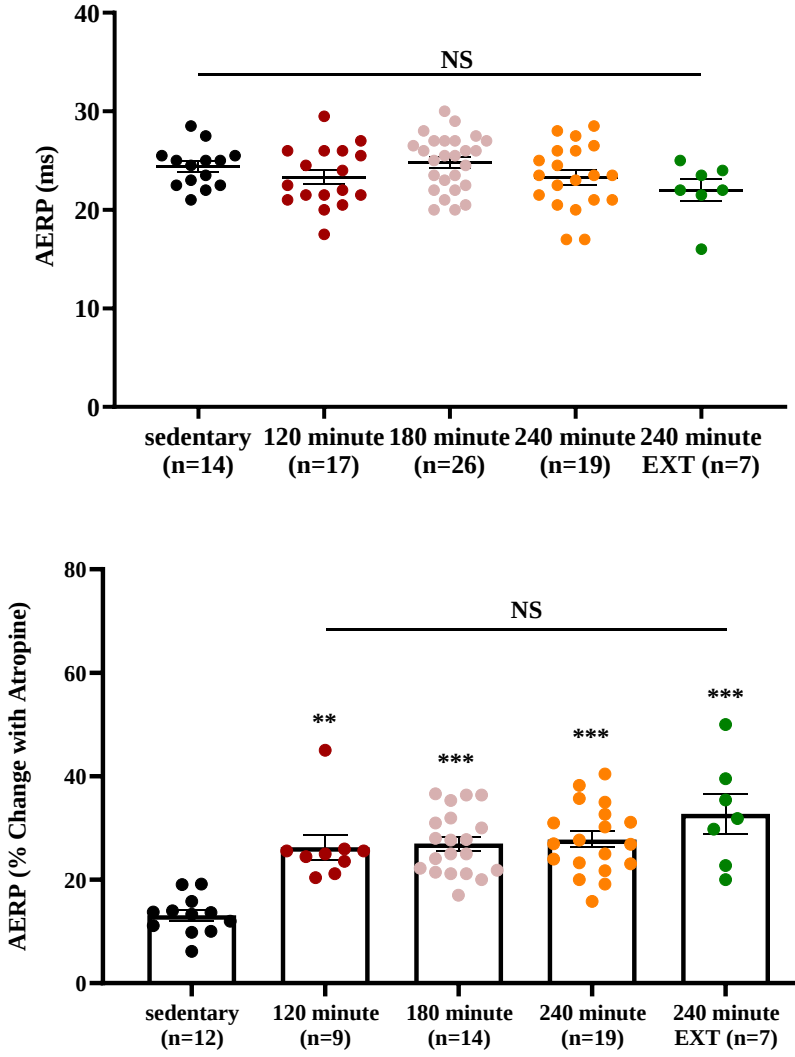

Appendix Figure A.3. Refractory Periods With and Without Parasympathetic Blockade (Extended). The *top panel* shows atrial effective refractory periods (AERPs) measured *in vivo*. The *bottom panel* shows % Change in AERP following atropine administration. The *n* values indicate the number of mice included. Data are Mean±SEM, $^{**}P<0.01$, $^{**}P<0.01$, $^{****}P<0.0001$ relative to sedentary mice using one-way ANOVA with Tukey's multiple comparisons.

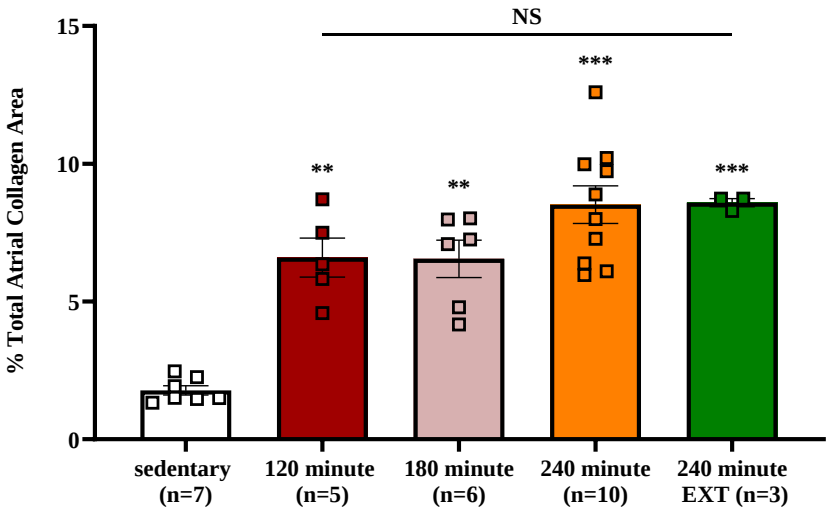

Appendix Figure A.4. Swim Training Induced Atrial Collagen Deposition (Extended). Left atrial appendage collagen content was identified using picrosirius red and imaged using a slide-scanner brightfield microscope at 20x. Total collagen quantification involved selecting and counting pixels based on brightness. The *n* values indicate the number of mice included. Data are Mean±SEM, **P*<0.05, ***P*<0.01, ****P*<0.0001, relative to sedentary mice using a one-way ANOVA with Tukey's multiple comparisons test.